AD NUMBER: AD0825180

LIMITATION CHANGES

TO:

Approved for public release; distribution is unlimited.

FROM:

Distribution authorized to US Government Agencies and contractors; Export Controlled; 1 Dec 1967. Other requests shall be referred to Rome Air Development Center (EMIRA), Griffiss AFB, NY 13440.

AUTHORITY

RADC, USAF ltr dtd 3 Mar 1977

RADC-TR-67-552
Final Report

CALIBRATION OF THE AERIAL PHOTOGRAPHIC SYSTEM

Dean C. Merchant
Syracuse University Research Institute

TECHNICAL REPORT NO. RADC-TR-67-552
December 1967

Rome Air Development Center
Air Force Systems Command
Griffiss Air Force Base, New York

CALIBRATION OF THE AERIAL PHOTOGRAPHIC SYSTEM

Dean C. Merchant
Syracuse University Research Institute

AFLC, GAFB, N.Y., 4 Jan 68-65

FOREWORD

Photogrammetrists have long been aware of the importance of the calibration of their complete measurement system. On the other hand, practical considerations have directed their interest toward adoption of selected approximations to calibration. These compromises were encouraged in part by the burdensome computational loads imposed by a realistic calibration and in part by the inability of the conventional analog approach to make use of other than nominal or characteristic type information concerning the photographic system.

Recent advances in computational techniques have virtually eliminated the earlier basis for compromise regarding photographic system calibration. Indeed, the lack of a reliable photographic system calibration is the limiting factor pertaining to the attainable accuracy of aerial photogrammetric processes when employing the purely analytical (computational) method. In appreciation of this trend, the International Society of Photogrammetry as early as the Seventh International Congress (1952) considered a draft specification regarding camera calibration in which was stated "Calibration should preferably be done photographically under conditions approaching closely that which the camera will encounter in service". This view is firmly endorsed by, among others, such photogrammetric authorities as Proctor of England, Hallert of Sweden and Cruset of France.

The notion of system calibration was developed by Dr. Churchill Eisenhart in a paper presented at the 1962 Standards Laboratory Conference, National Bureau of Standards, Boulder, Colorado entitled Realistic Evaluation of the Precision and Accuracy of Instrument Calibration Systems. He states:

> Calibration of instruments and standards is a refined form of measurement. --- it becomes evident that a particular measurement operation cannot be regarded as constituting a measurement process unless statistical stability of the type known as a state of statistical control has been attained. In order to determine whether a particular measurement operation is, or is not, in a state of statistical control it is necessary to be definite on what variations of procedure, apparatus, environmental conditions, observers, operators, etc., are allowable in "repeated applications" of what will be the measurement of the same quantity under the same conditions.

With reference to this concept of the measurement process it may be stated that current aerial photographic system calibration methods,

with few exceptions, fall far short of the ideal. Accordingly, it was the objective of this investigation to explore the feasibility of providing an aerial photographic system calibration procedure which, as a minimum, conforms to Eisenharts' concept of a measurement process applied to the measurement of the same quantity under the "same conditions." The task of "repeated applications" to attain the ideal state of statistical control is necessarily left to others.

The considerate advice and guidance offered by Dr. A. Brandenberger of Laval University and Dr. S. Ghosh of the Ohio State University during the course of this investigation is gratefully acknowledged.

The author is appreciative of the able assistance and support provided by the Syracuse University Computing Center which work was supported in part by the National Science Foundation under Grant GP - 1137.

Thanks are extended to Mr. Douglas S. Johnston for his capable work in connection with the observing and processing of data.

This document is submitted by Syracuse University Research Institute, Department of Civil Engineering, Syracuse, New York to Rome Air Development Center, Griffiss Air Force Base, New York, as the Final Report under Contract AF 30(602)-4329, Project 5569, Task 556902. Mr. Joseph Del Vecchio, EMIRA, was the RADC Project Engineer.

Particular thanks are due Mr. Del Vecchio and Mr. Don Zulch, EMASI, for his cooperation in providing suitable photography over the McClure camera calibration range.

This technical report has been reviewed and is approved.

Approved: John R. Callander
JOHN R. CALLANDER

Approved: James J. Dimel
JAMES J. DIMEL
Colonel, USAF
Chief, Intel & Info Proc Div

FOR THE COMMANDER: Irving J. Gabelman
IRVING J. GABELMAN
Chief, Advanced Studies Group

ABSTRACT

Emphasis on greater accuracy from photogrammetric methods has stimulated interest in the problem of calibration of the aerial photographic system. To be realistic, the calibration procedures must be accomplished under circumstances of environment and technique which are equivalent to those to be expected operationally. It was the purpose of this study to develop and investigate the feasibility of providing a realistic aerial photographic system calibration.

Computational procedures were developed, programmed and verified with artificial data. These computations included comparator calibration, single photo resection and multiple photo resection. The multiple photo resection employed up to four photographs using a common six parameter model to express interior orientation.

All procedures were verified further by use of real photography made at 14,000 feet over the U. S. Coast and Geodetic Survey, McClure, Ohio camera calibration range. Results of the computations using real data indicated a need for improvement in the reseau techniques employed for compensation of film shrinkage. Recommendations were made for this purpose.

Procedures were developed and studied for determination of the camera constant independently from the flying height of the aircraft. This is of particular importance for photographic systems intended for use over mountainous regions. The characteristics of this method of aerial calibration were discussed.

Technical Evaluation

1. As early as 1952, it was realized throughout the photogrammetric community that, in order to achieve the precise determination of calibration data necessary in the photographic collection system, it is essential to perform this calibration under the actual conditions which the camera encounters in service. Without external tracking information, this becomes exceedingly difficult due to the high degree of correlation which exists between the focal length and the actual flying height.

2. Dean C. Merchant has successfully demonstrated that this correlation can be suppressed by deriving the projection equations employed in terms of height differentials. The results hold a great deal of promise for a dynamic calibration procedure. A follow-on program is planned in which such a procedure will be used over a night calibration range over the Arizona test area, during FY 69.

JOHN R. CALLANDER
Project Engineer

TABLE OF CONTENTS

TABLE OF CONTENTS (cont'd)

LIST OF ILLUSTRATIONS

LIST OF ILLUSTRATIONS (cont'd)

LIST OF TABLES

LIST OF TABLES (cont'd)

1

INTRODUCTION

1.1 Background

The report of Commission I of the International Society of Photogrammetry to the Seventh International Congress [Commission I, 1952] states:

> Increasing accuracy requirements have led to increasing attention to calibration and to the relation between calibration measurements and the performance of the camera in service. Closer correspondence is being sought by increasing use of photographic methods which simulate service conditions, ---

The intent of this statement was to stimulate interest in reducing the differences that exist between conditions of environment, equipment and procedures employed operationally and the corresponding conditions used for purposes of calibration. These differences are departures from the basic conditions for realistic calibration as discussed by Eisenhart [1963]. In fact, according to Eisenhart, operational use of system calibrations obtained under these circumstances "cannot be regarded in any logical sense as measuring anything at all". Obviously, the situation is not quite so bleak in aerial photogrammetry. Even laboratory calibrations have produced reasonably accurate results. [Woodcock, Lampton, 1964] However, the vast majority of aerial photogrammetric applications that attempt to extract the maximum attainable accuracies inherent in their system are quite likely limited by the approximations introduced during the calibration.

It was the purpose therefore of this investigation to study the feasibility of providing a complete aerial photographic system calibration.

During the course of this investigation the author has drawn from the work of many. Of particular note is the work of Eisenhart [1963] for the fundamental concepts with regard to calibration; of Hallert [1962, 1962a, 1965] for the investigations and comments in many areas pertaining to aerial camera calibrations; of D. Brown [1964]for an adaptation of a thin prism mathematical model for decentered lenses; and of Leyonhufvud [1952] for his analysis of the influences on photogrammetric refraction by the assumption of a standard atmospheric model.

1.2 Scope

To assure that this investigation might reasonably lead to logical conclusions, the scope of the work was limited. It was defined to include only those factors which bear on the obtaining, controlling and reducing of aerial photography necessary for calibrating a standard precision aerial film camera.

During the course of this investigation two standards of dimension were adopted. The first standard was the McClure camera calibration range geodetic control data which were accepted as if without error. The second standard was the calibrated glass scale by which the photo comparator was calibrated. Both standards were secondary; that is they were related only numerically to the primary length standard defined in terms of wave lengths of Krypton 86. Secondary standards must always be used with caution and means provided for periodic verification.

A major obstacle to realistic calibration has been the substitution of a photographic plate for the film and magazine combination. Accordingly, considerable effort was directed to the use of film rather than plates for photography and the associated problem of overcoming the difficulties with film shrinkage.

The uncertainty of variations of the actual atmosphere from the accepted model and its influence on photo coordinates was studied and suitable corrections were introduced into the data reduction procedure.

Verification of much of the procedural development was undertaken by using photography taken with a Fairchild KC1B camera at an altitude of 14,000 feet over the McClure, Ohio range.

Finally, the important question of unfavorable strong correlation that exists between the camera constant and the object distance was studied. This question would have particular importance for cameras intended for use in mountainous regions. A method was devised based on the assumption that a calibration range would be available with a significant difference in ground target elevations. The method was evaluated using various combinations of artificial control distribution and certain recommendations were presented.

II

TECHNICAL DISCUSSION

During the course of discussions pertaining to aerial camera calibration, reference is repeatedly made to certain terms and acronyms which are germane to this investigation alone. They are defined at the beginning.

The term fiducial center is taken to mean the point on the image plane defined by the intersection of lines connecting two pairs of opposing fiducial mark images. In general, other terms are taken as defined by the Committee on Nomenclature of the American Society of Photogrammetry. [1966]

Acronyms which appear in the discussion make reference to computer routines. They are fully discussed in connection with the computation in which they first appear. To aid in subsequent references to these acronyms, Table 1 presents a brief note concerning their meanings, and indicates the respective locations in which they are more fully described. Symbols are defined in connection with the respective formula derivations in which they appear.

TABLE 1. ACRONYMS REFERRING TO COMPUTATIONAL ELEMENTS OF THE CALIBRATION PROCEDURE

Acronym	Purpose of Computation	First Reference (section)
COMCO	Comparator correction sub program	2.1.1.2
CRP	Comparator to photo coordinate transformation	2.1.2
SPR	Single photo resection	2.1.3
MPR	Multiple photo resection	2.1.4
CER	Correlation Elimination Resection	2.3.2

2.1 Derivation of Significant Formula With Real Data Applications

In each of the computational phases referred to in Table 1, an adjustment of redundant data was required. In all cases the method of least squares was used. In particular, the method of "variation of parameters" was used exclusively. [Uotila, 1963]. In the event

conditions were imposed on the solution, they were introduced directly into the functional relationships between the observations and the parameters.

2.1.1 Comparator Calibration

To assure meaningful results in subsequent phases of the investigation it was evident that a thorough calibration of the comparator would be required. Earlier work on the Syracuse University Mann 422C comparator indicated that it could be depended on from the standpoint of stability although the character of the comparator errors could not be described as linear.

2.1.1.1 The General Adjustment for Comparator Calibration

For purposes of the calibration a glass grid was ordered from Zeiss (Jena) on December 23, 1965. The grid was to consist of 272 intersections distributed over a 9" x 9" area with calibration data accurate to ±0.3 microns standard error. Based on the availability of such a grid standard a general mathematical model was selected using first, second, and third degree terms and an axis non-orthogonality term.

Observations were to be made directly on the grid standard in the comparator. Temperature would be stabilized to 22° C with a 1/2 degree maximum variation.

The results of the calibration were to be the values of the model parameters, estimates of their standard deviations and a computed standard deviation of unit weight.

The general functional relationship between observed comparator coordinates and the parameters of the calibration for the comparator with reference to Figure 1 are:

$$\hat{x} = (\Delta\hat{x} + A\hat{x}^2 + C\hat{x}^3 - x\cos\alpha - y\sin\alpha)K_x$$

$$\hat{y} = (\Delta\hat{y} + B\hat{y}^2 + D\hat{y}^3 - x\sin(\alpha - \beta) + y\cos(\alpha - \beta))K_y$$

where:

x, y = calibrated coordinates of the grid standard

$\hat{x}$, $\hat{y}$ = directly observed comparator coordinates

$\Delta\hat{x}$, $\Delta\hat{y}$ = the difference in origins between the comparator and grid systems along the $\hat{x}$ and $\hat{y}$ axis respectively

α = swing of the $\hat{x}$ axis with respect to the x axis

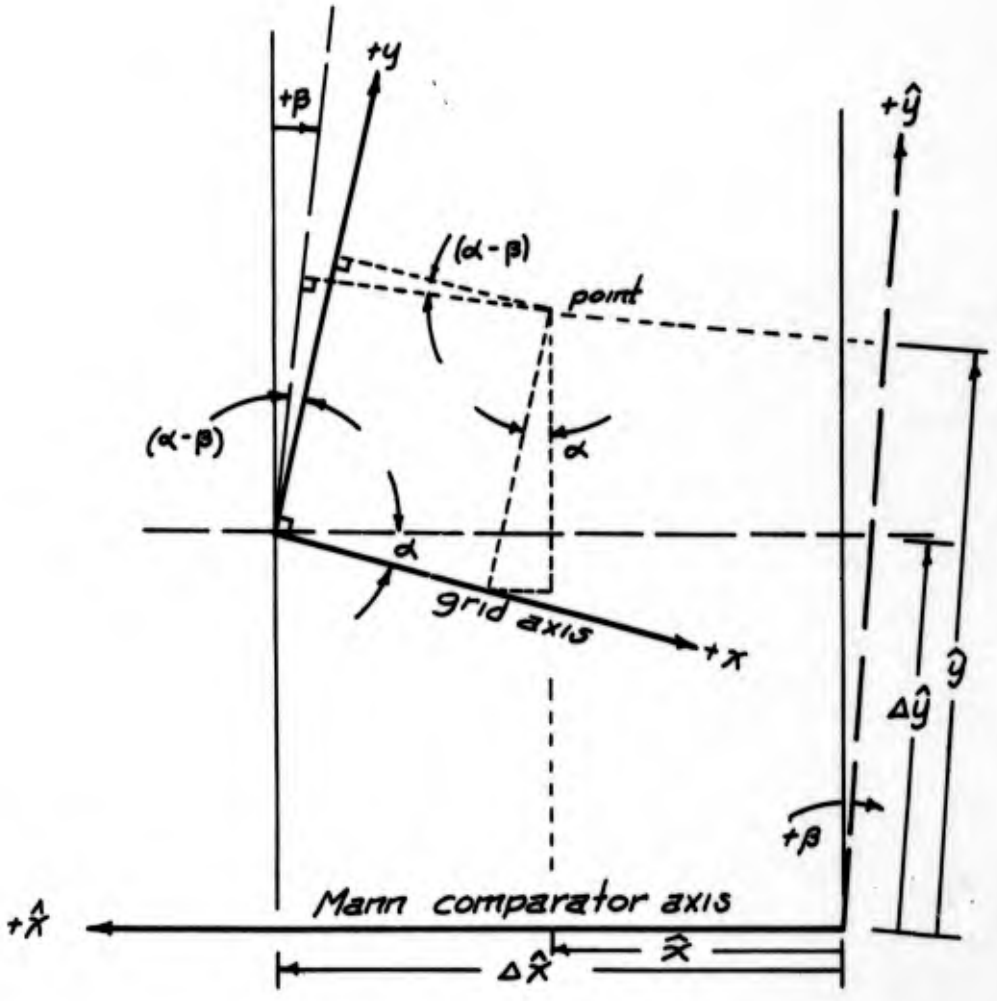

Figure 1. Elements of Transformation From Grid to Comparator Coordinates.

β = non-orthogonality term

K_x, K_y = scale terms in $\hat{x}$ and $\hat{y}$ coordinate directions respectively

A through D = additional constants of the calibration

A conventional least squares adjustment by the method of "Variation of Parameters" was employed. All observations were assumed to be of equal weight.

The adjustment was programmed for all ten parameters and verified with artificially computed data. The results of the adjustment computation on artificially generated data is presented in Tables II and III.

TABLE II. RESULTS OF GENERAL COMPARATOR CALIBRATION ADJUSTMENT USING ARTIFICIAL DATA (10 parameter adjustment)

Parameter	Initial Values (assumed)	True Values	Final Values (after 8 cycles)
α	+0.0 rad	+0.1 rad	+0.10000001 rad
K_x	1.000	1.01	1.0099988
K_y	1.000	1.01	1.0100010
$\Delta\hat{x}$	295.000 mm	300.000 mm	300.00006 mm
$\Delta\hat{y}$	295.000 mm	300.000 mm	299.99986 mm
β	0.0 rad	+0.001 rad	+0.00100000042 rad
A	0.0	$+0.4 \times 10^{-6}$	$+0.406 \times 10^{-6}$
B	0.0	$+0.4 \times 10^{-6}$	$+0.397 \times 10^{-6}$
C	0.0	$+0.4 \times 10^{-8}$	$+0.399 \times 10^{-8}$
D	0.0	$+0.4 \times 10^{-8}$	$+0.400 \times 10^{-8}$

2.1.1.2 The Modified Adjustment for Comparator Calibration

After the completion of the general comparator calibration program there was a delay in the receipt of the calibrated grid. In October, after a delay in excess of six months, it was decided to look for other means of providing an adequate comparator calibration. A method by

TABLE III. COORDINATES AND RESIDUALS AFTER A TEN PARAMETER ADJUSTMENT FOR COMPARATOR CALIBRATION (all units are mm)
XC, YC = comparator coordinates
XG, YG = grid coordinates
VX, VY = observational residuals

XC	YC	XG	YG	VX MM	VY MM
269.868	533.894	10.000	230.000	0.000030	0.000040
229.631	529.886	50.000	230.000	0.000030	0.000050
189.405	525.877	90.000	230.000	0.000020	0.000040
149.187	521.869	130.000	230.000	0.000010	0.000040
108.977	517.861	170.000	230.000	0.000030	0.000050
68.772	513.854	210.000	230.000	0.000020	0.000040
273.906	493.546	10.000	190.000	0.000020	0.000050
233.668	489.540	50.000	190.000	0.000040	0.000030
193.440	485.534	90.000	190.000	0.000030	0.000040
153.222	481.528	130.000	190.000	0.000020	0.000040
113.011	477.522	170.000	190.000	0.000020	0.000040
72.805	473.516	210.000	190.000	0.000003	0.000030
277.944	453.219	10.000	150.000	0.000020	0.000040
237.705	449.215	50.000	150.000	0.000020	0.000040
197.476	445.210	90.000	150.000	0.000010	0.000050
157.257	441.206	130.000	150.000	0.000010	0.000030
117.045	437.202	170.000	150.000	0.000020	0.000040
76.839	433.199	210.000	150.000	0.000006	0.000030
281.982	412.911	10.000	110.000	0.000020	0.000030
241.741	408.908	50.000	110.000	0.000010	0.000040
201.512	404.906	90.000	110.000	0.000020	0.000040
161.292	400.904	130.000	110.000	0.000010	0.000030
121.079	396.902	170.000	110.000	0.000020	0.000040
80.873	392.900	210.000	110.000	0.000000	0.000030
286.020	372.621	10.000	70.000	0.000020	0.000030
245.778	368.620	50.000	70.000	0.000020	0.000040
205.548	364.619	90.000	70.000	0.000020	0.000030
165.327	360.618	130.000	70.000	0.000020	0.000030
125.114	356.618	170.000	70.000	0.000030	0.000040
84.907	352.618	210.000	70.000	0.000002	0.000040
290.058	332.346	10.000	30.000	0.000020	0.000030
249.816	328.347	50.000	30.000	0.000030	0.000020
209.584	324.348	90.000	30.000	0.000030	0.000050
169.362	320.348	130.000	30.000	0.000010	0.000030
129.148	316.349	170.000	30.000	0.000020	0.000030
88.941	312.351	210.000	30.000	0.000005	0.000030

which a noncalibrated grid could be used to compute relative scale and the nonorthogonality term (β) was suggested. A useful grid for this purpose was already on hand. However, in April, 1966, a representative of the David Mann Co. [Zakrzewski, 1966] recalibrated the comparator and found it to contain a significant amount of nonlinearity of error. Accordingly, the noncalibrated grid approach had to be abandoned.

There was a suitable calibration of the $\hat{y}$-screw of the comparator provided by the Mann calibration. Unfortunately, during the observations for calibration of the $\hat{x}$-screw the operator noted some unusual results. The $\hat{x}$-screw data could not be considered as reliable from the Mann calibration. The $\hat{x}$-screw data exhibited an unusual degree of nonlinearity not found in other comparators of this type.

Beginning with a valid calibration of the $\hat{y}$-screw of the Syracuse comparator a method was devised to calibrate the $\hat{x}$-screw by measurement of a series of well distributed grid plate intervals using only the $\hat{y}$-screw. The intervals were corrected from the y-screw calibration data. By rotating the plate 90° and measuring the same intervals using the $\hat{x}$-lead screw, the discrepancies between corrected and observed intervals could be computed which would represent the corrections to the $\hat{x}$ comparator observations.

The interval data were computed from the mean of four sets of independent observations made by each of two observers. The set consisted of the average of five observations on each of twelve uniformly distributed points. This approach proved to be adequate if not ideal. To assure that no blunders existed in the theory, the final values of the calibration parameters were used in working equations. Agreement between the observed quantities and the corresponding standard were computed to a standard deviation in the $\hat{y}$-axis of ±0.2 microns and in the $\hat{x}$-axis to ±0.95 microns. The larger standard deviation in ($\hat{x}$) is the result of a more irregular distribution of corrections for the $\hat{x}$-axis than for the $\hat{y}$-axis. Further explanation is offered by the fact that the estimated standard error of the $\hat{y}$-screw calibration standard was ±1.0 microns and the $\hat{x}$-screw standard, computed from $\hat{y}$-screw observations, was ±1.34 microns.

The parameters of the comparator calibration were used to prepare a working sub-program for use in all computations in which raw comparator observations are to be used. The sub-program was checked again to assure that "true" or standard values were computed from observed values by the processing of the sub-program. The acronym for this sub-program is COMCO and will be referred to accordingly in subsequent paragraphs.

The working equations for screw corrections are:

$$x = \hat{x}K_x + A\hat{x}^2 + B\hat{x}\hat{y} + C\hat{x}^3 + D\hat{x}^2\hat{y}^2$$

$$y = \hat{y}K_y + E\hat{y}^2 + F\hat{x}\hat{y}$$

where:

x, y = corrected comparator coordinates

$\hat{x}, \hat{y}$ = observed comparator coordinates

K_x = $\hat{x}$-screw scale = 1.0000346

K_y = $\hat{y}$-screw scale = 0.9999925

A = coefficient of 2nd degree term in $\hat{x} = -0.5557 \times 10^{-6}$

B = coefficient of 1st degree mixed term for $\hat{x} = -0.2140 \times 10^{-6}$

C = coefficient of 3rd degree term in $\hat{x} = 0.2050 \times 10^{-8}$

D = coefficient of 2nd degree mixed term for $\hat{x} = 0.6431 \times 10^{-11}$

E = coefficient of 2nd degree term in $\hat{y} = 0.1511 \times 10^{-6}$

F = coefficient of first degree mixed term for $\hat{y} = 0.3437 \times 10^{-7}$

Figure 2 and Table IV indicate the locations of points used and the comparator corrections and residuals respectively after applying the working equations using the above parameters.

2.1.2 Comparator to Photo Coordinate Transformation

This phase of the computation is for the purpose of transforming the observed comparator coordinates into photo coordinates using an intermediate transformation through a reseau coordinate system. This will be referred to as the CRP program corresponding to Comparator to Reseau to Photo program. Included will be those computations necessary for correcting the comparator coordinates for calibration results and independent film shrinkage correction for each ground point image.

The necessary information to begin this phase of computation is:

a. directly observed comparator coordinates $(\hat{x}, \hat{y})$

b. coordinates of reseau marks in their own system $(\bar{x}, \bar{y})$

c. comparator correction subprogram (COMCO)

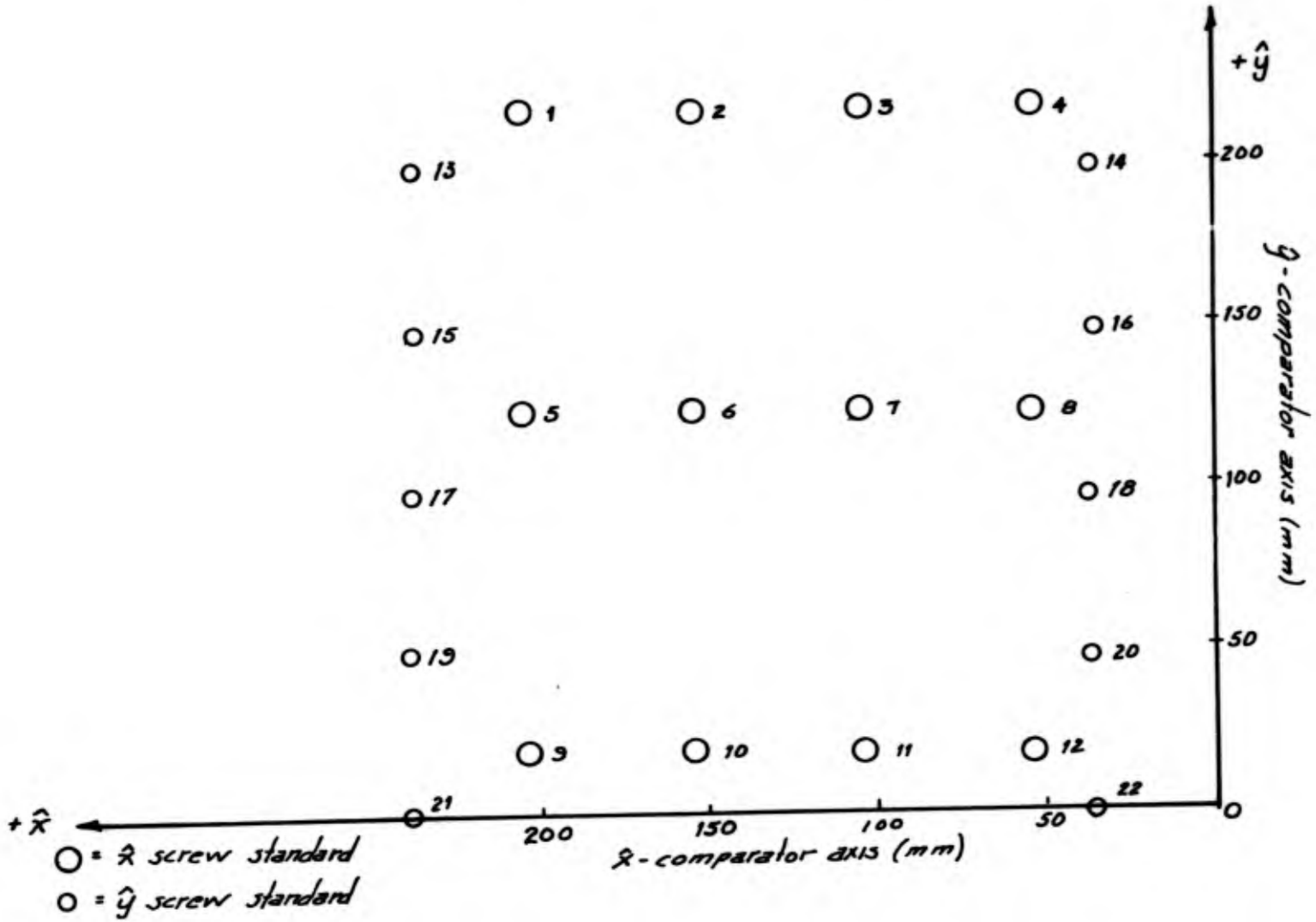

Figure 2. Location of Comparator Calibration Sample Points

TABLE IV. COMPARATOR CORRECTIONS AND RESIDUALS AFTER CALIBRATION

Point no.	x (microns) correction	residual	Point no.	y (microns) residual	correction
1	5.5	-0.2	13	0.3	-5.7
2	0.8	0.7	14	-0.1	-7.5
3	-1.7	-0.1	15	-0.4	-3.8
4	0.0	1.1	16	-0.1	-4.5
5	0.0	-0.4	17	-0.1	-1.6
6	-2.0	0.6	18	0.2	-1.9
7	-3.6	-1.7	19	0.3	0.0
8	0.0	0.6	20	0.1	-0.6
9	1.1	0.2	21	0.0	0.0
10	-0.1	0.8	22	0.0	0.0
11	-1.1	-0.4			
12	0.0	-0.3			

sum of x residuals = +0.9 microns
mean x residual = +0.075 microns
standard deviation of x residuals about zero = $\pm$ 0.80 microns

sum of y residuals = +0.2 microns
mean y residual = +0.020 microns
standard deviation of y residuals about zero = $\pm$0.20 microns

d. estimate of rotation of reseau coordinate system with respect to that of the comparator

e. additional information for automatic reseau point identification.

The results of this phase of computation in order of their printed appearance are:

a. the computed standard deviation of the mean of three observations on each fiducial mark

b. the comparator coordinates on each image point after correction for comparator calibration

c. the reseau point identifications in terms of the standard matrix notation (i, j)

d. the photo coordinate residuals after each coordinate transformation between corrected comparator and reseau coordinate system

e. the transformation parameters after adjustment with reference to Figure 3. ($\Delta\hat{x}$, $\Delta\hat{y}$, $\hat{\alpha}$, $\hat{x}$ scale, $\hat{y}$ scale)

f. computed standard deviation of unit weight.

The above results are provided for each ground point image based on independent least squares adjustments and for the fiducial mark observations which are treated in a common adjustment.

After each ground point image is individually adjusted into the reseau coordinate system it is transformed into the photo coordinate system. For this application the photo coordinate system is defined as that system lying in the plane of the positive photo having an origin at the intersection of the lines connecting opposite fiducials (fiducial center), having a (x) axis in the line defined by connecting the opposite fiducial pair which is most closely oriented to the flight direction (positive in the direction of flight) and having a (y) axis taken at 90° to the (x) photo axis. The (z) axis is taken as that axis passing through the fiducial center and normal to the (x, y) plane. A right handed coordinate system is assumed.

The results of adjustment computations for each point are summarized in a tabulation indicating the point identification, final photo coordinates corrected for film shrinkage and comparator calibration, the computed standard deviation of unit weight for each individual ground image point and the computed standard deviation of the mean of three observations in (x) and in (y) independently for each ground

image point.

Finally, since each ground point image was completely observed twice; that is, three repeated observations for each of two timewise widely separated sets, the final adjusted photo coordinates for each point were paired and the differences computed. The differences were used later to analyze the data for possible existence of significant bias between the two data sets. The mean photo coordinates from the two observational sets and the standard deviation of the mean value of the two sets are also computed. These data are tabulated in a final summation for each data point.

The CRP program punches on cards at a one card per point rate the point identification, final meaned photo coordinates, and computed standard deviations of the final meaned coordinates. A photo identification number is also punched on each card.

The computations in the CRP program proceed on a zone by zone basis for each image or group of images. The first zone is that zone which encompasses all fiducial marks. This zone in fact treats the overall photograph using pairs of reseau points in the vicinity of each of four fiducial mark images. By means of the eight widely spaced reseau marks, the parameters of transformation between comparator and reseau coordinate systems are computed by adjustment.

2.1.2.1. Functional Relationships Between Coordinate Systems

The functional relationships between observed coordinates and reseau coordinates for this computation and each subsequent computation on the independent gound point images is given below with reference to Figure 3:

$$\hat{x} = \Delta\hat{x} - (\bar{x} \cos \hat{\alpha} + \bar{y} \sin \hat{\alpha})/C_x$$

$$\hat{y} = \Delta\hat{y} - (\bar{x} \sin (\hat{\alpha} - \beta) - \bar{y} \cos (\hat{\alpha} - \beta))/C_y$$

where, with reference to Figure 3:

$(\hat{x}, \hat{y})$ = coordinates in comparator system

$(\bar{x}, \bar{y})$ = coordinate in reseau system

$(\Delta\hat{x}, \Delta\hat{y})$ = separation of respective origins measured along the comparator axis

(C_x, C_y) = linear film shrinkage coefficients measured along the respective comparator axis

$\hat{\alpha}$ = swing between comparator and reseau x axis

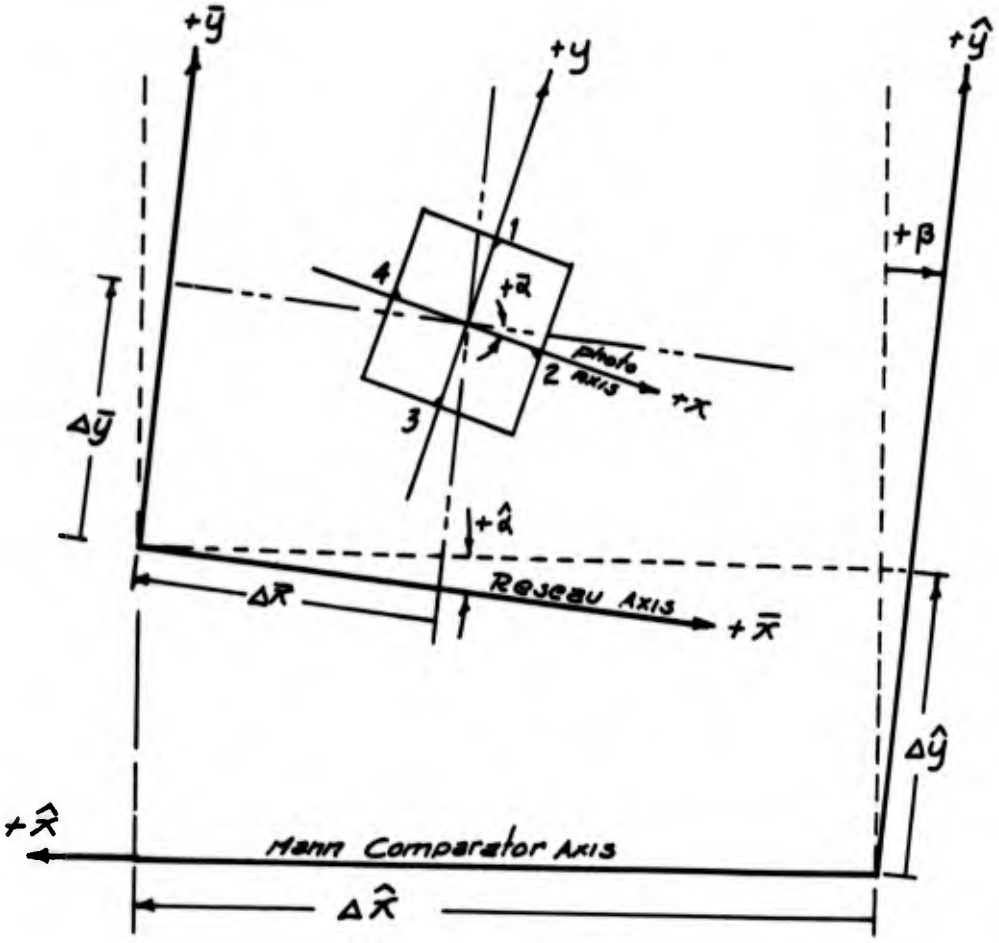

Figure 3. Relationships Between Comparator, Reseau and Photo Positive Systems of Coordinates.

β = nonorthogonality of comparator axis determined from the comparator calibration.

After each adjustment, the comparator coordinates of ground point images or fiducial images are transformed into reseau coordinates by the back solution indicated below. Details of the derivations are omitted.

$$\bar{x} = \frac{(\hat{x} - \Delta\hat{x})C_x \cos(\hat{\alpha} - \beta) + (\hat{y} - \Delta\hat{y}) \quad C_y \sin\hat{\alpha}}{\cos\hat{\alpha}\cos(\hat{\alpha} - \beta) + \sin\hat{\alpha}\sin(\hat{\alpha} - \beta)}$$

$$\bar{y} = \frac{-(\hat{x} - \Delta\hat{x})C_y \sin(\hat{\alpha} - \beta) + (\hat{y} - \Delta\hat{y})C_y \cos\hat{\alpha}}{\cos\hat{\alpha}\cos(\hat{\alpha} - \beta) + \sin\hat{\alpha}\sin(\hat{\alpha} - \beta)}$$

After the adjustment and transformation of fiducial image coordinates into reseau coordinates, the parameters of the transformation relating the photo coordinate system defined above the reseau coordinate system can be computed. The elements of this rigid body transformation will be rotation (α) about the (z) axis and translation along the reseau ($\bar{x}$, $\bar{y}$) axis. The working equations for the transformation are:

$$x = (\bar{x} - \bar{x}_o)\cos\bar{\alpha} + (\bar{y} - \bar{y}_o)\sin\bar{\alpha}$$

$$y = (\bar{x} - \bar{x}_o)\sin\bar{\alpha} + (\bar{y} - \bar{y}_o)\cos\bar{\alpha}$$

where:

(x, y) = photo coordinates

$\bar{\alpha}$ = swing between reseau and photo coordinate (x) axis

$(\bar{x}, \bar{y})$ = reseau coordinates

$(\bar{x}_o, \bar{y}_o)$ = reseau coordinates of the fiducial center

The swing angle $(\bar{\alpha})$ is computed from:

$$\bar{\alpha} = \arctan\left[\frac{\bar{y}_4 - \bar{y}_2}{\bar{x}_2 - \bar{x}_4}\right]$$

followed by testing for the quadrant. The subscripts refer to the fiducial position beginning with No. 1 at the (+y) fiducial and increasing clockwise in the plane of the positive photo.

The fiducial center coordinates were computed from the following formula. Derivations are omitted. The approach was to compute the coordinates of intersection of lines connecting opposite fiducials.

$$\bar{x}_o = [(\bar{x}_1 - \bar{x}_3)(\bar{x}_2\bar{y}_4 - \bar{y}_2\bar{x}_4) - (\bar{x}_4 - \bar{x}_2)(\bar{x}_3\bar{y}_1 - \bar{x}_1\bar{y}_3)]/D$$

$$\bar{y}_o = [(\bar{y}_2 - \bar{y}_4)(\bar{x}_3\bar{y}_1 - \bar{x}_1\bar{y}_3) + (\bar{y}_3 - \bar{y}_1)(\bar{x}_4\bar{y}_2 - \bar{x}_2\bar{y}_4)]/D$$

where

$$D = (\bar{x}_4 - \bar{x}_2)(\bar{y}_3 - \bar{y}_1) - (\bar{x}_1 - \bar{x}_3)(\bar{y}_2 - \bar{y}_4)$$

For examples of results of these computations please refer to Section 2.7.

2.1.2.2 Analysis of Paired Photo Coordinates

The differences of computed photo coordinates for the same image points measured at substantially different times provide data by which the adequacy of the procedure for elimination of systematic film shrinkage due only to changes occurring while the photo negative was in the comparator may be evaluated.

Comparator coordinates were determined during direct observation on the original photographic negative. Two complete observational circuits, each including all images, were made. The complete measurement process on each photo took, on the average, four days. Consequently, a time interval of approximately two days occurred between successive measurements of the same images. Substantial comparator coordinate differences were noted on the identical images ranging in magnitude up to ten microns. Since the temperature during the observations was maintained within ± 1/2°C and since the stability of the comparator had been demonstrated to be within one micron, the unusually large differences of "paired" points could reasonably be attributed to changes in film (combined influences of emulsion and base changes) due to changes in humidity. The film used in this experiment was Kodak Plus-X Aerographic (Type 5401). The dimensional change is 0.0070 percent per one degree (F) change [Kodak, 1966] for temperature. Further, according to Kodak "The reversible dimensional changes which occur as a result of a change in relative humidity are considerably more complex than those due to temperature changes." [Kodak, 1966]. Accordingly, the following tests of paired points in which each point having been measured at substantially different times is computed into the reseau system of coordinates and compared. This comparison will serve to indicate not only the adequacy of the procedure for eliminating film shrinkage occurring while the film is in the comparator due

to humidity changes but due to temperature changes as well.

This part of the data analysis was handled in three phases. The first phase consisted of eliminating obvious blunders by rejection criteria based on three times the standard error of one difference determined from experience. A rejection level of this magnitude can safely be expected to include only blunders without including statistically significant outlying observations. It cannot, in any sense, give assurance that all data subject to blunders has been eliminated. A standard error of a single difference of five microns was chosen as the apriori value of this test.

The second phase consisted of rejecting observational differences that exceed the limits established at the 99 percent confidence level using the computed standard deviation from the mean of the sample. [Parratt, 1961].

The third phase of analysis was used to confirm the hypothesis that the significant coordinate errors introduced during comparator observations through film shrinkage have been eliminated within the statistical significance of the experiment. This test was accomplished at the 99 percent confidence level using the null hypothesis that the average bias of the paired point differences is not significant. It was concluded that if the null hypothesis is accepted, the computational procedure for elimination of film shrinkage during comparator observations was adequate. Based on this analysis of observations on five actual photos, photograph 2825 was rejected as exhibiting a significant bias between means of the two observational sets.

Figure 4 presents the form used for anlysis of each photo independently. The analysis was designed according to Handbook No. 91 of the United States Department of Commerce [N.B.S. 1963]. Results of these analyses are discussed in Section 2.2.1.

2.1.3 Single Photo Resection

The Single Photo Resection (SPR) computation is accomplished primarily for the purpose of providing first approximations to the elements of exterior orientation for individual photographs. There data are required for each photo prior to its inclusion in a general adjustment of a series of photographs resulting in elements of interior orientation. The SPR computation also performs the secondary tasks of compensation for atmospheric refraction and of detection of errors due to image mis-identification or due to errors in ground control data. In addition, through study of photo coordinate residuals from all photos subsequently to be employed in a general adjustment, an estimate may be made of the parameters necessary to describe the complete interior orientation.

The information necessary to enter the SPR computation consists of:

a. photo coordinates with associated weights, corrected for comparator calibration and film shrinkage, and edited for observational blunders

Data Rejection and Coordinate Bias Significance Computations
by t-Distribution Testing

(Uses paired points, units are microns)
[Consistency of individual image point means]

Photo Number

x coordinates	y coordinates
Cycle number =	Cycle number =
n =	n =
Σx =	Σy =
$\bar{x} = \frac{\Sigma x}{n}$ =	$\bar{y} = \frac{\Sigma y}{n}$ =
x^2 =	y^2 =
$n\Sigma x^2$ =	$n\Sigma y^2$ =
$-(\Sigma x)^2$ =	$-(\Sigma y)^2$ =
$n(n-1)$ =	$n(n-1)$ =
S_x^2 =	S_y^2 =
S_x = ± microns	S_y = ± microns
$t_{(1-\frac{\alpha}{2})}$ =	$t_{(1-\frac{\alpha}{2})}$ =
Rejection Limits (99% confid. Lts.)	
Reject Pairs > $\bar{x}$ ±( )S_x	Reject Pairs > $\bar{y}$ ±( )S_y
Reject Pairs >	Reject Pairs >
Acceptance Range = ___ to ___	Acceptance Range = ___ to ___
Reject Points:	Reject Points:

Test of Significance of Bias of the Mean Differences
Hypothesis 1: no significant bias in differences exist
Hypothesis 2: a significant bias in differences exist
[Consistency of grand means]

$t_{(1-\frac{\alpha}{2})}$ =	$t_{(1-\frac{\alpha}{2})}$ =
$\mu_x = t\frac{S_x}{\sqrt{n}}$	$\mu_y = t\frac{S_y}{\sqrt{n}}$
Test:	Test:
$\mu_x > \lvert\bar{x}\rvert$ is favorable to H1	$\mu_y > \lvert\bar{y}\rvert$ is favorable to H1
$\mu_x < \lvert\bar{x}\rvert$ is favorable to H2	$\mu_y < \lvert\bar{y}\rvert$ is favorable to H2
Results:	Results:
Significant bias [does / does not] exist	Significant bias [does / does not] exist

Figure 4. Paired Photo Coordinate Analysis Form

b. survey coordinates in a plane coordinate system of targeted ground points corresponding to the photo points above

c. coefficients of the polynomial expressing the influence of atmospheric refraction according to Leyonhufvud [1952] and as adapted by the U.S.C. and G.S. [Harris, Tewinkel, Whitten, 1962]

d. gross first approximations to the exterior orientation

e. previous camera calibration data

The SPR computation results in photo coordinates corrected for effects of atmospheric refraction, film shrinkage, and edited for removal of blunders. The elements of exterior orientation computed from SPR are retained for the subsequent adjustment. The photo coordinate residuals after the SPR computation represent the discrepancies to be accounted for by the mathematical model of interior orientation. It is recognized that a certain portion of these residuals which rightfully should be attributed to interior orientation, were actually accommodated in the SPR adjustment by choice of the values for exterior orientation. The final general adjustment employing up to four photos simultaneously will be less subject to this compensating influence.

2.1.3.1. Derivations of Significant Formula Used By the Single Photo Resection Adjustment

The transformation formulas used to relate photo coordinates to survey coordinates are of the form originally attributed to Dr. Sebastian Finsterwalder. Briefly, they may be described with reference to Figure 5. Right handed coordinates are assumed for both the survey and photographic systems. When starting with survey coordinates, the primary rotation (ω) is taken about the (X') axis; the secondary rotation (ϕ) is taken about the (Y'') axis, and the tertiary rotation (κ) is taken about the (Z''') axis:

where: X' = axis through the air station parallel to the survey (X) axis

X'' = X'

Y'' = axis in a vertical plane, containing the air station, normal to the (X') axis and rotated from the horizontal by an angle (ω)

Z''' = axis passing through the air station and normal to the ($X'Y''$) plane.

All rotations are assumed to be right handed.

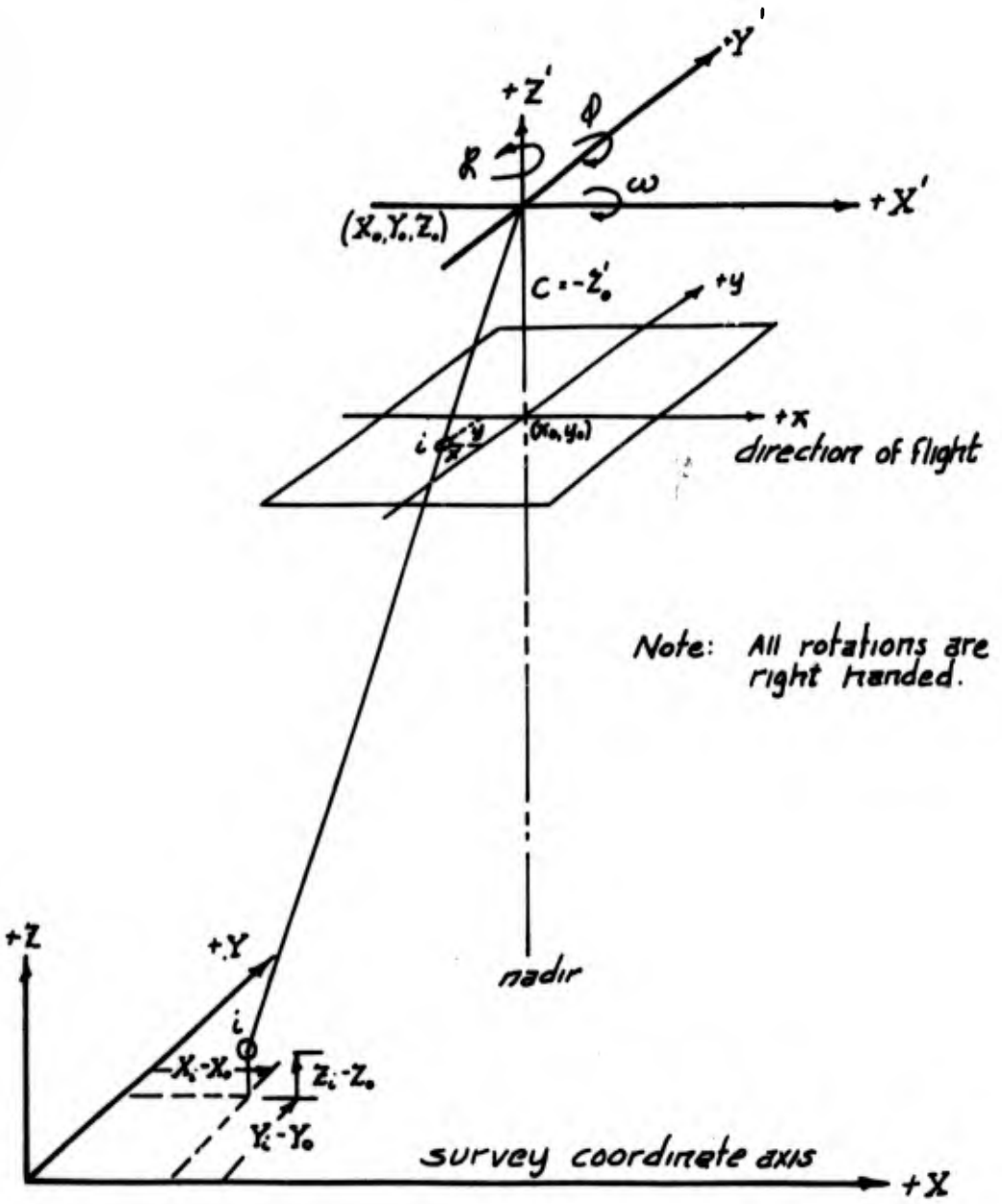

Figure 5. Relationships Between Survey and Photo Coordinate Axis

The coordinate transformation due to rotations only, may be expressed in matrix notation [Rosenfield, 1959]. A discussion of the selection of order of rotations appears below.

$$\begin{bmatrix} X_i' \\ Y_i'' \\ Z_i''' \end{bmatrix} = M_\kappa \cdot M_\phi \cdot M_\omega \begin{bmatrix} X_i - X_o \\ Y_i - Y_o \\ Z_i - Z_o \end{bmatrix}$$

in which:

M_κ; M_ϕ; M_ω = orthogonal rotational matrices

(X_i, Y_i, Z_i) = survey coordinates of any point (i)

(X_o, Y_o, Z_o) = survey coordinates of the air station

(X_i', Y_i'', Z_i''') = spatial coordinates of object point (i) in a coordinate system which is parallel to the photo coordinate system but with origin at the air station

The resulting equations are dependent on the order of selection of the rotation. In the event observations of elements of angular exterior orientation are to be made, or the adjusted values be used for instance with a plotter, it is required that the appropriate sequence of rotations be selected. In this application the survey coordinates were transformed into a system of rectangular coordinates parallel to the photocoordinate system. As seen from the above equation the rotation about the X-survey axis (ω) was chosen as the primary (ϕ) secondary and (κ) teritiary rotations. For the application at hand, the selection of the order of rotation is of no consequence. For the photographic case it remains only to scale the rotated survey coordinates by the ratio of the calibrated camera focal length (c) to the object distance measured in the direction of the Z''' axis. The photo coordinates are then:

$$x_i = \frac{-c}{Z_i'''} \cdot X_i'$$

$$y_i = \frac{-c}{Z_i'''} \cdot Y_i'$$

The need for a negative camera focal length in the above equations is the result of the arbitrary consistent choice of right handed coordinate systems. If the Z''' axis had been chosen as positive nominally downward through the air station, a positive camera constant would be required.

The fully expanded equations relating photo and survey coordinates are published extensively elsewhere [Harris, Tewinkel, Whitten, 1962] [Rosenfield, 1959], consequently they will not be reproduced here.

The adjustment computation was performed by the method of variation of parameters. No restraints were used on the orientation elements. Weights determined from the CRP computation were applied to the photo coordinate observations. The process of linearization of the parameters with respect to the observations by means of the Taylor's series required partial differentiation of (x,y) with respect to each element of exterior orientation. This exercise is also omitted in the interest of brevity. A detailed example of a specific linearization process may be found in the published work of the Coast and Geodetic Survey [Harris, Tewinkel, Whitten, 1962].

2.1.3.2. Derivation of the Compensation Computation for Effects of Atmospheric Refraction

The effect on photo coordinates of the influence of varying densities of atmospheric layers has been studied by others. For purposes of this investigation the work of Leyonhufvud [1952] is used. A discussion of influences of refraction is treated in paragraph 2.2.2.1. The work of Leyonhufvud has been adapted by the Coast and Geodetic Survey [Harris, Tewinkel, Whitten, 1962] for application to a fictitious vertical camera of 153.00 mm focal length. Variables are height of the air station and mean elevation of the terrain above sea level. The corrections for a given altitude and terrain elevation lend themselves to expression by means of an odd power third degree polynomial.

$$d = k_1 \cdot r + k_2 \cdot r^3$$

where:

d = correction to photo radial distance

r = radial distance to image from fiducial center (assumes that the principle point coincides with the fiducial center)

The expression is valid for a fictitious vertical camera with an arbitrarily selected focal length to agree with the coefficients (k_1, k_2). For application therefore, it is required that the uncorrected photo coordinates be rotated and scaled to correspond to the fictitious vertical photograph. After correction of the artificial data for effects of refraction, the coordinates are transformed back to the actual photo orientation.

The procedure for these photo coordinate transformations makes use of the rotational transformation developed between survey and photo parallel coordinate systems. The three rotations used in that transformation may be combined into a single orthogonal rotation matrix.

$$M = M_{\kappa} \cdot M_{\phi} \cdot M_{\omega}$$

The true photo coordinates may be related to their equivalent vertical photo coordinates by:

$$\begin{bmatrix} x \\ y \\ -c \end{bmatrix} = M \begin{bmatrix} x_v \\ y_v \\ z_v \end{bmatrix}$$

Post multiplying both sides by M^{-1} yields:

$$\begin{bmatrix} x_v \\ y_v \\ z_v \end{bmatrix} = M^{-1} \begin{bmatrix} x \\ y \\ -c \end{bmatrix}$$

Advantage is taken here of the orthogonality of the matrix (M). A characteristic of an orthogonal matrix is that its transpose equals its inverse. Therefore, without further derivation beyond what was required for the first transformation, the required rotational transformation may be taken as:

$$\begin{bmatrix} x_v \\ y_v \\ z_v \end{bmatrix} = M^{T} \begin{bmatrix} x \\ y \\ -c \end{bmatrix}$$

The equivalent vertical coordinates may then be scaled to correspond to the fictitious vertical photography for which the correction coefficients apply.

$$x_{vs} = \frac{153}{z_v} \cdot x_v$$

$$y_{vs} = \frac{153}{z_v} \cdot y_v$$

where:

x_{vs}, y_{vs} = scaled equivalent vertical photo coordinates

The correction terms are then computed using the aritifical coordinates. After corrections for refraction are added to (x_{vs}) and (y_{vs}), the coordinates are rescaled to correspond to corrected (x_v) and (y_v) coordinates. Finally, the corrected equivalent vertical photo coordinates are transformed back into their original orientation by:

$$\begin{bmatrix} x \\ y \\ -c \end{bmatrix} = M \begin{bmatrix} x_v \\ y_v \\ z_v \end{bmatrix}$$

The computation for correction of atmospheric refraction influences was prepared as a sub-program and employed in the SPR computation. The working program was verified with artificial data and found to agree with the tabulated corrections to a standard error of less than one micron.

2.1.3.3 Representative Results of the SPR Computation

To prove the program, a set of artificial photo coordinates without errors was computed based on a series of well distributed arbitrarily chosen survey coordinates and elements of exterior orientation. The computation was supplied with substantially different values of exterior orientation. The test of the computation would be its ability to produce the "true" (artificially chosen) elements of exterior orientation and photo coordinate residuals. The result of this test using 9 points is presented in Table 5.

TABLE V. RESULTS OF ADJUSTMENT BY SPR COMPUTATION BASED ON ARTIFICIAL DATA (for 9 points)

Exterior Elements	True	Initial Estimation	Computed	Discrepancy
X_o (ft)	10,000.	10,500	9,999.9990	+ 0.0010
Y_o (ft)	10,000.	10,500	10,000.0010	- 0.0010
Z_o (ft)	11,000.	10,500	11,000.9390	- 0.9390
κ (rad)	0.0000	0.017453	0.0000000	0.0
ϕ (rad)	0.0000	0.017453	-0.0000003	$+ 0.3 \times 10^{-6}$
ω (rad)	0.0000	0.017453	+0.0000062	$- 6.2 \times 10^{-6}$

The relatively large elevation discrepancy was due to the introduction of a correction for atmospheric refraction when, in fact, the artificial data had not been influenced by refraction.

An example of the results of the SPR computation working with real data is presented in Table 6. The first information identifies the photo by number, and indicates the number of control points employed. The values of the elements of angular orientation are printed followed by estimates of their respective standard errors. The covariance matrix from which these variances were extracted was computed using photo coordinate residuals after adjustment on data which had been corrected by information from a prior laboratory calibration. The air station coordinates in feet are printed next followed by estimates of their standard errors. The final information is the tabulation on a point by point basis of:

a. point identification number

b. photo coordinates corrected for film shrinkage and atmospheric refraction but with no alterations due to lens distortion

c. computed standard errors of photo coordinates derived from the CRP computation

d. photo coordinate residuals corrected for film shrinkage, atmospheric refraction but with no alterations due to lens distortion

Additional information such as the variance co-variance matrix is also printed out but is not included in Table 6. The information is also punched out for subsequent use in graphically displaying the residuals.

The graphical display of photo coordinate residuals after the SPR adjustment are presented in Figures 7 through 10.

2.1.4 Multiple Photo Resection

The Multiple Photo Resection (MPR) computation is intended to provide the final adjusted parameters of interior orientation. In addition, as a matter of necessity, the complete exterior orientation for each of a series of up to four photos is also computed. In principle there is no limit to the number of photos that may be used in the MPR program. In practice, the limitation of number of photos that may be simultaneously treated in in the MPR adjustment computation is normally imposed by storage capacity of the computer.

The information necessary to enter the MPR computation is as follows:

TABLE VI. REPRESENTATIVE SINGLE PHOTO RESECTION RESULTS IN WHICH THE RESIDUALS INCLUDE THE TOTAL LENS DISTORTION.

PHOTO NUMBER 2822
NUMBER OF CONTROL POINTS 36
DETERMINANT OF NORMAL COEFFICIENT MATRIX 0.75E-42

ORIENTATION WITH RESPECT TO RANGE (RADIANS).

KAPPA	+OR-	PHI	+OR-	OMEGA	+OR-
-0.0598182	0.0000282	-0.0147448	0.0000792	0.0042368	0.0000818

AIR STATION COORDINATES

X	+OR-	Y	+OR-	Z	+OR-
1602525.6000	1.1596	601041.9500	1.1879	13751.0720	0.4269

PHOTO COORDINATES ALTERED FOR REFRACTION

POINT	X MM	Y MM	MX MM	MY MM	VX MM	VY MM
0.067	-41.9973	-72.8231	0.0009	0.0016	-0.0031	-0.0339
0.103	-104.4201	-76.5924	0.0010	0.0018	-0.0107	-0.0181
0.038	-42.7905	-57.5123	0.0011	0.0020	0.0016	-0.0137
0.116	17.5036	-40.8810	0.0009	0.0015	-0.0058	0.0086
0.003	-13.1834	-39.6234	0.0017	0.0011	0.0101	-0.0011
0.032	-24.9529	-41.0610	0.0010	0.0015	0.0119	0.0052
0.037	-43.6712	-41.5708	0.0006	0.0018	0.0114	-0.0013
0.044	-59.4367	-42.4974	0.0013	0.0012	0.0071	0.0123
0.099	-106.8434	-29.8712	0.0017	0.0021	0.0055	0.0048
0.120	-91.6230	-28.1499	0.0012	0.0011	-0.0159	-0.0061
0.005	-45.1823	-28.3678	0.0012	0.0008	0.0033	0.0050
0.052	80.2380	-34.4222	0.0008	0.0015	0.0011	-0.0013
0.084	17.2225	-23.7935	0.0015	0.0009	-0.0061	-0.0004
0.035	1.4346	-23.7582	0.0007	0.0014	0.0014	0.0035
0.091	-44.8024	-11.1571	0.0021	0.0018	0.0175	0.0019

TABLE VI. CONTINUED.

0.046	15.4937	-7.6294	0.0012	0.0007	-0.0073	0.0042
0.062	76.9555	-4.1776	0.0019	0.0007	0.0007	-0.0043
0.096	14.7777	5.6393	0.0012	0.0013	-0.0103	-0.0075
0.111	-46.3018	4.2463	0.0017	0.0010	0.0133	0.0046
0.001	-93.9803	17.4833	0.0021	0.0019	-0.0046	-0.0007
0.090	-47.7710	19.8442	0.0010	0.0009	0.0121	0.0013
0.012	14.6158	23.3179	0.0006	0.0011	-0.0110	-0.0180
0.070	74.7498	25.6826	0.0013	0.0011	0.0154	-0.0080
0.083	13.7741	38.0103	0.0022	0.0015	-0.0033	-0.0132
0.040	-47.7686	34.8194	0.0011	0.0023	0.0070	0.0012
0.118	-111.6788	47.4061	0.0014	0.0013	0.0207	0.0007
0.085	-48.6581	50.1327	0.0009	0.0006	0.0019	0.0011
0.034	-96.3904	63.4096	0.0006	0.0023	0.0129	0.0208
0.113	12.9342	52.6224	0.0011	0.0006	0.0133	-0.0047
0.023	73.7190	56.3757	0.0008	0.0014	-0.0069	0.0152
0.050	11.3255	68.4587	0.0012	0.0013	0.0057	-0.0209
0.060	-3.4651	67.7109	0.0009	0.0017	0.0048	-0.0055
0.063	-49.2406	65.4737	0.0005	0.0007	-0.0178	0.0063
0.033	-35.0022	81.7305	0.0010	0.0015	-0.0015	0.0059
0.107	-19.5150	81.6663	0.0012	0.0004	0.0099	0.0043
0.065	-50.7649	96.0414	0.0011	0.0016	-0.0127	-0.0007

a. photo coordinates with associated weights corrected for comparator calibration, film shrinkage and free from blunders, (weights are taken as the inverse of a representative photo coordinate variance)

b. survey coordinates in a rectangular system and free from blunders

c. first approximations to all parameters of the adjustment including interior orientation (common to all photos) and exterior orientation for each photo independently.

d. the camera constant and coordinates of the principal point in a fiducial center origin system

The MPR computation results are printed out after each adjustment sequence to permit monitoring of the solution. After final adjustment the printed results consist of:

a. the adjusted values of the six parameters expressing lens distortion (Distortion will be discussed in Section 2.1.4.1.)

b. a listing of the final coordinates, weights and photo coordinate residuals for each point in the computation

c. the computed standard error of unit weight

d. the complete variance covariance matrix is printed out for up to thirty unknown parameters.

2.1.4.1 Significant Formula Used by the Multiple Photo Resection Computation

For purposes of this program the mathematical model suggested by D. Brown [1964] is employed. Brown's model is used since it is representative of a currently popular model capable of accommodating in a general fashion both radial and tangential lens distortions. For purposes of this study other equally general models would have been as appropriate.

The model accounts for the usual symmetrical lens distortion by means of an odd power polynomial to the seventh degree neglecting the first order term which is entirely equivalent to a radial scale term. The radial symmetrical distortion is treated by the following polynomial:

$$\delta r_s = K_1 r^3 + K_2 r^5 + K_3 r^7$$

where:

δr_s = radial component of symmetrical lens distortion

(K_1, K_2, K_3) = coefficients of polynomial expressing radial symmetrical lens distortion

r = radial distance from principal point to image point

The tangential component of distortion assumed entirely due to decentering of the individual objective lens elements is expressed by an adaptation of the thin prism model suggested by D. Brown [1964]. The earlier work of Connrady [1919] is theoretically more accurate but computationally awkward. The thin prism model suggested by Brown [1964] is used here. The rectangular tangential components are expressed by:

$$x_t = -(J_1 r^2 + J_2 r^4) \sin \phi_o$$

$$y_t = +(J_1 r^2 + J_2 r^4) \cos \phi_o$$

where:

(x_t, Y_t) = rectangular components of tangential distortion

(J_1, J_2) = coefficients of polynomial expressing maximum tangential distortion

r = radial distance from principal point to image point

ϕ_o = clockwise angle between the positive (x) photo axis and the direction of maximum tangential distortion.

The two model distortions are then combined. The results are photo coordinates corrected for both radial and tangential lens distortion.

$$x = (1 + \frac{\delta r_s}{r})(\bar{x} - x_o) - (J_1 r^2 + J_2 r^4) \sin \phi_o$$

$$y = (1 + \frac{\delta r_s}{r})(\bar{y} - y_o) + (J_1 r^2 + j_2 r^4) \cos \phi_o$$

where:

(x,y) = fiducial center coordinates corrected for lens distortion

$(\bar{x},\bar{y})$ = fiducial center coordinates uncorrected for lens distortion

(x_o,y_o) = fiducial center coordinates of the principle point

After expanding the (δr_s) term, the expressions for corrected photo coordinates are:

$$x = (1 + K_1r^2 + K_2r^4 + K_3r^6)(\bar{x} - x_o) - (J_1r^2 + J_2r^4) \sin \phi_o$$

$$y = (1 + K_1r^2 + K_2r^4 + K_3r^6)(\bar{y} - y_o) + (J_1r^2 + J_2r^4) \cos \phi_o$$

Six elements or model parameters are used to express the complete objective distortion. The remaining elements of interior orientation are not included due to their strong correlation with certain elements of exterior orientation. In a later section of this report, several suggestions are made for elimination of correlation between the calibrated focal length and the elevation of the air station for a nominally vertical camera.

To form the general observation equations for use in the MPR computation, the above equations are introduced into the expanded equations relating photo coordinates and survey coordinates described earlier in Section 2.1.3.1. In abbreviated notation the final formulas used in the MPR computations are:

$$\bar{x} = x_o + \frac{Ax + By + Cz}{Gx + Hy + Iz} + (J_1r^2 + J_2r^4) \sin \phi_o \quad (1 + K_1r^2 + K_2r^4 + K_3r^6)^{-1}$$

$$\bar{y} = y_o + \frac{Dx + Ey + Fz}{Gx + Hy + Iz} - (J_1r^2 + J_2r^4) \cos \phi_o \quad (1 + K_1r^2 + K_2r^4 + K_3r^6)^{-1}$$

where:

$(\bar{x},\bar{y})$ = photo coordinates uncorrected for lens distortion

(x,y,z) = differences between exposure station and ground point,

$$(X_o - X),\ (Y_o - Y),\ (Z_o - Z)$$

(A,B,C,D,E,F,G,H,I) = coefficients of the projective transformation discussed in Section 2.1.3.1

(J_1, J_2, ϕ_o) = coefficients of tangential objective distortion

(K_1, K_2, K_3) = coefficients of radial objective distortion

r = radial distance from principal point to image

(x_o, y_o) = fiducial center coordinates of principal point

For use in a least square adjustment these equations are put in linear form with respect to the calibration coefficients and elements of exterior orientation for each photograph employed. The least squares adjustment is accomplished according to the method of variation of parameters. The adjustment is repeated until no significant improvement in residuals is noted. Each repetition of the adjustment employs the previous adjusted parameters as first approximations.

From the general MPR equations above, it is seen that before adjustment, a value for at least (J_1) is required so that alterations to (ϕ_o) are provided after each adjustment. For this application, the values computed from a stellar calibration on the same camera and published by Autometrics Corp. [Raytheon, 1965] were used. If previous calibration data were not available, an estimate could be made for (J_1) and (ϕ_o) using the graphical display of residuals from the SPR computation.

The National Bureau of Standards procedure for camera calibration locates the principal point. The fiducials are affixed to the camera cone to provide a means for referencing the location of the principle point. Errors in this procedure will be absorbed by the mathematical model chosen for the MPR computation.

2.1.4.2 Representative Results of the MPR Computation

The validity of the MPR program was established by means of artificial data generated by a separate computation. For this purpose twenty-four well distributed ground points were selected with elevations ranging from zero to fifty meters. The elements of interior and exterior orientation were assumed and a set of artificial photo coordinates were computed. These coordinates were free from all errors and tabulated to the nearest micron. Equal weights were assigned to all photo coordinates. With these photo coordinates, the MPR computation was entered using four photos, each 90° in azimuth from the other. The photo coordinate residual was ± 0.28 microns standard error after seven iterations. This can be attributed entirely to the fact that the least significant figure in the observations was one micron. The results of the MPR computation regarding interior orientation are presented in Table 7.

TABLE VII. RESULTS OF ADJUSTMENT BY MPR COMPUTATION BASED ON ARTIFICIAL DATA

Interior Elements	True	Initial Estimate	Computed	Deviations
K_1	$+0.24988\times10^{-7}$	$+.25\times10^{-7}$	$+.24668\times10^{-7}$	$-.0032\times10^{-7}$
K_2	-0.13896×10^{-10}	$-.13\times10^{-10}$	$-.13828\times10^{-10}$	$-.00068\times10^{-10}$
K_3	$+0.51406\times10^{-15}$	$+.50\times10^{-15}$	$+.51143\times10^{-15}$	$-.00263\times10^{-15}$
J_1	$+0.39642\times10^{-6}$	$+.40\times10^{-6}$	$-.40059\times10^{-6}$	$-.00417\times10^{-6}$(1)
J_2	-0.31691×10^{-11}	$-.32\times10^{-11}$	$+.30545\times10^{-11}$	$+.01146\times10^{-11}$(1)
ϕ_o(rad)	+1.3401	+1.30	-1.7855	$+.016 + \pi$

(1) deviations after allowance for sense change induced by a π radians change in ϕ_o.

At an altitude of 15000 meters, the deviations were consistently less than several centimeters in exposure station position and angular orientations deviated consistently by less than one half arc second from the true value.

In Table 7, note the reversed sense but correct magnitude of the (J_1) and (J_2) terms. This is explained by noting that the (ϕ_o) term deviates nearly π radians from the true value. The combined influences on the calibration of the (J_1), (J_2) and (ϕ_o) terms taken together is equal to the influence of the true values for these terms. Further, the rather large deviations in some terms indicate the relative insensitivity of the solution to these terms. Fortunately, the consequence on photo coordinate correction of the larger deviations in application will be relatively small. The prime test for validity of the solution lies in the magnitude of the observational residuals and not the amount of parameter deviations from the true values. In this case, the mean photo coordinate residual of $\pm$0.28 microns is quite satisfactory as indicated above.

The significant results using four photos taken over the McClure range are presented in Section 2.7 of this report. The photo coordinate residuals after adjustment are plotted for these photographs and are presented in Figures 13 through 20.

2.2 Discussion of Significant Problems

2.2.1 Photo Coordinate Errors

Errors in photo coordinates may be attributed to several sources. First, errors may arise during the measurement process. These are due primarily to uncompensated comparator errors, and observational pointing errors. The second general error source class arises from characteristics of the film itself. These are film shrinkage non-linearity and emulsion/base thickness irregularity. A third class of error arises from such sources as approximations in refraction corrections or due to computational expediencies.

Based on results from real data discussed in some detail earlier and on the findings of others regarding characteristics of film, this section attempts to combine these components of error to provide a realistic estimate of the errors in photo coordinates.

Because of the difficulty experienced with film shrinkage caused by changes in relative humidity, the results from real data have value only for computation of precision. A full discussion of this problem is presented in Section 2.3.3. The real data would have provided computed values for photo coordinate errors arising from all sources at the end of the MPR computation had the reseau been flashed onto the film at very nearly the instant the film was exposed in the camera. The following discussions will be directed toward estimating the error that would have occurred had the reseau technique been effective.

The precision of the measurement process is best estimated from the analysis of photo coordinate differences between the two values determined independently as described in the CRP computation. An analysis was made after the CRP computation for detection of significant bias in photo coordinates determined from observations made at significantly different times. As part of this analysis described in detail in Section 2.1.2, a standard deviation was computed for paired coordinate differences. Table 8 presents the computed standard deviation of paired differences for the four photos which displayed no significant bias.

TABLE VIII. STANDARD DEVIATION OF PAIRED PHOTO COORDINATE DIFFERENCES (± microns)

Photo No.	s.d. for Δx	s.d. for Δy
2729	3.52	3.14
2822	3.26	4.21
2826	3.68	3.19
2829	3.51	2.91
Average	3.49	3.34

It appears that ±3.5 microns is a representative standard deviation of paired coordinate differences. Since they do not exhibit significant bias, it is assumed that a standard error (m) of an individual photo coordinate is:

$$m = \frac{m_{difference}}{\sqrt{2}}$$

Also, the standard error of the mean of the paired coordinates will be:

$$m_{\bar{x}} = \frac{m_x}{\sqrt{2}} \qquad \text{and} \qquad m_{\bar{y}} = \frac{m_y}{\sqrt{2}}$$

The computed standard deviation of the mean of the two paired photo coordinates is then:

$$m_{\bar{x}} = \frac{m_{difference\ (x)}}{2} \qquad \text{and} \qquad m_{\bar{y}} = \frac{m_{difference\ (y)}}{2}$$

The result is that the standard deviation of the mean value due to the precision only of the observation is ±1.75 microns. For purposes of weighting, a value of ±2.0 microns was used.

The systematic error introduced by the comparator was discussed in section 2.1.1. The standard deviation of computed corrections was ±1.0 microns in (y) and ±1.34 microns in (x). These are representative of the magnitude of comparator calibration errors and will be systematic to some extent.

The second source of errors arising from the film consists primarily of effects due to non-affine or irregular film shrinkage and due to irregularity of the effective emulsion plane with respect to the fixed camera platen. By use of the one half inch interval reseau and assuming that it could be exposed on the film concurrently with the image from the ground, the irregular and affine film shrinkage influence would be effectively reduced to the micron level. [Brock, Faulds, 1962].

The irregularity of the effective plane of the emulsion may have a greater effect than residual shrinkages. Dr. Ahrend [1966] describes this problem as consisting of five contributing factors.

The first factor is that of platen flatness. In the application to airborne system calibration in which film rather than plate photography is used, the influence of platen flatness anomalies may be to some extent absorbed within the parameters of the calibration.

Secondly, the question of full flattening of the film against the platen and the influence of combined film base and emulsion thickness irregularities must be considered. Registration is grossly a question of adequate vacuum applied for a sufficient period of time. Vacuum failure would of course require rejection of the photography. Thickness variations on representative aerial films have been reported by Hallert [1962]. The thickness standard deviation was found to range from ± 0.8 to ± 2.1 microns. Peak deviations of 10 microns were found to exist. The thickness variation appeared periodic in nature with a repetition interval of about 40mm. The presence of such disturbances emphasizes the need for at least use of a series of photos for adjustment into a common set of camera calibration parameters.

The third factor influencing image flatness arises from a honeycomb structure occurring during the first fractional part of a second after application of the vacuum [Ahrend, 1966][Clark, Cooper, 1964]. This is caused by the fact that small pockets of air trapped between the film and the platen require time to escape to the vacuum source points. This influence should be avoided by proper vacuum distribution design and provision of ample time for air pocket dissipation.

Dust and emulsion particles between the film and platen must be avoided. It is recommended that thorough, frequent cleaning of the platen by compressed air be accomplished to avoid this problem [Ahrend, 1966].

The final contributing factor suggested by Ahrend is the warping of plates with emulsion coating on one side only. In the application at hand, the original negative was measured. This factor is evidently of no interest in this discussion.

The third class of photo coordinate error arises from incomplete correction for such influences as atmospheric refraction, irregularities of the survey control and computational approximations. These influences have been discussed in this paper individually as they arise. The calibration procedures have been designed to keep these individual influences below one micron in the worst case of coordinate position.

Of particular interest in computation of photo coordinates based on a fiducial center origin system is the accuracy which is obtained in determining the fiducial center. Without regard to comparator errors, the error in coordinates of the fiducial center (x_o, y_o) is approximately equal to the standard deviation of the respective coordinate means at opposite sides of the format. Assuming that (x_o) is the mean of (x_1) and (x_3);

i.e.:
$$x_o = \frac{x_1 + x_3}{2}$$

$$\therefore \quad m_{x_o}^2 = \left(\tfrac{1}{2} m_{x_1}\right)^2 + \left(\tfrac{1}{2} m_{x_3}\right)^2 = \tfrac{1}{4}\left(m_{x_1}^2 + m_{x_3}^2\right)$$

If it is assumed that they are of equal precision;

$$m_{x_o} = \frac{1}{\sqrt{2}} m_x$$

The results from the CRP computation regarding precision of repeated pointings on the standard side fiducials of KC1B camera are presented in Table 9. From these results, the standard deviation in the x coordinate of the fiducial center (s_{x_o}) is $\pm$1.03 microns, and for (s_{y_o}) is $\pm$0.50 microns. The disparity in precision may be explained by the superior images of fiducials at the left and right fiducial positions.

TABLE IX. PRECISION OF OBSERVATIONS ON FIDUCIAL MARKS USING A FAIRCHILD KC1B CAMERA

Photo No.	standard deviations	$\pm$ x (microns)		$\pm$ y (microns	
	fiducial identification	f1	f3	f2	f4
2729		1.73	0.88	2.03	2.58
2822		1.45	2.60	0.33	0.33
2826		0.58	0.58	0.00	0.00
2829		0.00	0.88	0.33	0.58
Fiducial Average		1.28	1.65	0.90	0.50
x or y Average		$s_x = \pm$ 1.46		$s_y = \pm$ 0.70	

The error in determining the fiducial center will vary from photo to photo with the precisions indicated above. Because of the nature of this and other errors contributing to what is defined as the photo coordinate error it would be inappropriate to combine them quadratically to compute their total effect. The combined photo coordinate error may be obtained most realistically from the standard error of unit weight and the appropriate photo coordinate weight after the MPR adjustment provided the technique of film shrinkage control by means of a reseau is effective.

2.2.2 Atmospheric Refraction and Earth Curvature

The discussions of the influences of atmospheric refraction and of the assumption that the geoid can be replaced by a plane over the limited

range of the control field are presented in this section. They will be treated separately. In each case it is intended to demonstrate that their respective influences are so well predictable that they need not be treated as unknowns in the resection adjustments in the usual aerial photographic case over the McClure range.

2.2.2.1 Refraction

The work of Leyonhufvud [1952] is particularly outstanding with regard to the influences of optical refraction through the standard atmosphere for the aerial case. The results are developed for the ICAN (International Commission for Air Navigation) atmosphere and compared with results obtained from other models. For purposes of this investigation, the adaptation of Leyonhufvud's results by the U.S. Coast and Geodetic Survey [Harris, Tewinkel, Whitten, 1962] has been used.

The comparison of results using various atmospheric models originally presented by Leyonhufvud [1952] has been adapted to the specific case at hand. Table 10 presents a comparison of influences of atmospheric refraction according to several sources assuming a camera focal length of 153.0 mm, an altitude of 4000 meters above the ground assumed to be at sea level. Only the extreme case of the ray at 45° off the vertical (nadir distance) is compared. It is seen that the maximum discrepancy of 0.95 micron exists between ICAN and the model proposed by Gast [1937].

TABLE X. COMPARISON OF INFLUENCE OF ATMOSPHERIC REFRACTION ON THE AERIAL CASE FOR SEVERAL ATMOSPHERIC MODELS

(alt. = 4000 meters, ground elev. = 0 meters, nadir distance = 45°, focal length = 153 mm.)

Source	sexigesimal arc sec.	radial microns	differences from ICAN (microns)
ICAN	9.11	13.50	0.00
Aschenbrenner [1937]	8.96	13.27	-0.23
Schutte [1937]	9.50	14.08	+0.58
Gast [1957]	9.76	14.45	+0.95

An attempt was made to estimate the influence of variations of the actual atmosphere from the assumed ICAN atmosphere. The separate influences of temperature, pressure, lapse rate and relative humidity were considered. Apparently, due to lack of information concerning the variability of these factors at different altitudes, Leyonhufvud computed only maximum influences and unit rates of influence of these factors. Again they were computed for the extreme ray of 45° off the nadir, and a ground

elevation of 0 meters. His results have been converted to the case at hand for an altitude of 4000 meters and focal length of 153. mm. and are presented in Table XI.

It is seen that by assuming the most wide range of temperature, and to a lesser degree other properties, a significant range of photo coordinates could be expected for the extreme ray. This gives also an indication of the unit rates of change of photo coordinates for the extreme ray per unit change of the influencing property. Information concerning the temperature for various altitudes with associated standard deviations has been published recently by Cole and Nee [1965]. This data along with the standards of the ICAN atmosphere permit an estimate of the standard error that may be expected due to variations of temperature from the assumed values for the aerial case of 4000 meters altitude and for the extreme ray. The influence of lapse rate, pressure and humidity variations appear to be of secondary significance as compared to temperature variations.

The ICAN atmosphere as used for refraction correction represents an estimated seasonal mean. Accordingly, variations in photogrammetric refraction will occur due both to departures from seasonal means and to standard deviations of temperature.

The ICAN atmosphere uses 288°K (where (K) denotes degrees Kelvin) as the absolute temperature standard at sea level. The maximum spread from the standard for the geographical sample points occurs at Great Falls, Montana at the surface. The seasonal departures from the standard are -14°C in winter to +7°C in summer [Cole, Nee, 1965, p. 12]. These are predictable and may be used to compute systematic photocoordinate corrections if considered significant. Using Leyonhufvud's unit rates adapted to the case at hand, the seasonal change in temperature would require a radial image correction at 45° nadir distance of =1.2 microns in January and +0.6 microns in July. The maximum variation in temperature of $\pm$9°C standard deviation about the monthly mean also occurs at the surface at Great Falls, Montana during January. For the extreme ray, the temperature variation will introduce a standard deviation of $\pm$0.72 microns. The influences of variations of the atmosphere from the ICAN standard atmosphere were not considered significant for this application.

2.2.2.2 Earth Curvature

The elevations of targeted survey control points were published in terms of elevation above sea level. These elevations when used with the assumption that the reference surface is a plane will introduce a distortion of a magnitude several times greater than that introduced by refraction and with an opposite sense. It is convenient to treat regular earth curvature influences as a distortion and correct the photo coordinates directly. An alternate approach would be to convert the published geodetic coordinates to rectangular spatial cartesian coordinates, thus removing the need for artificial corrections.

TABLE XI. MAXIMUMS AND UNIT RATES OF INFLUENCE OF PRINCIPAL PHYSICAL PROPERTIES ON PHOTOGRAMMETRIC REFRACTION ADAPTED FROM LEYONHUFVUD [1952].

(nadir distance = 45°, ground elevation = 0 m., focal length = 153 mm)

properties, units (range)	total influence		unit rates of influence	
	(arc sec.)	(microns)	arc sec./ unit of property	microns/ unit of property
pressure, mm (730 to 790)	0.72	1.07	0.012	0.017
temperature, deg. C. (-15 to +45)	3.46	5.13	0.058	0.086
lapse rate of temp., deg. C/100 m (0.35 to 0.95)	1.02	1.51	1.69	2.50
relative humidity percent at +45°C (0 - 100)	0.15	0.22	0.0016	0.0024

The method employed during this investigation was to compute and apply corrections to the observed photo coordinates to compensate for the plane assumption for the vertical datum. For this purpose, the separation between the plane and the local spherical normal may be calculated from [Brandenberger, 1951]: (Referring to Figure 6)

$$\Delta H' \quad R - \sqrt{R^2 + X^2} = R\left(1 - \sqrt{1 + \frac{X^2}{R^2}}\right) \approx \frac{X^2}{2R} + \ldots$$

where:

$\Delta H'$ = separation

R = a mean earth radius of curvature computed from $(a + a + b)1/3$ using the parameters of Clarke 1866 (6,370,977 meters)

X = distance of point from the nadir point

Then:

$$X^2 = H^2 \tan^2 \eta$$

$$\therefore \quad \Delta H' = -\frac{H^2}{2R} \tan^2 \eta$$

where:

η = nadir distance

For small values of (η), the elevation departure $(\Delta H')$ may be approximated by (ΔH).

Converting to influence on nadir distance:

$$\eta = \arctan\left(\frac{X}{H}\right)$$

$$d\eta/dH = -\frac{1}{1 + \frac{X^2}{H^2}}\left(\frac{X}{H^2}\right)$$

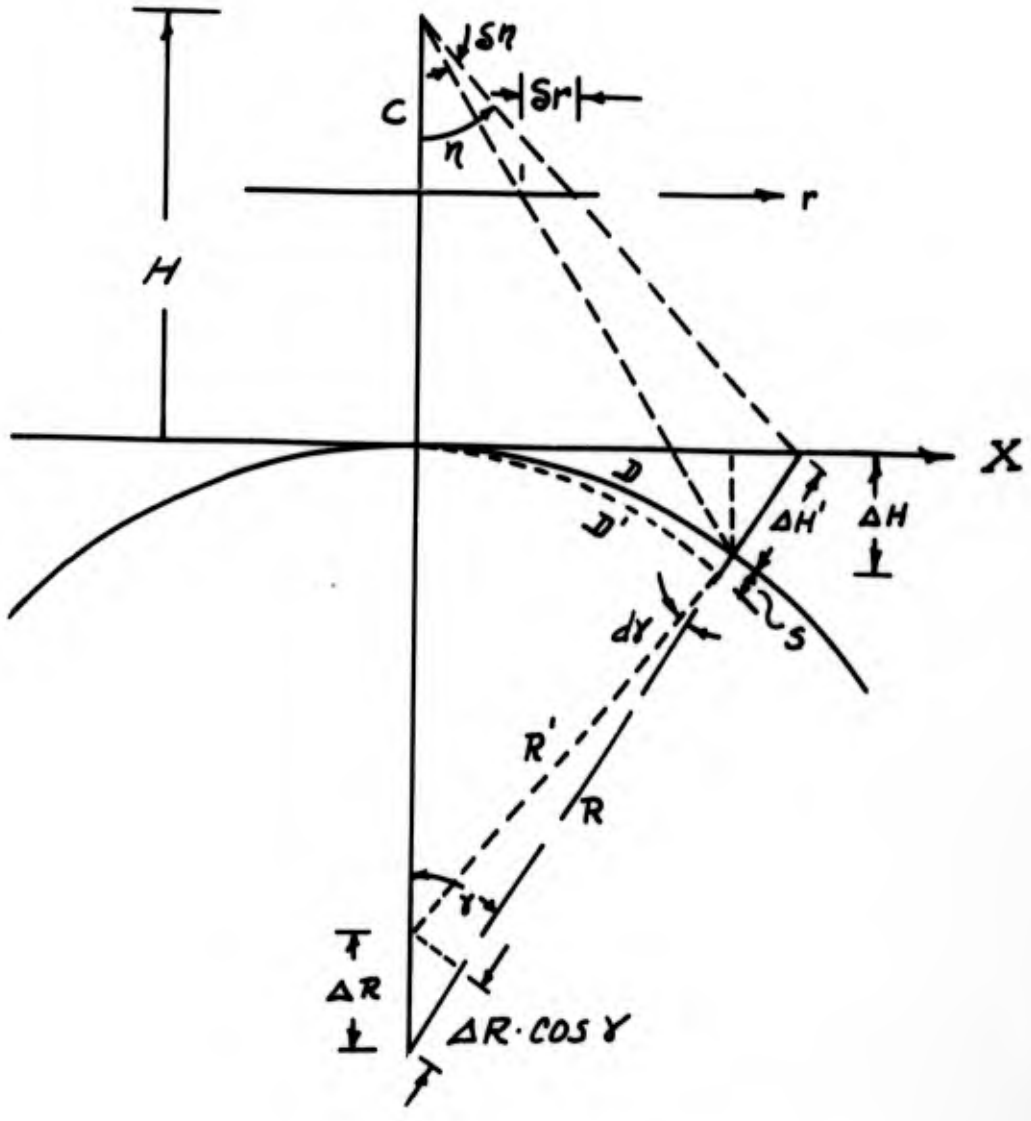

Figure 6. Departure of Reference Plane from Spherical Earth

This is equivalent to:

$$\delta\eta = \frac{1}{1 + \frac{X^2}{H^2}} \left(\frac{X}{H^2}\right)\left(\frac{X^2}{2R}\right) = \frac{H \sin^3 \eta}{2R \cos \eta}$$

(note: The change in notation from (d) to (δ) corresponds to the change in assumption from a differential to a finite quantity.)

where:

$\delta\eta$ = the change in nadir distance in radians due to earth curvature

The change in photo coordinate per radian unit change in nadir distance is then:

$$\delta r = c \sec^2 \eta \cdot \delta\eta$$

$$\therefore \delta r = c \frac{H}{2R} \tan^3 \eta$$

The correction ($+\delta r$) for influence of earth curvature may be computed from the above formula assuming a vertical photo of focal length (c) for an altitude of (H). The units of (H) and (R) must be the same. The units of the correction will be those of (c). This correction is conveniently computed and applied at the same time atmospheric refraction is treated during data processing. This was accomplished during this investigation.

2.2.2.3 Spherical Assumption Influence on Photo Coordinates

In Section 2.2.2.1 the vertical datum was assumed to be plane. In that section an expression was developed to correct for the assumption that the earth is planar rather than spherical. The validity of that expression is investigated here from the standpoint of use of the sphere to approximate the reference ellipsoid. The expression relating change in photo coordinate due to a spherical assumption (i.e., constant radius earth) was:

$$\delta r = c \frac{H}{2R} \tan^3 \eta$$

The change in displacement of the photo image ($\Delta\delta r$) due to the separation occurring between the spherical and ellipsoidal earth (S) is then derived by differentiation of the correction (δr) with respect to the nominal earth radius (R). The separation and earth radius are very nearly co-linear for small central angles (γ). Accordingly, the radial correction to the photo image position becomes:

$$\Delta\delta r = [- c \frac{H}{2R^2} \tan^3\eta]S$$

The separation (S) may be derived with reference to Figure 6.

Let $\Delta R = R - R'$

Then very nearly:

$$S = R - \Delta R \cdot \cos\gamma - R'$$

$$S = \Delta r \ (1 - \cos\gamma)$$

Substituting in the above expression for photo image displacement:

$$\Delta\delta r = -c \cdot \frac{H}{2R^2} \cdot \Delta R \cdot (1 - \cos\gamma) \cdot \tan^3\eta$$

where:

$\Delta\delta r$ = photographic image displacement

c = camera constant

H = elevation of exposure station

R = local earth radius of curvature

ΔR = change of local earth radius over the extremes of the camera field

γ = geocontric angle subtending the camera field

η = nadir distance of imaging ray

This derivation of image displacement is conservative in that it assumes an instantaneous change in earth's radius of curvature. In fact, of course, it is a gradual process. Further refinement of this derivation is

not necessary. If changes in curvature can be shown to be insignificant with the conservative formula above, they certainly will not be significant using a more refined formula.

The formula for image displacement due to changes of radius of curvature is evaluated for the meridian in the vicinity of the camera calibration range. Assuming a camera constant (c) of 150 mm, a flight height of 4000 m, a geocentric angle (γ) of one minute corresponding to the half field coverage of the camera and a change in the radius of curvature in the meridian of 16.7 meters as determined from Gossett [1950] for Clarke 1866, the image displacement is computed to be -0.50×10^{-12} mm. Obviously, the spherical assumption does not introduce a significant influence.

2.2.2.4 Earth Gravity Anomalies

Using the expression developed in Section 2.2.2.3 for relating image displacement ($\Delta\delta r$) to separation (S), the influences of anomalies of the earth's gravity field may be estimated. In recent studies of the earth's gravity in the State of Ohio it has been determined that the greatest rate of change of the deflection of the vertical occurs over a 30 km distance in the amount of 10 seconds [Uotila, 1967] [Heiskanen, Uotila, 1956]. With reference to Figure 6, the change in deflection may be related to the change in radius of curvature (ΔR).

Assuming:

$$D = D'$$

Then:

$$R = \frac{D}{\gamma}$$

$$\Delta R = -\frac{D}{\gamma^2} \cdot \Delta\gamma$$

Evaluating this expression over the 30 km distance and for a change in deflection ($\Delta\gamma$) of 10 arc seconds, the computed change in radius of curvature is 60 km. Assuming that the change in radius of curvature over the 30 km interval is representative of the rate of change that occurred within the interval, the change in radius may be scaled to correspond to the 4 km half field angle. The change of radius of curvature due to anomalies is then computed to be 8 km over the half field of the camera. Using the assumptions of Section 2.2.2.3 regarding the photography, the image displacement resulting from extreme anomalies of gravity in Ohio can be computed as before. The image displacement is computed to be 0.25×10^{-9} mm. It may be safely stated that gravity anomalies in Ohio will not introduce significant image displacements for purposes of this study.

2.2.3 Film Dimensional Stability and Reseau Control

The results of the investigation with regard to film/emulsion stability have revealed that significant non-linear image distortions occur under operational conditions due to the uncontrolled influences of relative humidity. A significant part of the process of providing reliable photo coordinate measurements lies in adequate consideration of humidity changes that occur prior to and after exposure.

Comparator observations were processed through the CRP (comparator to reseau to photo coordinate transformations) and the results were analyzed individually for four photos. Data were rejected as described for CRP in paragraph 2.1.2. The approved observations, corrected for comparator calibration and film shrinkage as computed from the reseau standard data were then processed through the SPR (single photo resection program). As described in paragraph 2.1.3 above, the SPR corrects for interior orientation using information obtained from a previous calibration. The photo coordinate residuals, however, are computed after adjustment assuming a purely projective relationship between the image and object space. Consequently, the residuals that remain should represent the components of the individual observations which require compensation by means of an appropriate mathematical model of the interior orientation. It was expected that the residuals should nominally describe one of a number of theoretically possible optical objective distortions. As an example, provided all other systematic influences had been removed and provided the magnitude of the residuals were sufficiently small, it was expected that the residuals could be described by Conrady's model for decentered objectives or by D. Brown's [1964] thin prism model.

The residuals for each photo were plotted independently by the graphical component (CAL-COMP) of the digital computer. Inspection of these plots indicate that a significant departure from the expected results has occurred. It is evident that a systematic influence which is considerably larger than could reasonably be attributed to the objective itself has resulted. The camera had been previously calibrated first by Fairchild Camera and Instrument Corp. (Syosset, N.Y.) using the "bank collimator" method and later by Autometrics Corp (Alexandria, Va.) using the stellar method. The results of these calibrations, although far from an agreement, at least indicate reasonably predictable residual patterns that can be adequately described by Brown's model.

Figures 7 through 10 present the photo coordinate residuals assuming a pure central point projection and employing a best available exterior orientation.

These residual plots indicate quite strongly that a significant affine disturbance has occurred in excess of the shrinkage which was compensated by means of reseau control and in excess also of that which may be expressed in terms of accepted mathematical models of interior orientation.

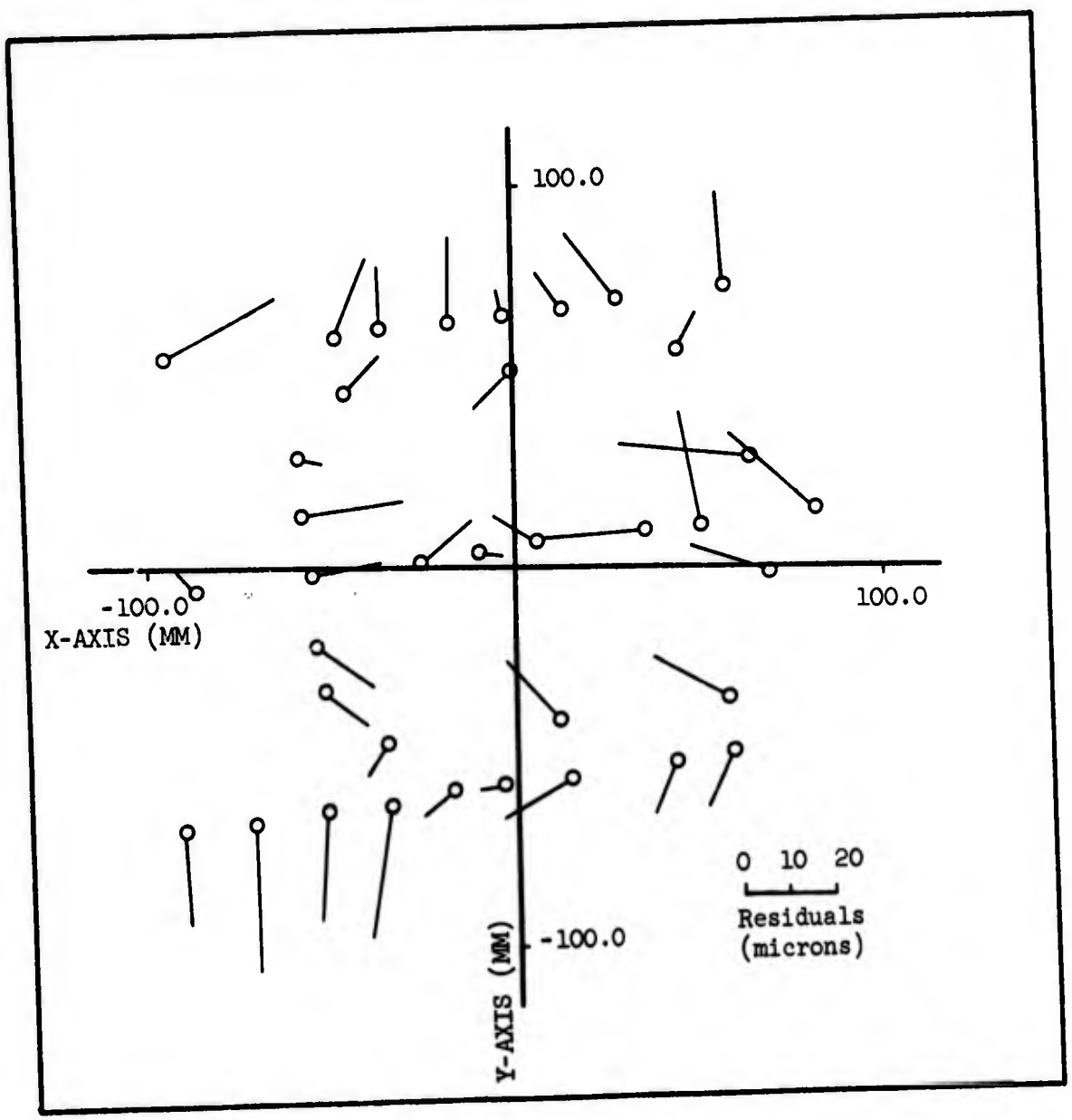

Figure 7. Photo Coordinate Residuals After SPR (Photo 2729).

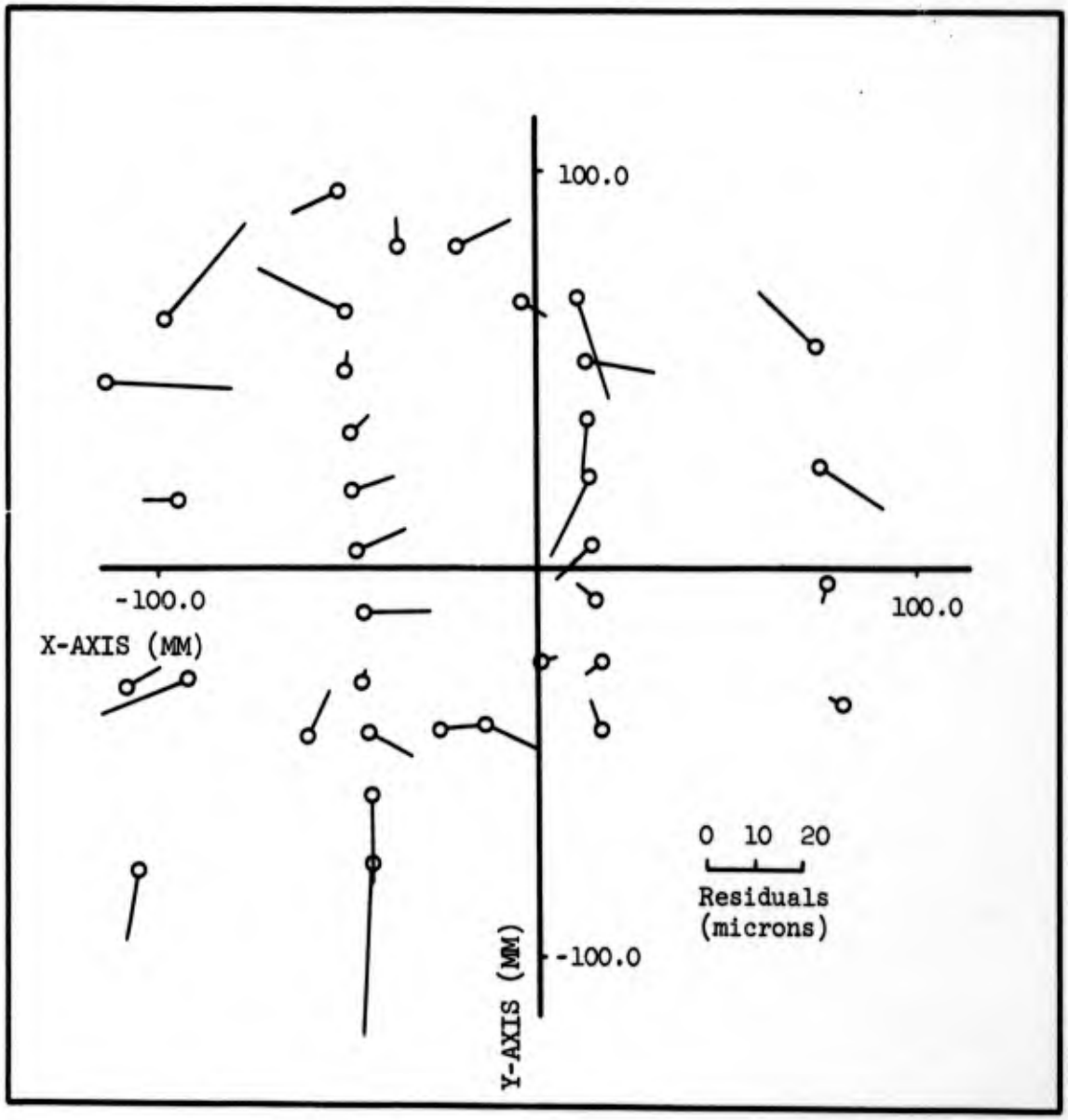

Figure 8. Photo Coordinate Residuals After SPR (Photo 2822).

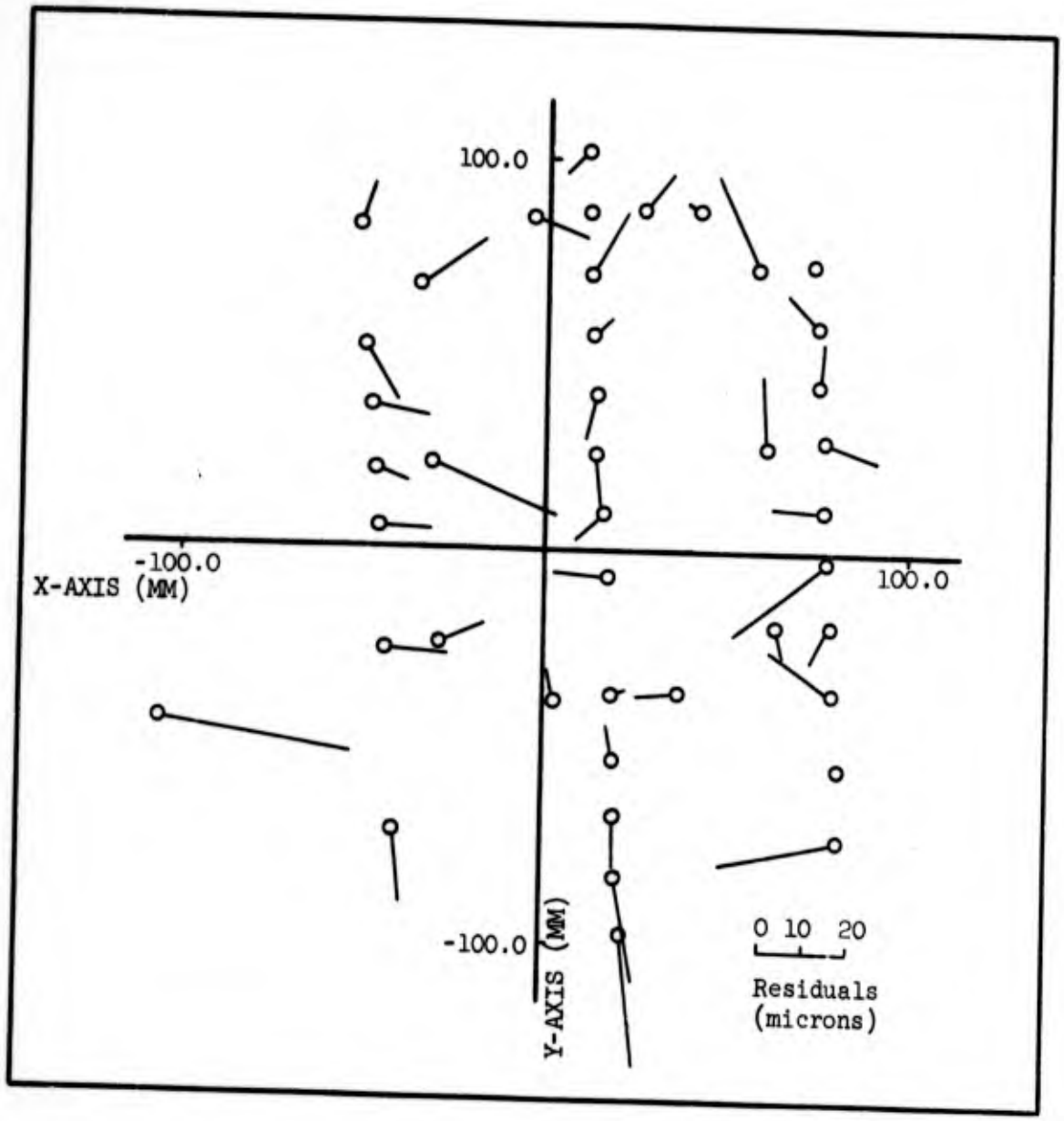

Figure 9. Photo Coordinate Residuals After SPR (Photo 2826).

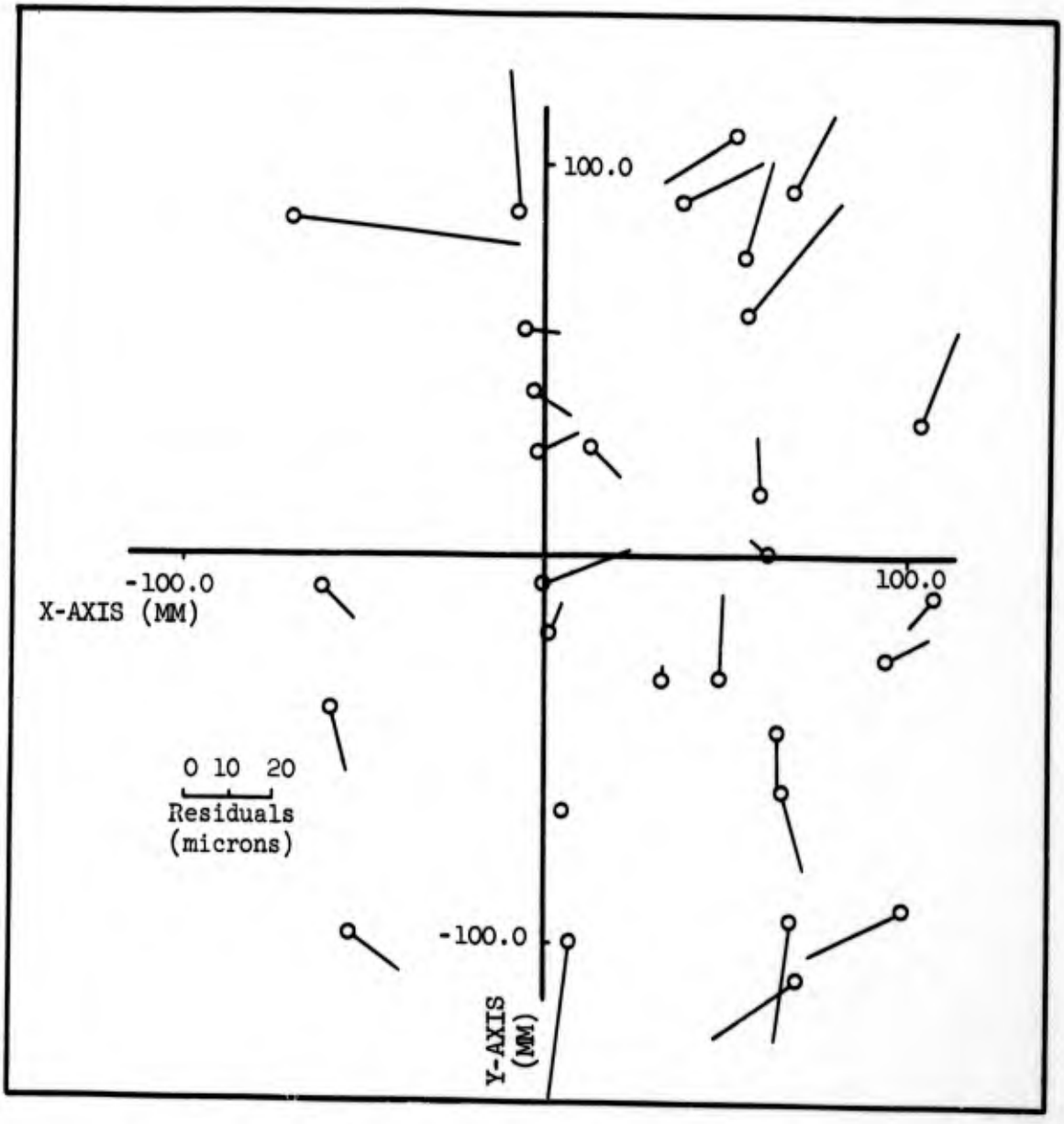

Figure 10. Photo Coordinate Residuals After SPR (Photo 2829).

2.2.3.1 Identification of Source of Error

The first step in location of the unusual systematic influence consisted of identifying the error as one of interior or exterior origin. The error was quite positively identified as one which was independent of the direction of flight. This is quite evident by comparison of residual plots for photo 2729 and the remaining photos. All exhibit the peculiar affine disturbance yet photo 2729 was exposed during a flight heading 90° from the other three and at the same altitude. It was concluded that the disturbance originated either within the camera or as a consequence of deformation of the photographic window. Since the window had been checked for quality according to military specification (refer to [Military Specification]) and was not subject to differential pressures, it was decided that the disturbance was caused by an element of interior orientation.

With the systematic disturbance identified as one of interior orientation, a vacuum failure was suspected. After some review of results, vacuum failure was discounted for the following reasons. The quality of the images of fiducials was excellent. This was substantiated by the fact that the standard deviation of the mean of three observations on a given fiducial was consistently less than two microns and nearly always less than one micron. Further, if vacuum failure were the cause of the disturbance, it would not be reasonable to expect consistency of the results from exposure to exposure as indicated in the plots of photo coordinate residuals. Accordingly, other sources of interior disturbance were studied.

The stability of the film was then considered. The ideal specifications for obtaining suitable photography required that the calibrated reseau be exposed in the camera simultaneously with the image of the photo control range. For practical reasons it was not possible to include the reseau within the camera. This would have provided the ideal control standard whereby film shrinkage could have been computed within acceptable limits. A compromise solution which appeared at the time to be satisfactory was required. The reseau was preflashed onto the unexposed film (Type 5401) and rerolled onto the film spool. This process was accomplished within the Base Photo Laboratory at R.A.D.C., Griffiss Air Force Base, New York. The temperature was maintained at 23°C plus or minus one degree during exposure and during the process of storage. The relative humidity during laboratory storage of the film within its closed container may be taken as 50 percent [Kodak, 1966]. Prior to flight the film was loaded into the magazine also at 23°C and installed in the camera located in the camera compartment of the B-57 aircraft. The camera body temperature was also approximately 23°C. The loading of the film into the magazine and aircraft was accomplished at about 08.30 on December 21, 1965. The camera compartment was then subject to temperature control but open to ambient pressure for the remainder of the photographic mission. Photography over the McClure, Ohio range was exposed at about 13:00 the same day [Flight Log, 1965]. Temperature within the camera during exposure over the range averaged 27°C [Flight Log, 1965]. No attempt was

made to measure the relative humidity during any portion of the photographic mission. With this as background, the influence of possible changes in relative humidity in the camera compartment from that which existed at the time the reseau was flashed on the film was investigated. From material supplied by Eastman Kodak [1966] regarding mechanical properties of rolled film subject to change in surrounding relative humidity it was discovered that indeed relative humidity could be responsible for the systematic disturbance of photo residuals. It is noted [Kodak, 1966] that the rate of moisture loss increases substantially with decrease in atmospheric pressure and also with decrease in winding tension. Two figures are reproduced in part below from the Kodak [1966] manual to indicate the nature of the influence on film dimensions as a result of relative humidity changes. Figure 11 indicates the changes in relative humidity of film completely stabilized initially at fifty percent relative humidity and at 70 degrees (F) (approximately 21°C). The film was then rolled and subjected to an external environment of five percent relative humidity still at 70 degrees (F). The changes in relative humidity across the width of film for various periods of time are remarkable non-linear. Note that these results refer only to widths of 70 mm. for film Type 8402 and Type 4401. Some variation may be expected for Type 5401 but the nature of the influence of relative humidity will be essentially the same.

Figure 12 indicates the dimensional changes that may be expected due to changes in relative humidity for film Type 5401, unprocessed, at 70 degrees (F). It may be noted that a change in relative humidity of only 14 percent from the stored or initial condition of 50 percent causes a dimensional changes of 0.1 percent. In terms of photo coordinates, the result for a uniform change in relative humidity at a point 100 millimeters from the principal point is a shift of the image equal to 100 microns. Quite evidently, the cause of the unexpected residuals after the SPR program could be explained by a change in humidity. It may be further noted that the unprocessed film exhibits a dimensional hysteresis. Beginning at a relative humidity of 5 percent and increasing to 80 percent, the film exhibits a certain dimensional change. However, as the relative humidity is gradually returned to 5 percent, the dimensional changes are somewhat different for any given relative humidity. That is, according to Calhoun and Leister [1959], the dimensions for any given relative humidity are dependent on the direction from which the humidity was approached. As an example, a point located at 100 millimeters from the origin would undergo a 25 micron dimensional shift even when the initial and final measurements were made at 50 percent relative humidity. This would result before and after the occurrence of a change from 50 percent to 55 percent and back to 50 percent relative humidity. These examples assume uniform changes of humidity across the total film width. From Figure 11 it is seen that some non-linear humidity conditions are to be expected. However, the magnitude of dimensional changes due only to a 14 percent change in relative humidity may be reduced to equal the magnitude of the disturbing photo coordinate residuals which are of concern here.

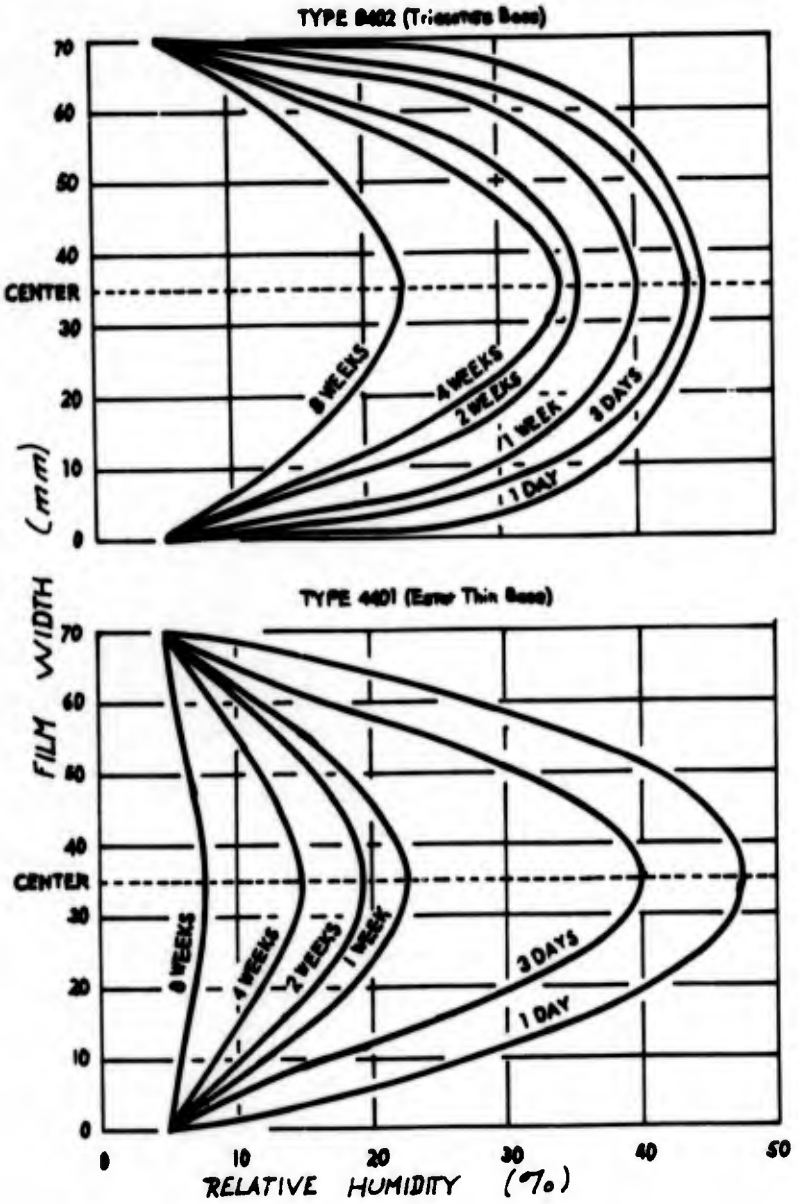

Figure 11. Typical Equivalent Relative Humidity Distribution of Roll Film [Kodak, 1966].

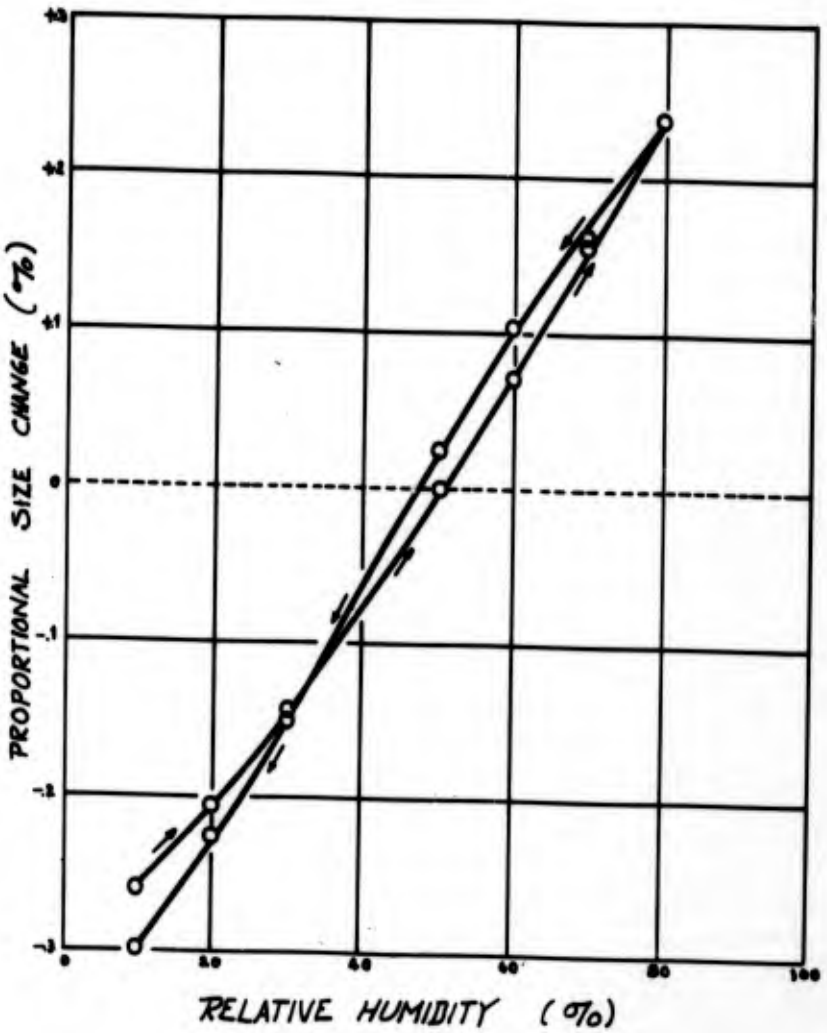

Figure 12. Typical Dimensional Hysteresis Loop for Unprocessed Film (type 5401) [Kodak, 1966].

In summary, it was evident that changes of perhaps 10 percent relative humidity between the laboratory exposure of the calibrated reseau and exposure in the camera could explain the unexpected photo coordinate residuals. The nature of the dimensional changes during a photo mission could be complicated by a series of independent factors: (1) variation of retive humidity with time, (2) variation of film winding tension, (3) acceleration of film humidity changes under reduced atmospheric pressure.

A detailed verification of the shrinkage due to change in relative humidity is not possible for the McClure photography. However, a comparison of scale coefficients as determined by reseau data and as determined by a direct comparison to calibrated fiducial separation indicates that substantial shrinkage did occur in the y-coordinate direction while little if any was experienced in the x direction. The shrinkage differences are direct measures of the overall photo shrinkage that occurred between the exposure of the reseau and of the photo within the camera. Table 12 indicates that an average scale difference of -24.6 parts per 100,000 exists in the y-coordinate direction. Only +4.2 parts per 100,000 exists in the x-coordinate direction.

The scale factors (K_x,K_y) were computed from:

$$K_x = \frac{\Delta F_x(\text{true})}{\Delta F_x(\text{observed})}$$

$$K_y = \frac{\Delta F_y(\text{true})}{\Delta F_y(\text{observed})}$$

where:

$\Delta F(\text{true})$ indicates the separation of the respective fiducial determined either from the calibrated reseau value or the initial camera calibration

$\Delta F(\text{observed})$ indicates the comparator value corrected for rotation and comparator calibration

These scale differences verify that an overall film shrinkage has occurred which is in agreement in character and magnitude with that which can be expected from moderate changes in relative humidity within the camera compartment.

TABLE XII. COMPARISON OF COORDINATE AXIS SCALE FACTORS DETERMINED BY A RESEAU STANDARD TO THAT DETERMINED BY A CALIBRATED FIDUCIAL STANDARD

Photo No.	Reseau Standard		Fiducial Standard		Scale Difference (Parts per 100,000)	
	K_x	K_y	K_x	K_y	ΔK_x^*	ΔK_y^*
2729	1.00062	1.00046	1.00053	1.00062	+9	-16
2822	1.00034	1.00008	1.00042	1.00038	-8	-30
2825	1.00071	1.00050	1.00066	1.00078	+5	-28
2826	1.00098	1.00072	1.00097	1.00100	+1	-28
2829	1.00076	1.00054	1.00062	1.00075	+14	-21

* $\Delta K = (K_{reseau} - K_{fiducial})/100{,}000.$

$\bar{\Delta K}_x = +4.2$ $\bar{\Delta K}_y = -24.6$

2.2.3.2 Scaling of y-Coordinate to Correct For Uncompensated Film Shrinkage

With the origin of the unexpected photo coordinate residuals identified, it was understood that no simple linear corrections would be adequate. In fact, the consequences on film dimensions of the influences of changing humidity, film spool tension and decreased atmospheric pressure would make any attempt to compute corrections for film distortions impractical. The question of film stress induced by shrinkage strains due to continuously varying humidity across the film width would further seriously complicate any attempt at complete shrinkage compensation.

However, a measure of the improvement of results offered even by a simple y-coordinate scaling was of interest. For this investigation, the MPR (multiple photo resection) was used first with photo coordinates corrected for shrinkage based only on the calibrated reseau. Then MPR was used with the same photo coordinates except with the y-coordinates scaled by the average difference of scale of -25 parts per 100,000 as computed above. By use of the MPR solution, the influence of lens distortion would be removed thereby accentuating the systematic errors attributed to film shrinkage caused by humidity changes. Unfortunately, some of the film shrinkage would also be compensated by the model for interior orientation. However, due to the magnitude of the disturbing shrinkages, this compensation was felt to be of secondary importance. Figures 13 through 16 indicate the nature of the photo coordinate residuals after simultaneous processing through the MPR program without alterations to the y-coordinate scale. As expected, the magnitude of the residuals is reduced as compared to the results of the SPR program since allowance is made for interior orientation. Two points exhibited extraordinarily large residuals in the results of the MPR program which were not apparent earlier. Points 0.011 on photo 2829 and point 0.010 on photo 2826 were investigated and rejected. The y-photo coordinates were then scaled by 1.000258 and the MPR program repeated. Figures 17 through 20 indicate the improvement of the rescaled solution over the previous solution in which only reseau controlled scaling was used.

The computed standard deviation for a typical residual before rescaling is $\pm$ 10 microns. After rescaling of the y-coordinates only, the typical residual standard deviation is computed as $\pm$ 8 microns. The typical residual standard deviation was computed as the square root of the product of the unit variance and the reciprocal of a typical photo coordinate weight. Based on the precision of coordinate observations made to this point in the camera calibration process it would be reasonable to expect that the residuals should be several microns smaller than those computed after y-rescaling in the MPR program. It is evident that the difference in residuals between the best result and the expected result could be explained by the uncompensated residual film shrinkages.

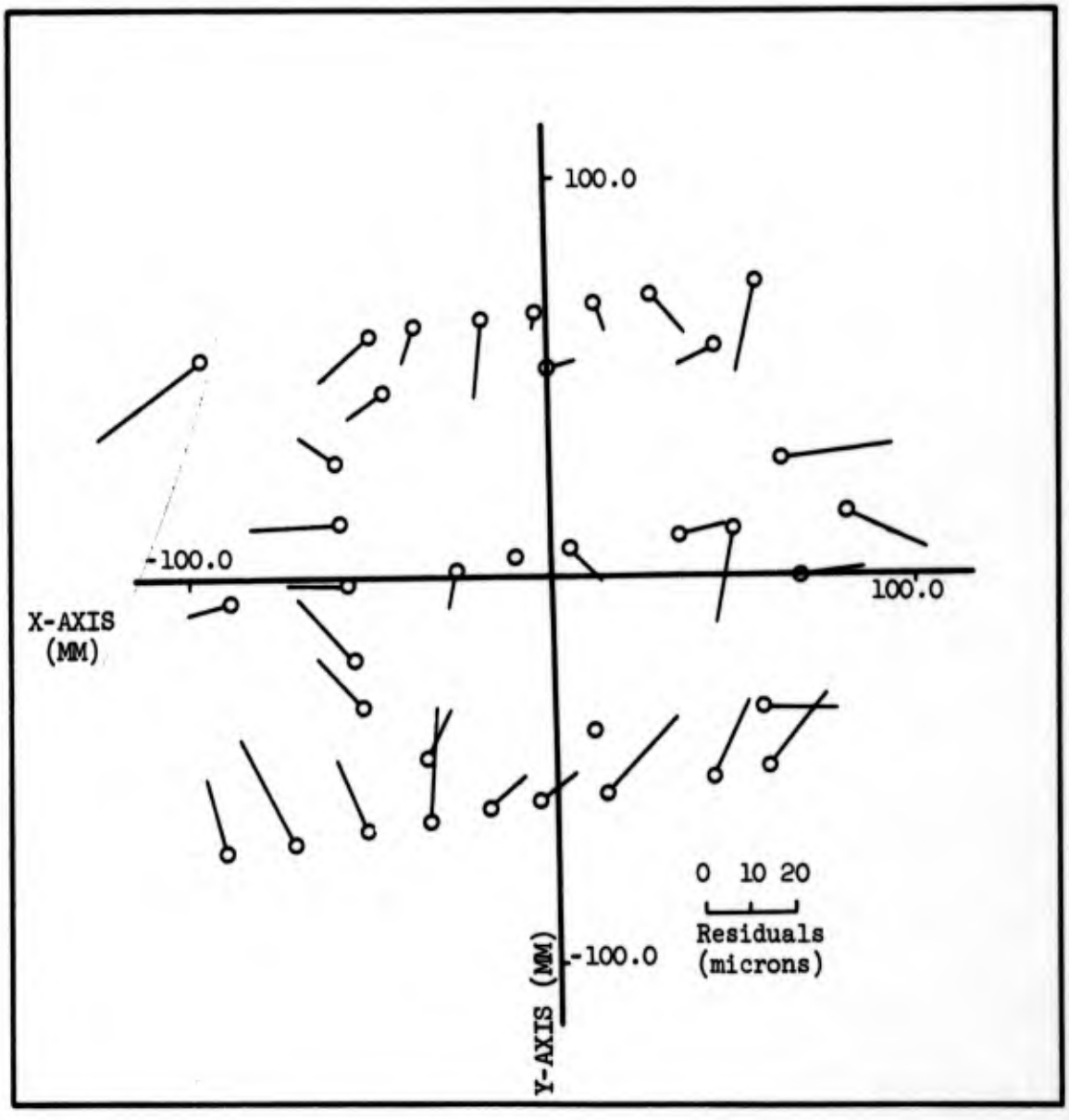

Figure 13. Photo Coordinate Residuals After MPR But Before y-Coordinate Corrective Scaling (Photo 2729).

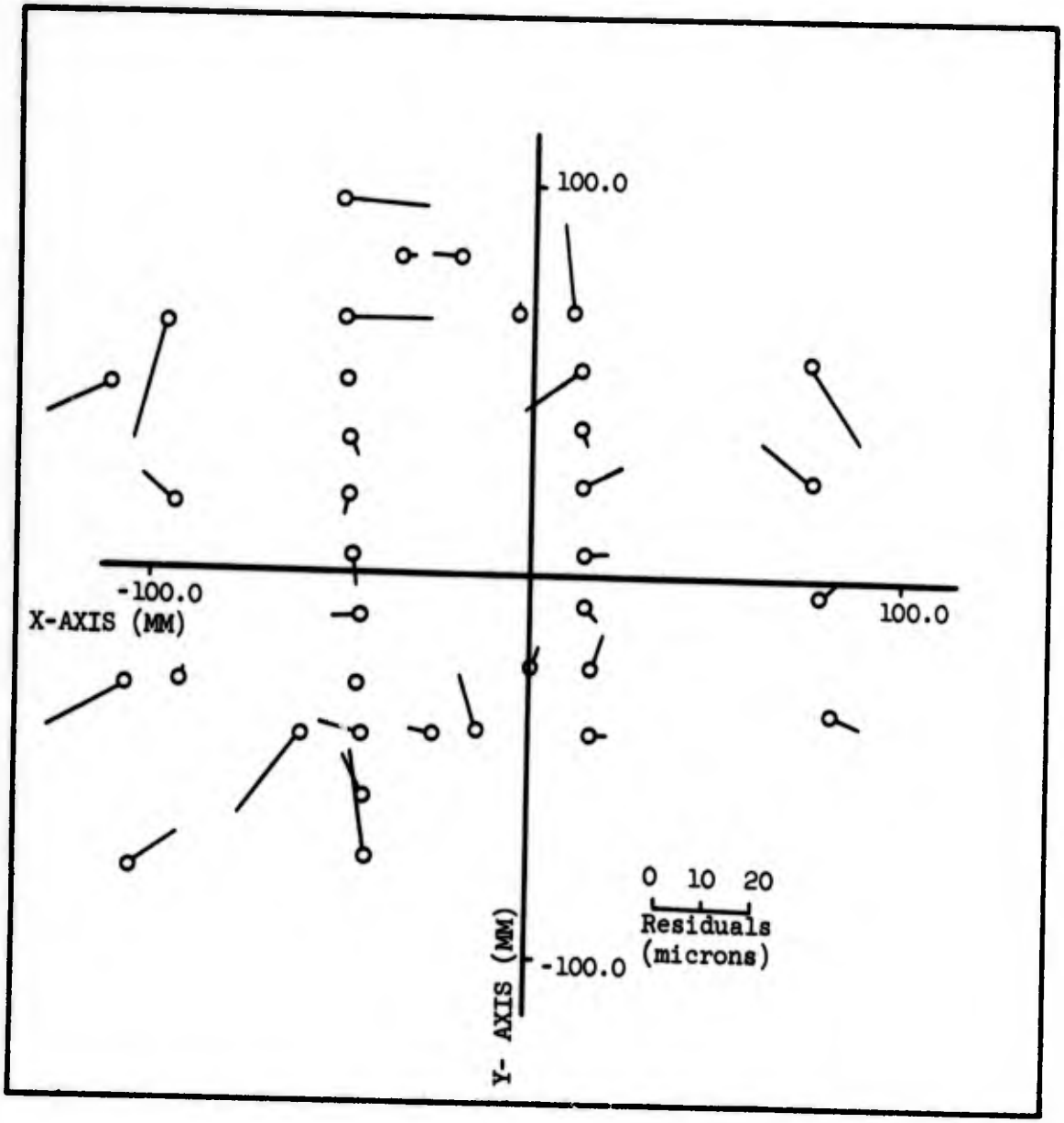

Figure 14. Photo Coordinate Residuals After MPR But Before y-Coordinate Corrective Scaling (Photo 2822).

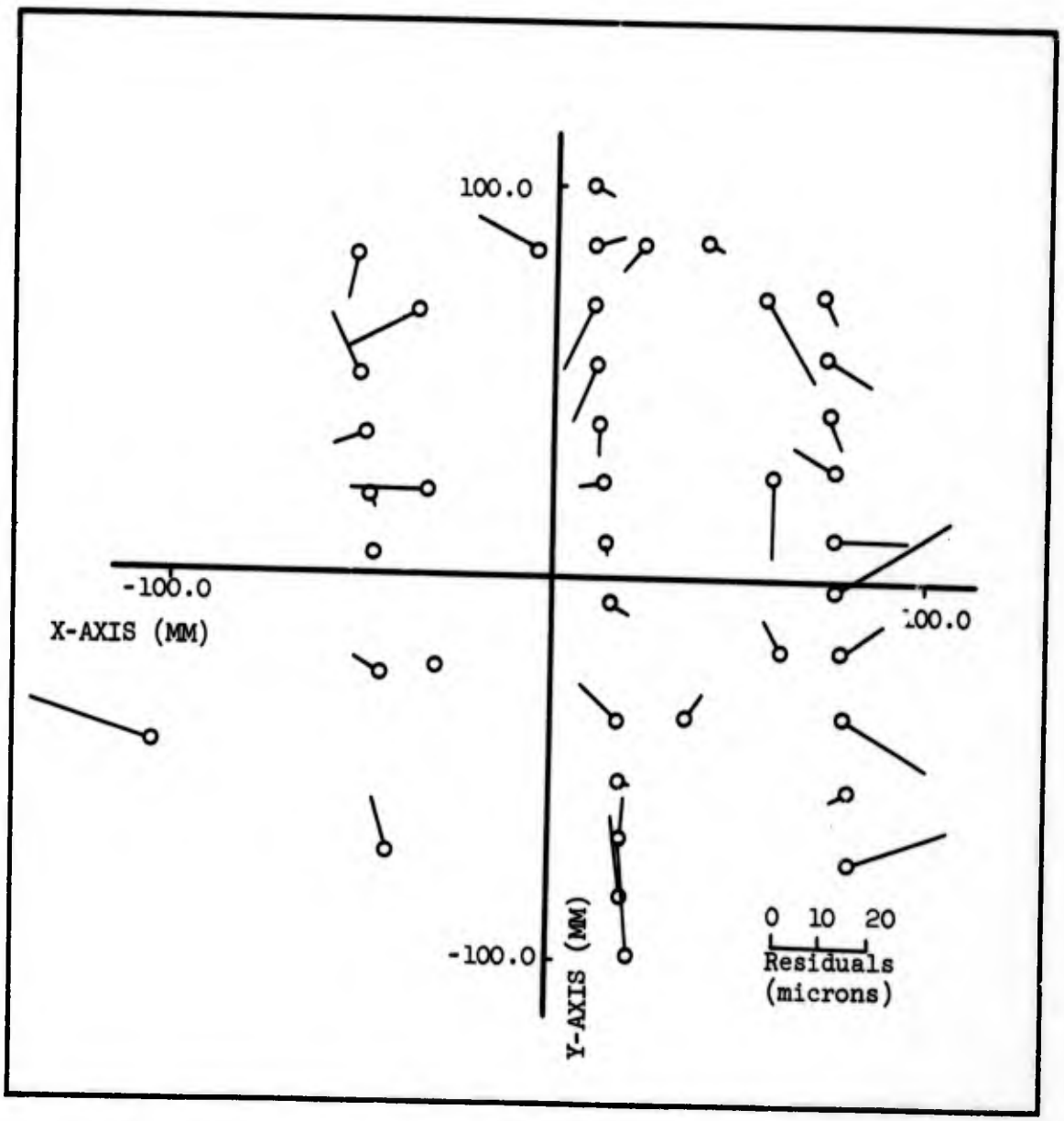

Figure 15. Photo Coordinate Residuals After MPR But Before y-Coordinate Corrective Scaling (Photo 2826).

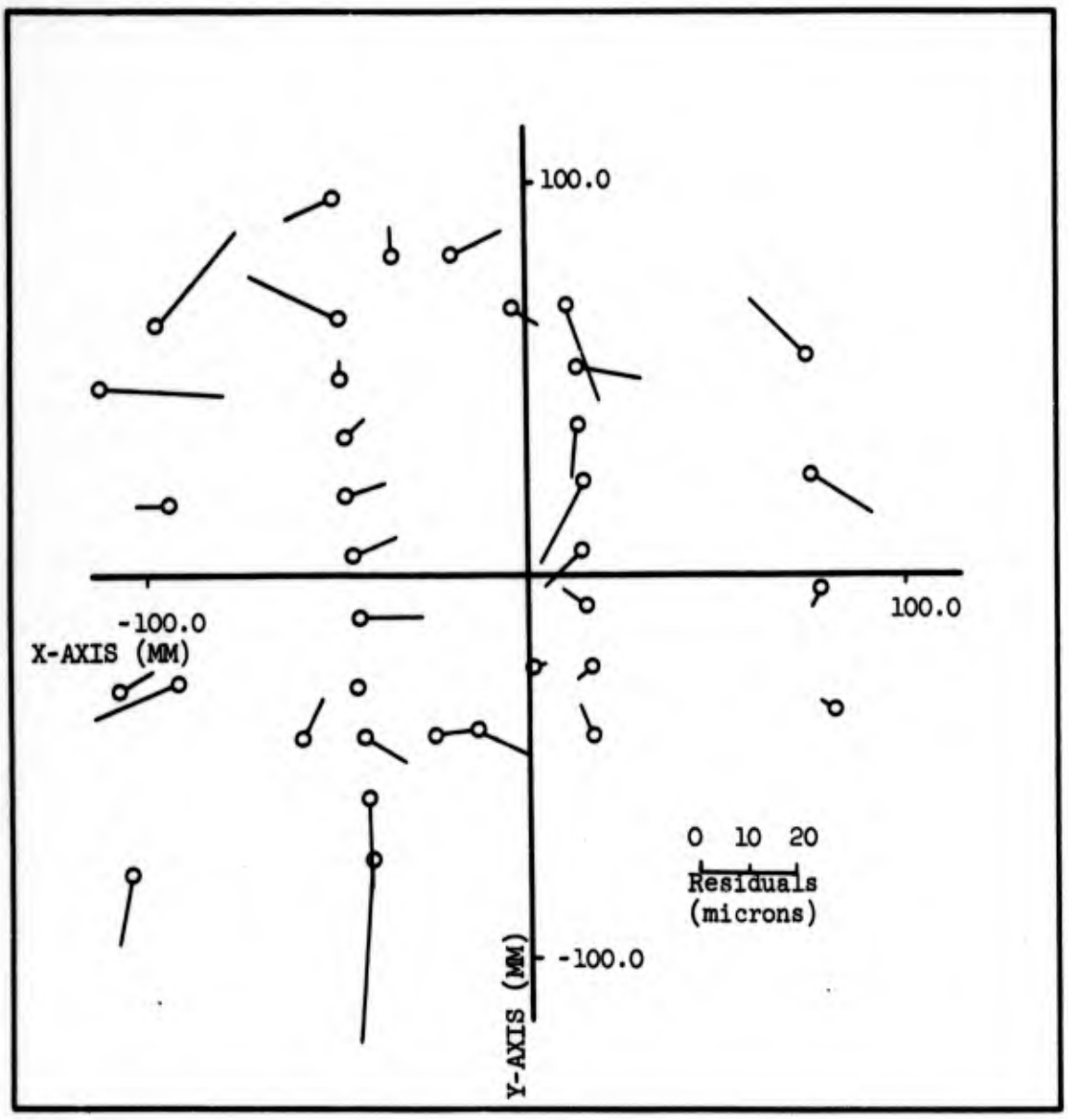

Figure 16. Photo Coordinate Residuals After MPR But Before y-Coordinate Corrective Scaling (Photo 2829).

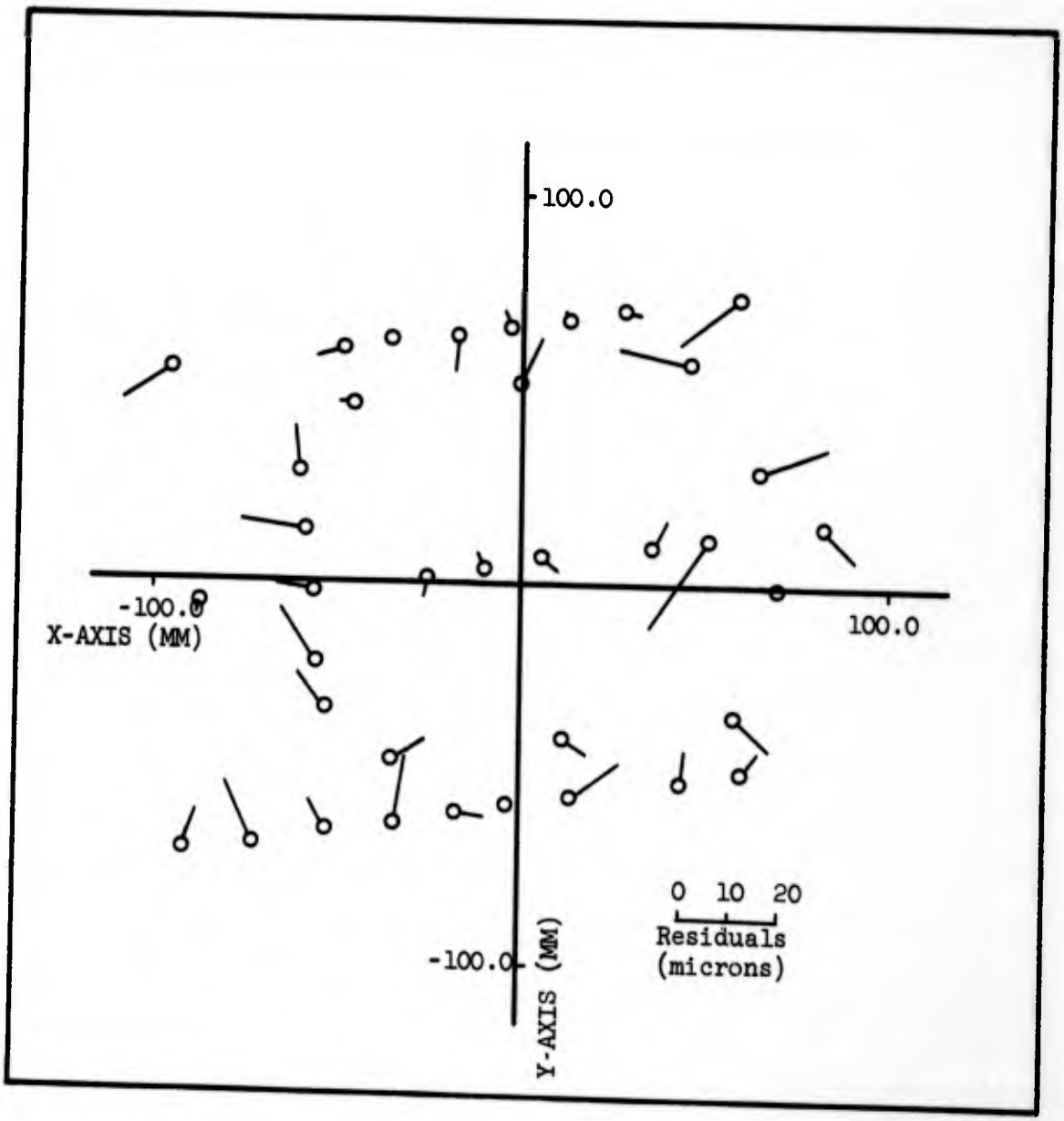

Figure 17. Photo Coordinate Residuals After Corrective Scaling and MPR (Photo 2729).

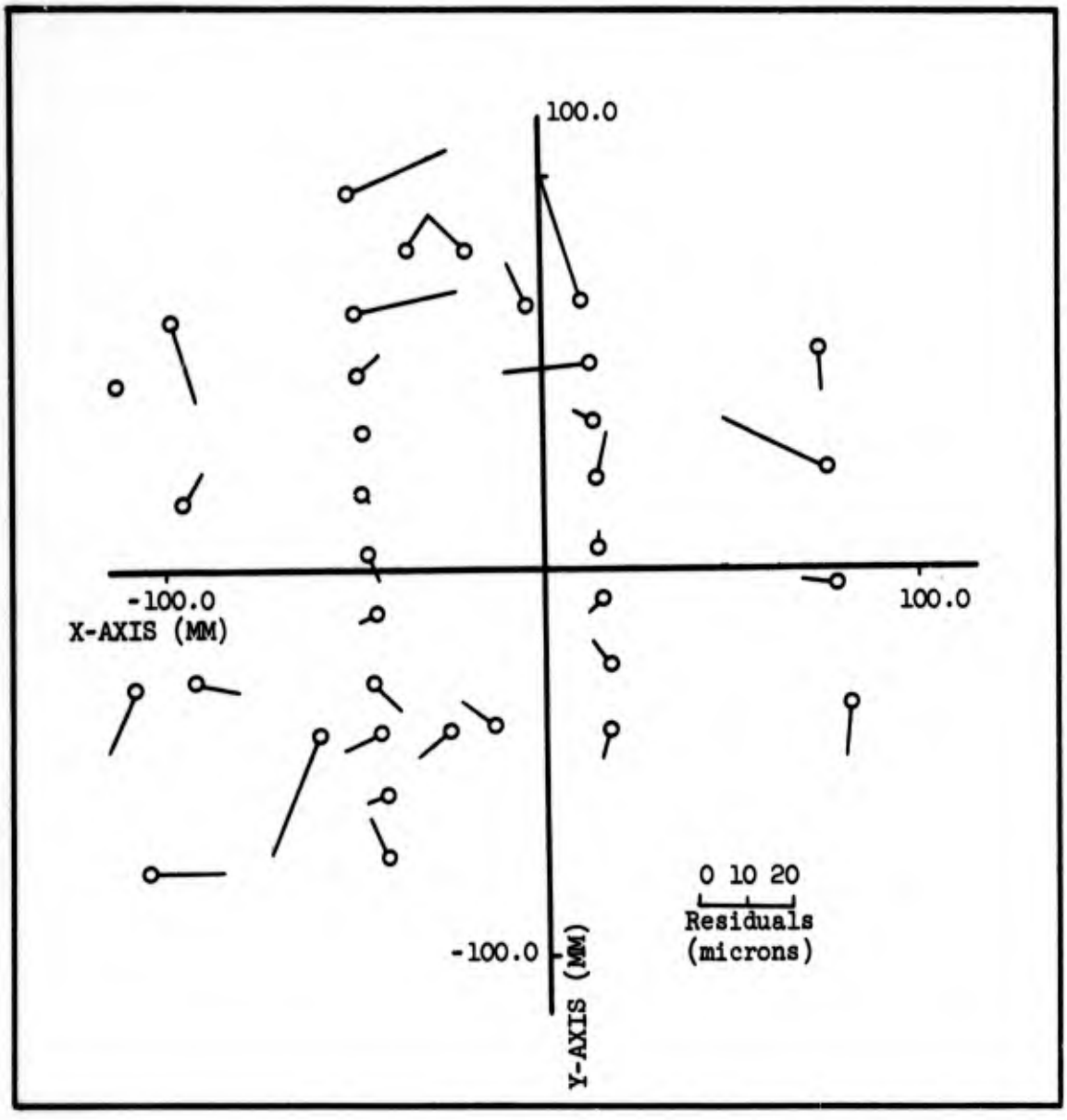

Figure 18. Photo Coordinate Residuals After Corrective Scaling and MPR (Photo 2822).

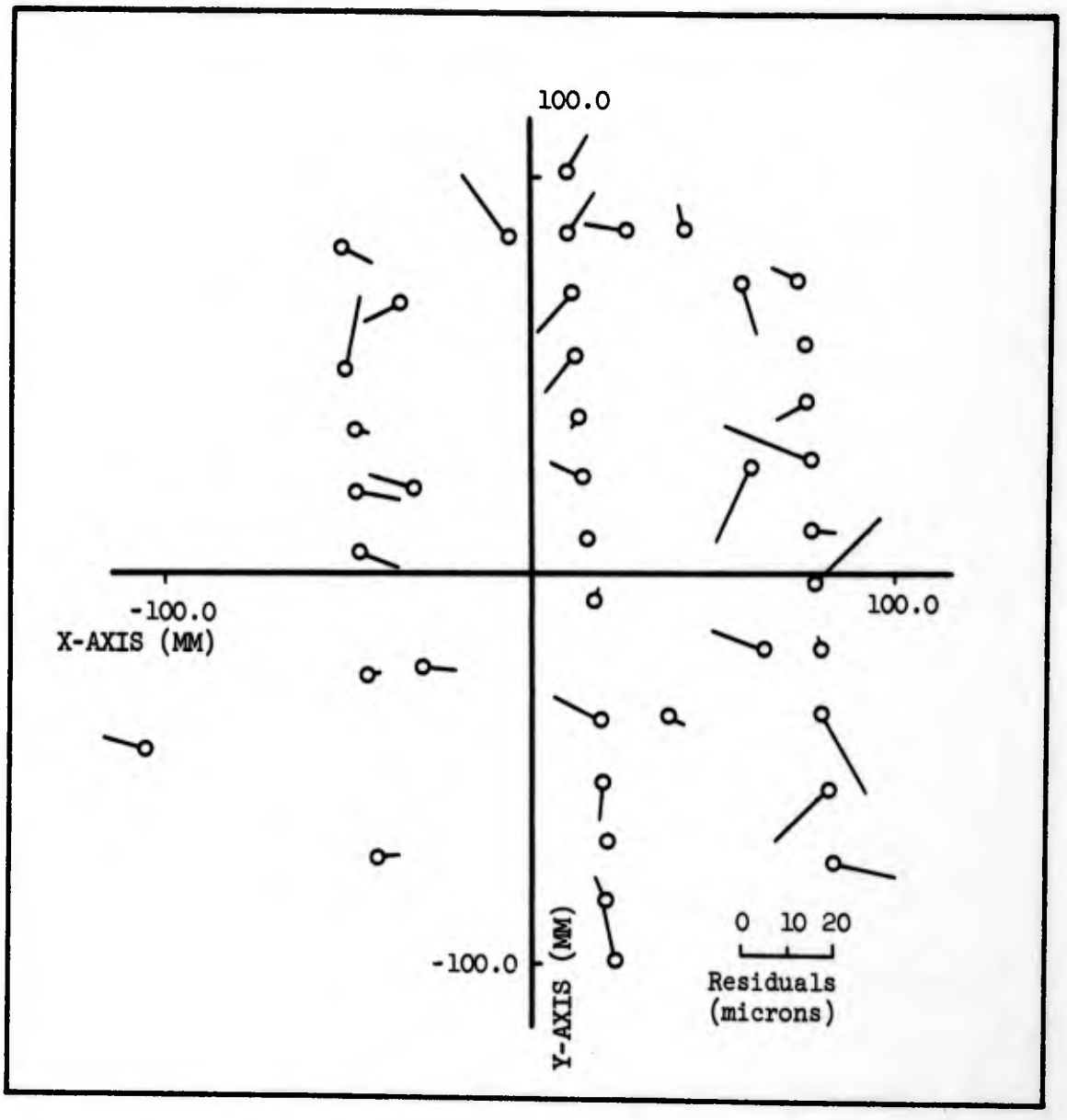

Figure 19. Photo Coordinate Residuals After Corrective Scaling and MPR (Photo 2826).

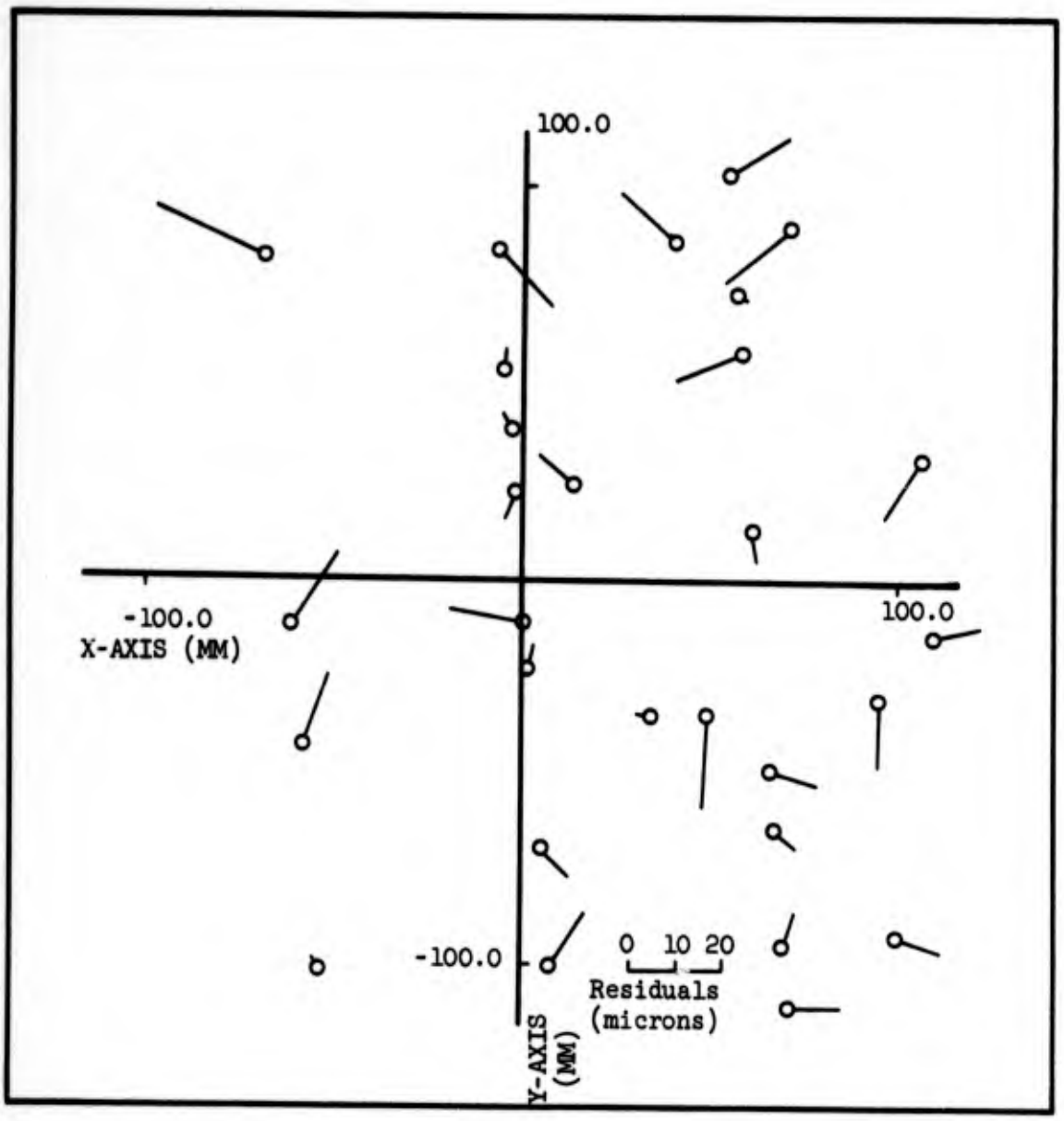

Figure 20. Photo Coordinate Residuals After Corrective Scaling and MPR (Photo 2829).

2.2.3.3 Alternate Solutions to the Problem of Operational Film Stability

A possible solution to the problem of film stability when used with conventional cartographic (precision) cameras subject to changes of humidity environment will be considered from two points of view. First, the problem as it applies to calibration photography will be considered. Consideration will then be given to the problem as it applies to operational photography.

The fundamental concept on which this study is based is that calibration processes shall metrically define the photographic system under circumstances as equal as possible to those anticipated operationally. The introduction of a glass plate substitute for the film would seriously mitigate the value of the calibration. Further, no modification of the camera to include a reseau within the plane of focus would be permitted for the same reasoning. Accordingly, what may be termed a "reseau bonnet" is suggested which will permit the control reseau to be pre-flashed (or post-flashed) on the film within six seconds from the instant of esposure in the camera itself. The term "bonnet" is used here to indicate that the device is positioned above the camera when in use. Reference is made to Figure 21 in which a schematic diagram of the reseau bonnet is presented. By means of air conditioning, the film supply and camera magazine would be maintained at 50 percent relative humidity; the value under which film is stored [Kodak, 1966]. Temperature would be stabilized to a value anticipated for the specific photographic system operationally. Film tension, although of less importance, could be measured and adjusted by means of a drag roller to equal that found in the operating camera. No special requirements exist for pressurization other than attempting to equal that found operationally within the system being calibrated. Note that for most precision camera types, no modification whatever is required to adapt the reseau bonnet. No significant load changes are introduced on the camera.

By means of the reseau bonnet as suggested above it is visualized that a given airborne photographic system will provide suitable photography for purposes of calibration. The photography would be exposed under conditions as close to those anticipated under normal operational conditions as predictions of temperature and relative humidity will permit.

The problem of film stability for routine operational photography does not appear to have been given the consideration warranted by its large systematic influence on the measured photo coordinates. Perhaps it was felt that little could be done to improve the overall photogrammetric system by careful film dimensional control since many other factors also introduced systematic errors. As an example, the assumption that laboratory calibrations on glass plate are metrically equivalent to the characteristics of the operational camera apparently introduces systematic errors of approximately the same magnitude. However, if the airborne photographic system calibration is to be exploited operationally, a practical refinement to achieve a higher degree of film dimensional stability or at least con-

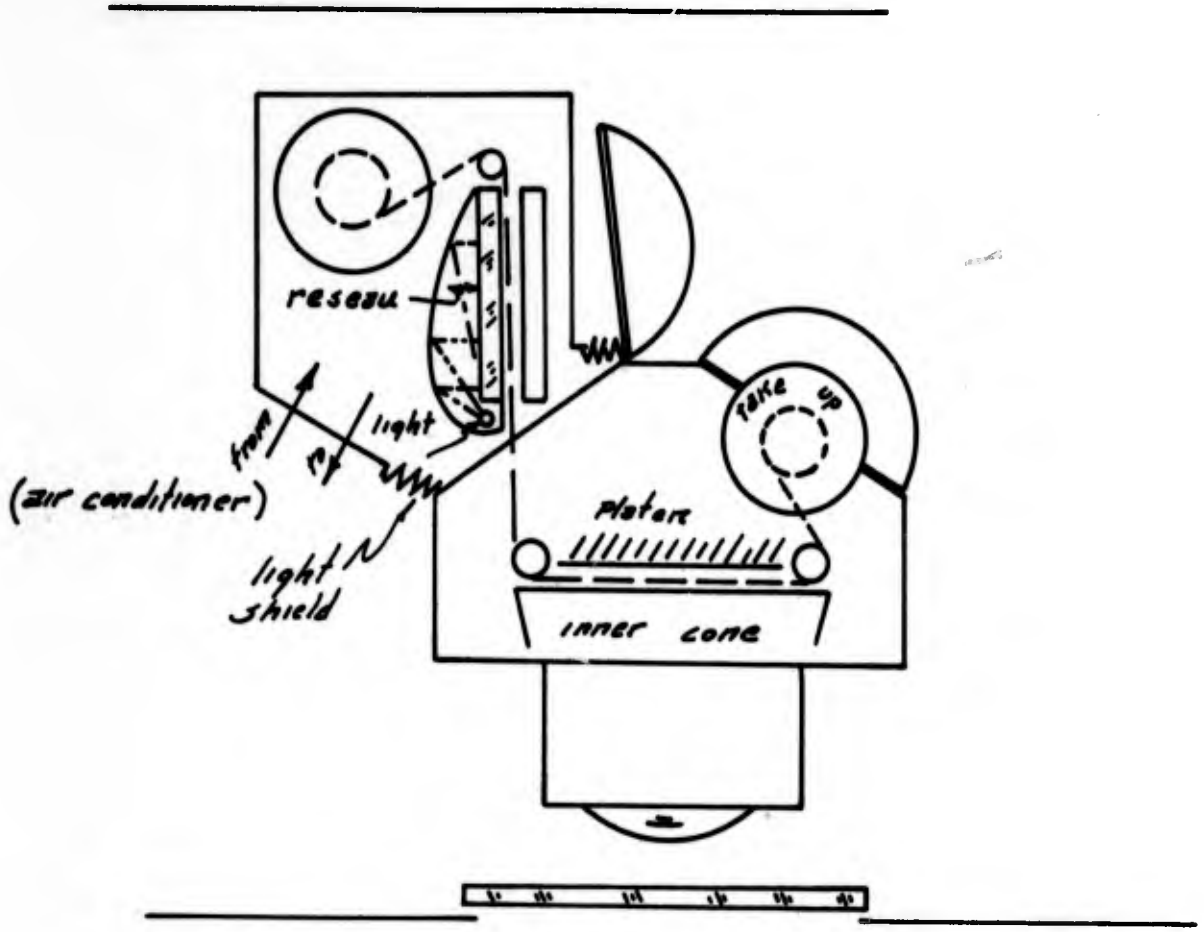

Figure 21. Reseau Bonnet

trol must be employed. If the aircraft normally stabilizes temperature to room temperature (21°C), then it remains to stabilize the camera compartment to the relative humidity under which the film was stored; that is, 50 percent relative humidity [Kodak, 1966]. Care must be taken to not permit the film to depart from these conditions for any appreciable length of time for a period of perhaps three months prior to exposure. This will reasonably assure a uniform moisture content across the width of the rolled film. If such a period of preconditioning is not practical for a film roll, special handling of unspooled film would also be satisfactory from the point of view of dimensional stability.

In the event the camera compartment is not stabilized to 21°C, an estimate of the expected operational temperature should be made and the film spool temperature soaked at that value for several days [Kodak, 1966]. Under these circumstances however, the relative humidity of the stored film (sealed in a storage container) will change according to a predictable amount. Three months of storage at the predicted temperature and induced relative humidity will then be required unless special handling by unspooling the film in the new humidity environment is undertaken. A stabilization of the camera compartment to the predicted film storage relative humidity is then required.

Any attempt to expose photography under conditions in which no relative humidity stabilization to an appropriate value is accomplished must be subject to doubt concerning the dimensional fidelity of the photography. Relative dimensional disturbances as large as 0.2 percent can reasonably be expected due to the non-linear moisture content of the film alone. It appears that serious camera system calibration in which film is used should not be undertaken without stabilization of relative humidity within the camera body and magazine.

Other factors may seriously influence the stability of film. The amount of tension introduced to the film during the drying period after photographic processing influences the longitudinal film stability. However, the result would be substantially linear and consequently of a less damaging nature. Kodak [section 9, p. 26, Figure 9-8, 1966] indicates that approximately 2.2 pounds per linear inch of width applied as tension during the drying period will stretch the film by 0.10 percent. It is suggested that care be taken during all phases of photographic processing to employ the minimum required tension under prevailing circumstances and that the tension be maintained at a constant level.

The dimensional hysteresis due to change in relative humidity could introduce dangerous dimensional disturbances if the film were subjected to only a 10 percent change in relative humidity for perhaps a week prior to processing [Kodak, 1966, section 9, p. 22, Figure 9-4]. The influence of the hysteresis after exposure could reasonably result in 0.025 percent relative dimensional change and would be of non-linear nature across the film width.

In summary, calibration photography should ideally be made on photography subject to a relative humidity environment of 50 percent, and a temperature environment of 21°C. Both should be maintained without interruption for a period of several months prior to exposure and during exposure. Reseau control should be exposed onto the film as nearly simultaneously with exposure of the ground control imagery as is permitted without camera modification. This will provide further assurance that the small changes in relative humidity and temperature that will occur under even controlled conditions will not unduly disturb the calibration. Finally, film tension should be minimized during the processing period and applied uniformly throughout.

2.3 Supression of High Correlation Between Camera Constant and Object Distance

In an operational or field calibration of an aerial photographic system, a question arises concerning the strong geometric correlation that exists between the camera constant (c) and the flying height (object distance). In the usual projection equations relating photo and survey coordinates through elements of interior and exterior orientation, the ratio of camera constant to flying height above a ground target tends to be constant, that is, the correlation between these two factors approaches unity. In the event that the survey control field is a plane , the consequence of using an erroneous camera constant for vertical photography will be fully off set by use of an appropriate flying height. For the case in which the survey control field contains a third dimension, the compensation afforded by the use of an appropriate flying height can be only approximate. Cameras intended for use over mountainous terrain should be calibrated with particular attention to this question. The following discussions pertain to possible solutions for the camera constant under circumstances that closely simulate those expected operationally.

The direct approach would consist of directly observing either the calibrated focal length or the camera station elevation coordinate. The usual approach is to determine the calibrated focal length as part of a conventional laboratory calibration; however, this defeats the purpose of the airborne system calibration. The independent observation of the camera station elevation conceivably could be accomplished by such means as use of a radio altimeter operating over a lake, or by space intersection using simultaneous tracking either by cine-theodolite or directly by theodolite. It is felt that none of these methods offer assurance that the necessary spatial coordinate accuracies would be achieved. The use of three or more ballistic cameras employing a star field background for control would probably achieve sufficient accuracy and esti ates of reliability; however, the night operations require that the photo control zone be provided with illuminated targets thereby introducing undersirable artificial circumstances. Synchronization between the aerial and ballistic camera exposures would be required. The ballistic camera appears to be an excessively expensive and unrealistic approach.

The tilting of the camera through some appreciable angle for at least one of several calibration photos followed by a common adjustment in which all photos are used does not suppress the correlation of focal length satisfactorily unless the horizontal coordinates of the camera are observed in some manner. As a result, the large correlation factor between focal length and elevation in the vertical case, becomes equally large with respect to the direction defined by the extension of the camera's optical axis. Since this direction (the direction of the extension of the optical axis) is defined in terms of the horizontal as well as vertical coordinates of the photo station and since the horizontal coordinates are also unknown, the unfortunate correlation remains.

The method investigated here for development and subsequent application is a variation on the well known method for indirect measurement of the principal distance of a stereo plotter projector. Rather than observing the height of the camera directly, the difference of target height is measured. This difference may be related functionally to the principal distance. In general, this suggests that a target field in which there is substantial elevation difference between targets would provide the solution required necessary to suppress the correlation. A similar suggestion was made by Hallert regarding the possibility of using relief in the control field [Hallert, 1965].

Preliminary investigations indicate that correlation remains strong between focal length and elevation coordinate of the camera even when using the most extreme elevation differences under combinations of selected target locations. Computations using six to nine target points selected for best strength of solution, at height differences ranging up to one half the flying height have indicated that the correlation factor between focal length and camera station elevation still ranged from 0.934 to 0.988. It is apparent that a moderately weak suppression of the correlation is achieved by providing depth in the control field when the usual resection equations extended to include elements of interior orientation are employed. A geometrically stronger solution is desirable.

The plotter projector calibration equations mentioned above provide an interesting alternate concept for an approach. They may be modified to express the observed photo coordinates as a function of focal length, target height differences and horizontal coordinates of the camera station. For photography taken close to a vertical orientation, these equations are independent of photo station elevation. In the following paragraphs an approach to correlation elimination based on control field depth is suggested, derived and, studied by means of artificial data. The development assumes that the photo coordinates are free from systematic errors due to film shrinkage and atmospheric refraction.

2.3.1 A Method for Elimination of Correlation Between Flying Height and Focal Length

This method makes use of a series of paired control points selected such that a marked difference in elevation exists between them. Figure 22

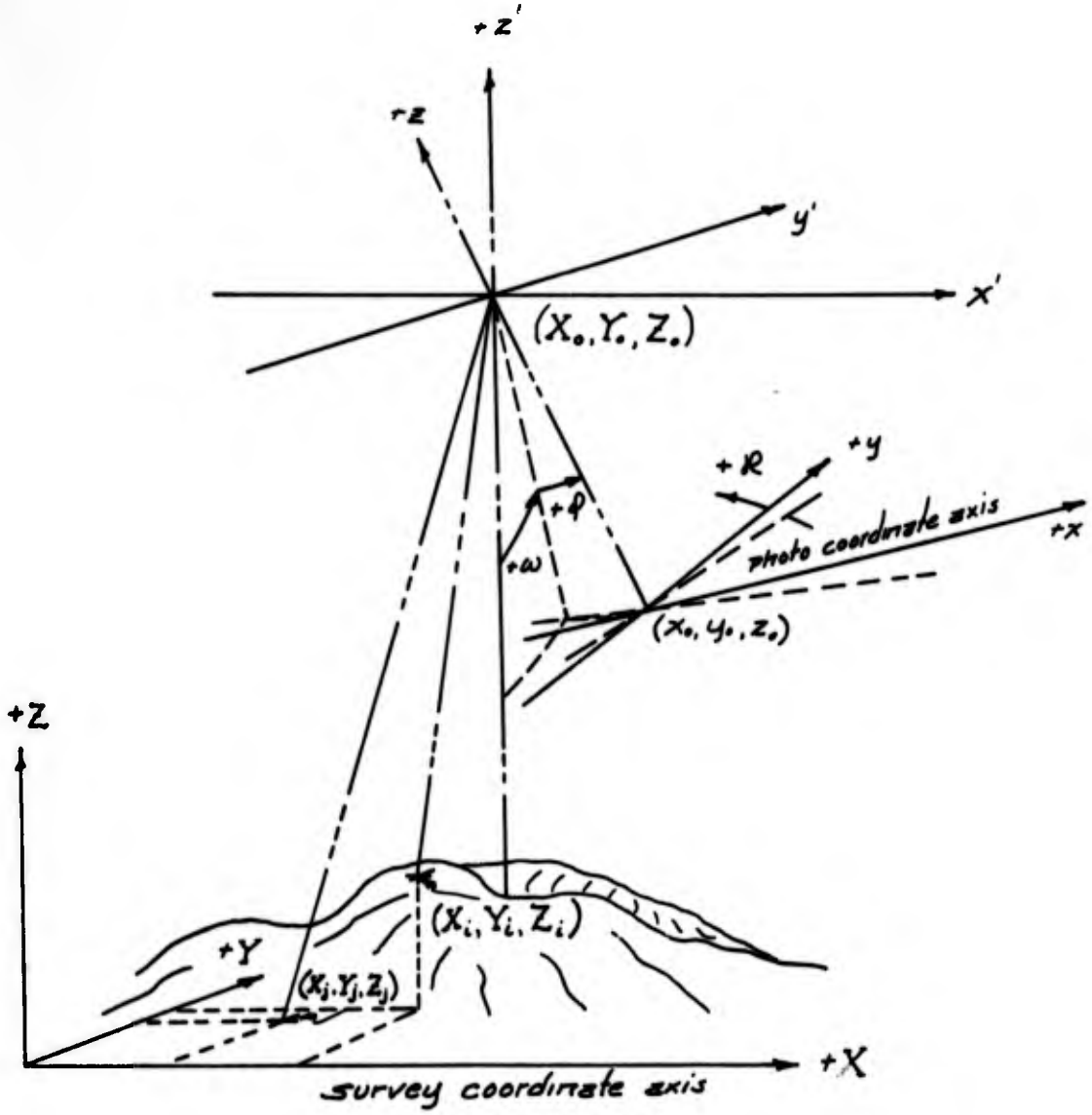

Figure 22. Relations Between Photo and Survey Coordinates.

indicates the relationships between paired ground control points used during this development.

The (x', y', z') coordinate system is defined as that system which is parallel to the survey system of coordinates (X,Y,Z) but with its origin at the exposure station. The photo coordinate system (x, y, z) is defined as a right handed rectangular system whose axis are rotated sequentially from the (x', y', z') system beginning with a rotation about the (x') axis (ω) followed by a rotation (ϕ) about the displaced (y') axis, and finally by a rotation (κ) about the twice rotated (z') axis. The origin of the photo coordinate system is then displaced a distance from the exposure station equal to the focal length (c) measured in a negative (z) direction.

Beginning with these as difinitions, the derivation of the equations relating photo coordinates to paired survey coordinates independent of flying neight may begin. First, by proportionality:

$$\frac{x'_i}{z'_i} = \frac{X_i - X_o}{Z_i - Z_o} \quad \text{and} \quad \frac{y'_i}{z'_i} = \frac{Y_i - Y_o}{Z_i - Z_o}$$

also:

$$\frac{x'_j}{z'_j} = \frac{X_j - X_o}{Z_j - Z_o} \quad \text{and} \quad \frac{y'_j}{z'_j} = \frac{Y_j - Y_o}{Z_j - Z_o}$$

The immediate task is to eliminate the elevation coordinate of the exposure station (Z_o) from the above equations. By writing each expression such that (Z_o) is the dependent variable and then subtracting, two equations free of (Z_o) will result. After some development, the equations may be written with the equivalent vertical coordinates as the dependent variable. The basic relationships are then:

$$x'_i = \frac{(X_i - X_o)\, z'_i}{Z_i - Z_j + \frac{z'_i}{x'_j}(X_j - X_o)}$$

$$y'_i = \frac{(Y_i - Y_o)\, z'_i}{Z_i - Z_j + \frac{z'_i}{y'_j}(Y_j - Y_o)}$$

These equations are free from the (Z_o) term but assume verticality. To transform the (x', y', z') system into the photo coordinate system, use is made of the rotational matrix suggested in section 2.1.3. Since the development at hand is novel, a more complete derivation of the relationships will be presented in this section. It is assumed that beginning from the (x', y', z') system and with reference to Figure 22, the primary rotation is (ω), the secondary is (ϕ) and the tertiary rotation is (κ). This may be expressed as in section 2.1.3 as:

$$\begin{bmatrix} x \\ y \\ -c \end{bmatrix} = M \begin{bmatrix} x' \\ y' \\ z' \end{bmatrix}$$

The rotational matrix (M) was determined from the ordered product of three orthogonal independent rotation matrices. Accordingly, (M) is also orthogonal permitting the following equality:

$$M^{-1} = M^{T} = T$$

That is, the inverse of the orthogonal rotation matrix is equal to its transpose and will be denoted by the symbol (T). The equivalent vertical coordinates (x', y', z') may be expressed in terms of photo coordinates by:

$$\begin{bmatrix} x' \\ y' \\ z' \end{bmatrix} = T \begin{bmatrix} x \\ y \\ -c \end{bmatrix}$$

Assuming a right handed coordinate system and right handed rotations, and according to the conventional practice of matrix subscript notation, the elements of (T) are:

$$T11 = \cos\phi \cos\kappa$$

$$T21 = -\cos\omega \sin\kappa + \sin\omega \sin\phi \cos\kappa$$

$$T31 = \sin\omega \sin\kappa + \cos\omega \sin\phi \cos\kappa$$

$$T12 = \cos\phi \sin\kappa$$

$$T22 = \cos\phi \sin\kappa$$

$$T32 = -\sin\omega \cos\kappa + \cos\omega \sin\phi \sin\kappa$$

$$T13 = -\sin \phi$$

$$T23 = \sin \omega \cos \phi$$

$$T33 = \cos \omega \cos \phi$$

Assuming Brown's model for expressing the objective lens distortion as described in section 2.1.4, the photo coordinates are modified.

$$x = (1 + K1\, r^2 + K2\, r^4 + K3\, r^6)(\bar{x} - x_o) - (J1\, r_2^2 + J2\, r^4) \sin \phi_o$$

$$y = (1 + K1\, r^2 + K2\, r^4 + K3\, r^6)(\bar{y} - y_o) + (J1\, r^2 + J2\, r^4) \cos \phi_o$$

In abbreviated notation, the corrected photo coordinates are:

$$x = K(\bar{x} - x_o) - J \sin \phi_o$$

$$y = K(\bar{y} - y_o) + J \cos \phi_o$$

where:

(x,y) = corrected photo coordinates

$(\bar{x},\bar{y})$ = photo coordinates subject to objective distortion

(x_o,y_o) = coordinates of principal point in a fiducial center system

$$K = 1 + K1\, r^2 + K2\, r^4 + K3\, r^6$$

$$J = J1\, r^2 + J2\, r^4$$

ϕ_o = angle between $\bar{x}$ axis and direction of maximum tangential distortion

After substitution, the expanded basic relationships using the above abbreviated notations become:

$$\bar{x}_i = x_o + \frac{1}{K}\left\{\frac{1}{T11}\left[\frac{(X_i - X_o)(x_i\ T31 + y_i\ T32 - c\ T33)}{z_i - z_j + (X_j - X_o)\left[\frac{x_j\ T31 + y_j\ T32 - c\ T33}{x_j\ T11 + y_j\ T12 - c\ T13}\right]} - y_i\ T12 + c\ T13\right] + J \sin \phi_o\right\}$$

$$\bar{y}_i = y_o + \frac{1}{K}\left\{\frac{1}{T22}\left[\frac{(Y_i - Y_o)(x_i\ T31 + y_i\ T32 - c\ T33)}{z_i - z_j + (Y_j - Y_o)\left[\frac{x_j\ T31 + y_j\ T32 - c\ T33}{x_j\ T21 + y_j\ T22 - c\ T23}\right]} - x_i\ T21 + c\ T23\right] - J \cos \phi_o\right\}$$

2.3.2 Correlation Elimination Resection

The Correlation Elimination Resection (CER) computation is intended to provide values of adjusted parameters including the camera constant. Use is made of the equations developed in section 2.3.1 which relate photo and survey coordinates independent of the camera station elevation. Although no real data were available to investigate characteristics of the CER computation, a limited study of the behavior of this method was undertaken by means of artificial data.

2.3.2.1 Verification of CER Computation

For purposes of adjustment computation, the equations developed in Section 2.3.1 were used to derive the observation equations. The usual process of arranging the observations as linear functions of the parameters by means of the first two terms of the Taylor's Series was employed requiring lengthy partial differentiation. In the interest of brevity, this work is not included here. However, the derivations were checked and verified by means of artificially generated data. Table 13 indicates the photo coordinate residuals after adjustment. These results serve to verify the derivations employed by the CER adjustment computation.

2.3.2.2 Geometric Strength of CER Computation

By means of artificially determined data, several combinations of control field depth and numbers of survey control points were used in the CER computation. Figure 23 indicates a representative pairing of high and low control. In all cases there were used four widely separated pairs of points in which the high and low points had the same horizontal positions. The remaining control was paired so that the high points occupied substantially different horizontal positions. This procedure provides a logical pattern within which the various combinations of control could be studied. All solutions were run assuming a photo coordinate error of $\pm$ 5 microns due to all unmodeled error sources. The weight number corresponding to the camera constant and the camera constant's standard error for the various combinations tested is presented in Tables 14 and 15. The term ($\Delta h/\Delta H$) denotes the ratio of the control field depth (Δh) to the height of the camera station above the low control (ΔH).

TABLE XIII. RESULTS OF THE ADJUSTMENT BY THE CER COMPUTATION
(ERRORLESS DATA)
X WT, Y WT = RECIPROCAL OF THE RESPECTIVE PHOTO COORDINATE OBSERVATIONAL VARIANCE.

POINT NO	X(MM)	Y(MM)	X WT	Y WT	X RESID(MM)	Y RESID(MM)
11.0000	-75.5753	100.7729	0.144E 05	0.334E 05	0.302E-03	0.330E-03
12.0000	-37.7520	151.0363	0.256E 05	0.662E 04	-0.238E-03	-0.570E-03
54.0000	25.1886	-100.7402	0.335E 05	0.334E 05	-0.398E-03	0.100E-04
14.0000	37.7671	151.0363	0.651E 04	0.653E 04	0.917E-03	0.180E-03
15.0000	75.5860	100.7729	0.360E 05	0.223E 05	0.921E-03	0.250E-03
21.0000	-150.7987	75.4016	0.396E 04	0.177E 05	0.269E-02	-0.220E-03
45.0000	100.7607	-50.3792	0.297E 05	0.381E 05	-0.560E-03	0.458E-03
51.0000	-112.5561	-150.0901	0.104E 05	0.189E 04	-0.108E-02	-0.212E-02
22.0000	-50.3407	50.3421	0.367E 05	0.381E 05	-0.557E-03	-0.525E-03
55.0000	112.5751	-150.0895	0.334E 04	0.195E 04	-0.181E-02	-0.240E-02
24.0000	50.3444	50.3421	0.334E 05	0.333E 05	-0.151E-02	0.940E-04
44.0000	75.5630	-75.5599	0.655E 04	0.673E 04	0.342E-02	0.185E-03
41.0000	-100.7518	-50.3792	0.334E 05	0.335E 05	-0.180E-03	0.890E-04
25.0000	150.8153	75.4014	0.669E 04	0.649E 04	-0.220E-03	0.219E-03
52.0000	-25.1810	-100.7402	0.381E 05	0.223E 05	0.200E-05	-0.140E-03
42.0000	-75.5550	-75.5599	0.192E 04	0.176E 05	-0.270E-04	0.104E-03

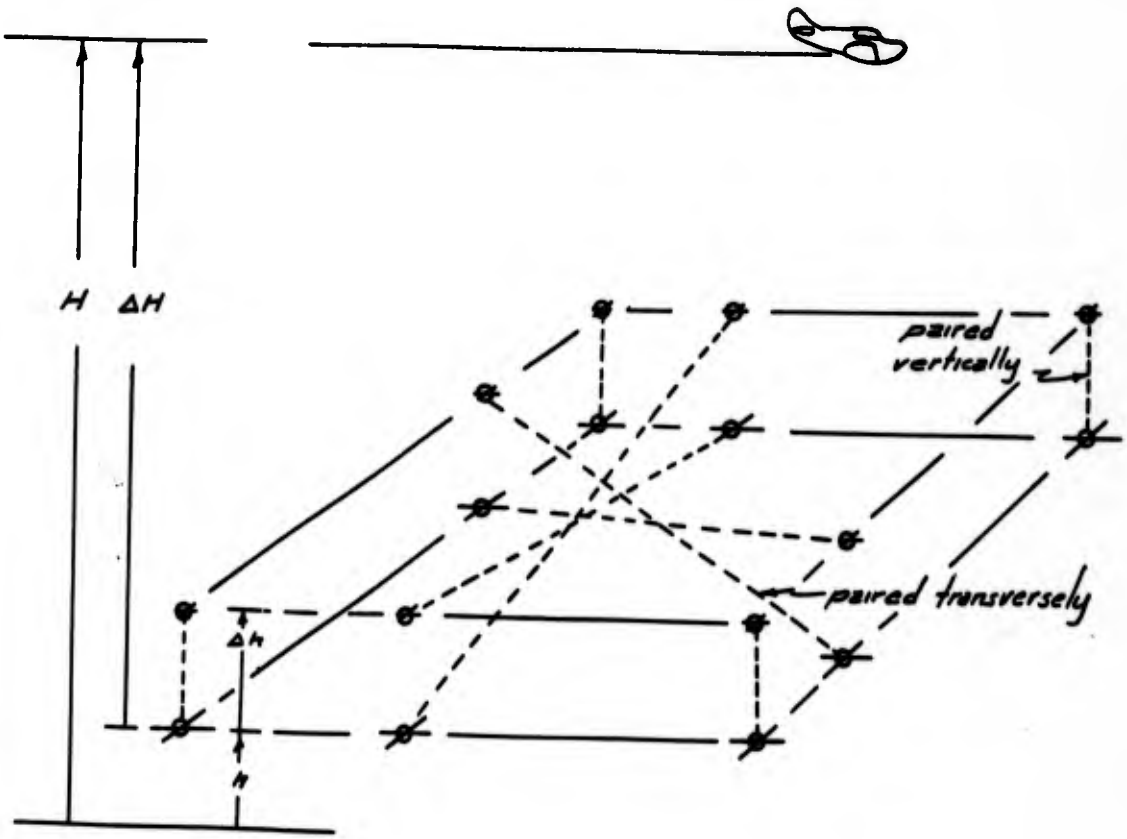

Figure 23. Representative Pairing of Survey Control

TABLE XIV. CAMERA CONSTANT WEIGHT NUMBER (QCC) (ASSUMED ALL PHOTO COORDINATE OBSERVATIONS WEIGHTED BY THE RECIPROCAL OF 0.005 MM., SQUARED)

Δh/ΔH \ No. of Points	40	32	24
1/3	0.159×10^{-4}	0.205×10^{-4}	0.223×10^{-4}
1/4	0.298×10^{-4}	0.410×10^{-4}	----------
1/5	0.505×10^{-4}	----------	----------

TABLE XV. CAMERA CONSTANT STANDARD ERROR (± MICRONS) AS COMPUTED FROM THE WEIGHT NUMBER AND AN ASSUMED PHOTO COORDINATE ERROR OF ± 5 MICRONS

Δh/ΔH \ No. of Points	40	32	24
1/3	0.159×10^{-4}	0.205×10^{-4}	0.223×10^{-4}
1/4	0.298×10^{-4}	0.410×10^{-4}	----------
1/5	0.505×10^{-4}	----------	----------

The results of these purely geometric considerations of the nature of the CER computation indicate accuracy that might be expected for the camera constant under various conditions. These results are further conditioned by the assumptions that no other systematic influences were present, the errors in photo coordinates were random about a zero mean, and were drawn from a parent population possessing a standard deviation of ± 5 microns. It also assumes that sufficient observations were used to assure that the parameters of the mathematical model do not tend to absorb observational errors. The results of a comparison of the camera constants computed in the CER solutions and the true values indicate that some model absorption of the observational errors probably did take place in those solutions employing less than 40 control points. These results are presented in section 2.3.2.3

2.3.2.3 Comparisons of True to Computed Camera Constant After the CER Computation

In solutions in which parameters are indirectly "observed" quantities, the influences of correlation between two or more parameters will tend to distort the impression received by comparing an individual parameter to its true value. Of course, true values are rarely available for comparison except under artificial circumstances such as this. The parameters have meaning only when all are taken together in the model in which they were determined. The evaluation of the result should be made with respect to the quantity that is intended to be measured by the system. However, it is still of interest in this case to extract the camera constant out of its mathematical context to observe its character under those conditions of control which were used in section 2.3.2.2. Table 16 indicates the difference or "error" in computation of the camera constant by the CER solution. The relatively large values of errors along the diagonal of Table 16 are not simply the result of geometric dilution but indicate a failure of the solution to converge.

TABLE XVI. TRUE ERRORS IN CAMERA CONSTANT (MICRONS) FOR VARIOUS COMBINATIONS OF SURVEY CONTROL (STD. DEVIATION IN PHOTO COORDINATES WAS ± 5 MICRONS).

No. of Points / Δh/ΔH	40	32	24
1/3	+2.9	+5.6	+30.8
1/4	+3.1	-58.3	
1/5	+38.4		

Due to the probabilistic nature of such solutions in which photo coordinate errors are subject to random errors, it is recognized that a great number more such computations are required before any firm conclusions may be drawn. However, the trend of the influences of control point density and depth can already be seen. For control fields with depth-height ratios (Δh/ΔH) of 1/3; more than thirty points should be used and for depth-height ratios of 1/4, more than forty points should be used. In the case of smaller depth-height ratios, the solution does not appear to be successful for even 40 points. The final test of success as mentioned earlier, however, is not the direct comparison of any one parameter, but a comparison of the result of the measurement process when all parameters are employed.

2.4 McClure Ohio Camera Calibration Range

The U. S. Coast and Geodetic Survey established an aerial camera calibration range near McClure, Ohio in 1947. Since then the range has been gradually improved by resurvey and addition of more targeted control. At present, the basic range consists of approximately 120 targeted points in a 5 mile by 5 mile flat area. Recently, an 85 mile southwesterly extension to the range has been added consisting of 25 stations.

The targets that were established up until 1959 consist of crushed limestone placed flush with the ground in circles of 6 foot diameter. Subsequently, targets have been made to the same specification but of concrete. Each target is fully described according to standard station description practice of the Coast and Geodetic Survey.

The horizontal control was established by means of triangulation and geodimeter traverse. The adjusted positional accuracy is assumed to be one part in 100,000. The coordinates are published in terms of State Plane Coordinates, Lambert Projection, North Zone for Ohio. The vertical control was established by fourth order leveling strengthened by first and second order level lines.

2.5 Camera Installation

The details of the camera installation are described by Major C. Fortney, USAF [1965] in a final report concerning the modification of a USAF B-57B for purposes of precision photography.

The camera, a KC1B (Fairchild), was installed on an ART-25 (Aeroflex) gyro-stabilized vertical mount. The camera compartment was expressly designed to maintain a constant temperature environment at 21°C. This was accomplished by means of a balanced design of compartment insulation, and servo controlled heat lamps. Temperature was controlled by means of a sensor located in the camera compartment. Three additional sensors were located within the camera, two of which were thermistors. One thermistor was attached to the objective assembly and the other against the registration frame. An excellent record of temperature at critical points may be obtained by means of these devices during the actual photo mission. No attempt was made to control either pressure or humidity environment in the aircraft.

The camera compartment and associated equipment was mounted directly on the bomb bay door of the B-57B aircraft. Figure 24 shows the compartment on the bomb bay door but detached from the aircraft.

The photographic window consisted of a 23" x 13" x 1/2" crown glass, shock mounted in a metal frame. This was installed and flared into the B-57B bomb bay door.

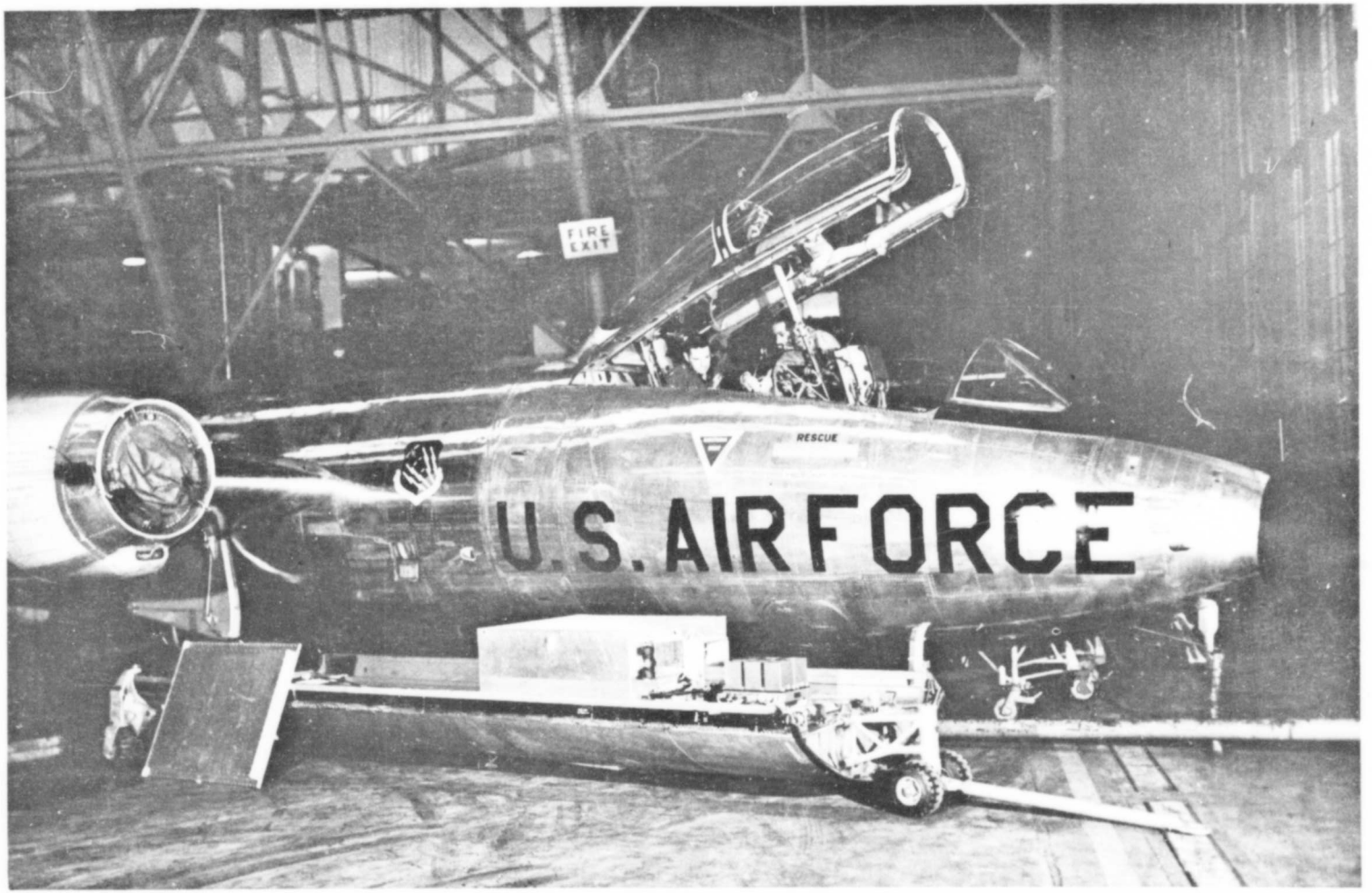

Figure 24. B57B Aircraft Showing Camera Chamber Installed on Bomb Bay Door

Results of flight tests presented in Figure 25 indicate the performance of the camera compartment and camera temperature stabilization equipment. [Fortney, 1965].

2.6 Photography of the McClure Range

Photography for purposes of the present investigation was taken with a Fairchild KC1B camera serial number 63-027 with lens number 289. The lens was a Goerz planigon, 6 inch focal length and was operated at its maximum aperture of f/6.3. The camera was calibrated on March 21, 1963 by Fairchild using the standard bank collimator photographic laboratory procedure [Norton, 1963]. This information was used as a starting point for the airborne calibration. Later, the same camera was calibrated according to the stellar method using glass based photography. This work was accomplished by the Autometrics Operations of Raytheon on June 22, 1965 [Raytheon, 1965].

For purposes of elimination of film shrinkage it was originally planned to flash a calibrated reseau grid onto the film during exposure in the camera. This would require camera modification and would not be in keeping with the requirements of a realistic camera calibration. Accordingly, a compromise was arranged whereby the reseau would be exposed onto the film in the laboratory prior to loading into the camera magazine. The consequence of this compromise is fully discussed in section 2.2.3 of this paper.

The film was type 5401, Plus-X Aerographic on an acetate butyrate base. Processing was accomplished at the base photographic laboratory at Griffiss Air Force Base, New York according to standard procedures.

The photo mission began at Griffiss Air Force Base on December 21, 1965 at 08:30 E.S.T. One hundred eighty five feet of film were loaded and a photo pre-flight check list completed. The first photography flown at 14,000 feet over the McClure range was obtained at 12:41 E.S.T. and completed at 12:56 E.S.T.

An example of the photography indicating the reseau overlay is presented in Figure 26.

2.7 Summary of Significant Results

The following paragraphs are a compendium of results taken from the various phases of the camera calibration investigation. They are intended to provide a quick reference to the most significant findings of this research. All references to photo coordinate errors assume that a standard mapping camera of 153 mm focal length is used.

The initial comparator calibration computation was developed based on the assumption that a calibrated grid standard with published coordinates

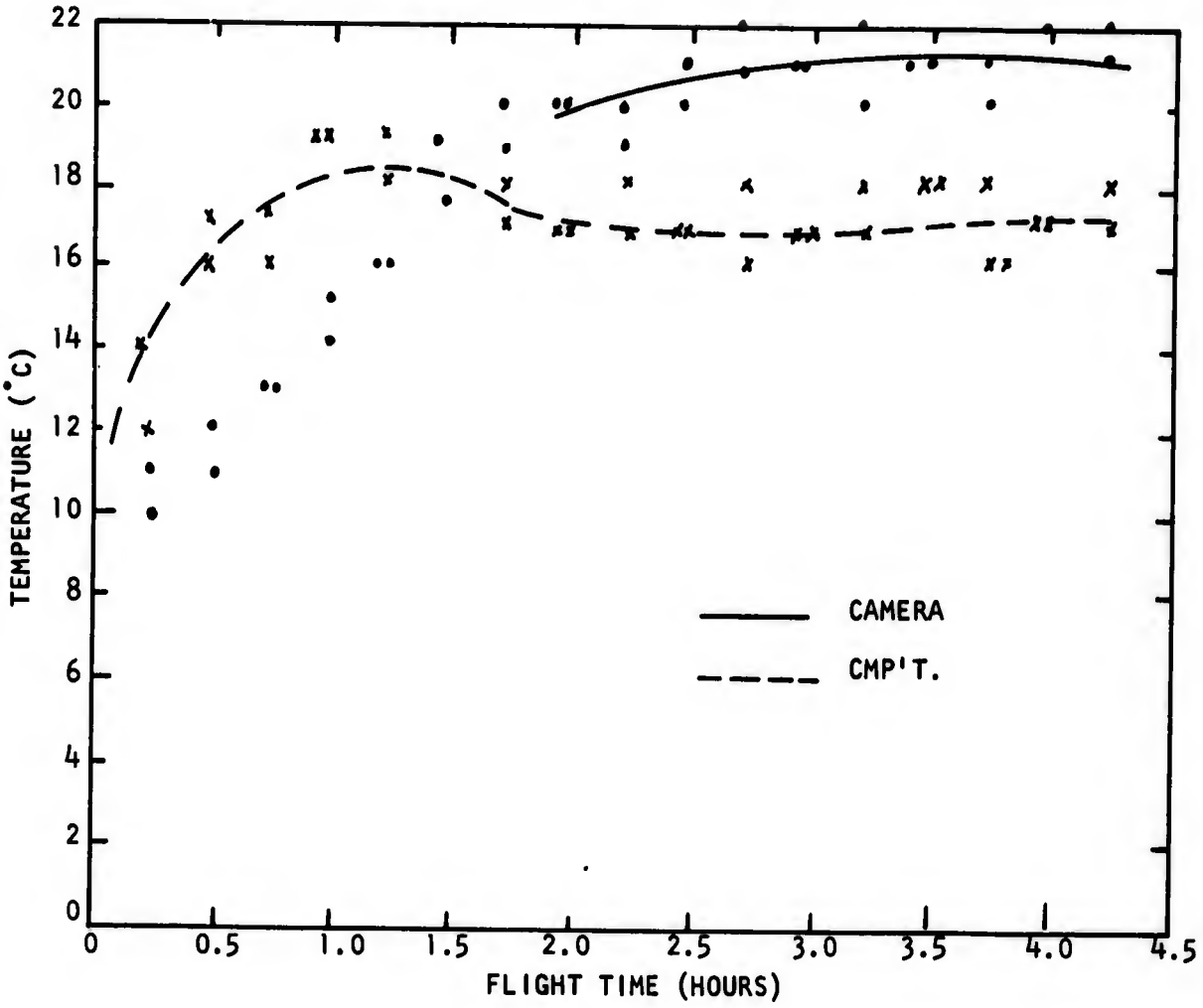

Figure 25. Compartment - Camera Temperature, Not Preheated. [Fortney, 1965]

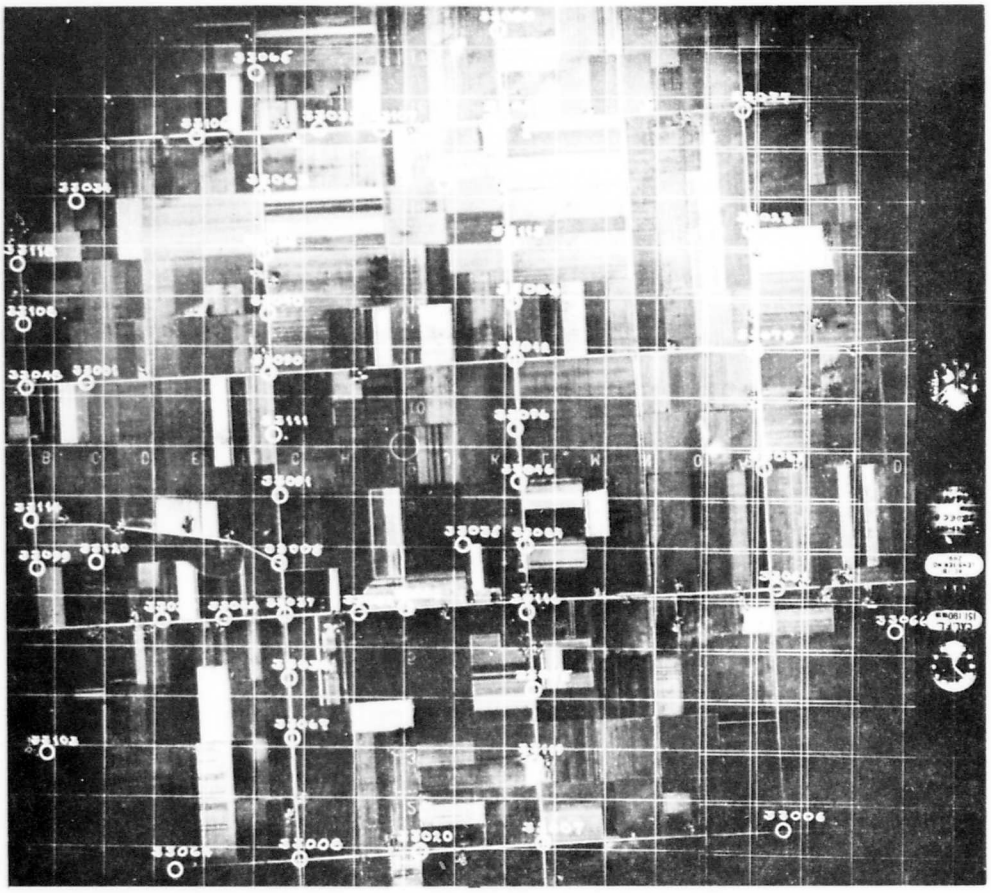

Figure 26. Sample Photo of the McClure, Ohio Calibration Range

accurate to ± 0.3 micron standard error would be available. An artificial data solution, using a ten parameter model and 36 grid intersections, produced residuals after adjustment of about 0.03 micron standard error.

The second attempt at comparator calibration was developed based on two observational sets along the (y) coordinate axis. A linear scale provided by the David Mann Corporation was used as a standard. The resulting standard error in the (y) coordinate direction was ±1.00 micron and in the (x) coordinate direction ±1.34 microns. The overall systematic error of a given set of comparator coordinates was estimated to be less than 2.0 microns.

The CRP computation provided a measure of observational precision. The standard error between observational sets taken at substantially different times on the same image of a ground point was ±3.5 microns. In this case, each set consisted of the mean of three observations. Tests were made to detect significant bias between the mean differences of observational sets by means of the t-test. Of the five photographs measured, one was rejected at the 99 percent level as exhibiting a significant bias between observational means. The average of the standard deviations of the mean of all pointings on a given image was computed to be ± 1.75 microns. This represents only the ability to repeat a mean of six observations on an image under circumstances that prevailed, and does not include significant bias. The precision with which the fiducial center was computed using observations on fiducial marks was ±1.03 microns standard deviation in (x) and ±0.50 micron in (y).

The compensation for film dimensional errors was not successful in the sample photography. The photo coordinate errors introduced by residual shrinkage, lack of film and emulsion flatness, and of platen flatness theoretically could be reduced to a combined error of about ±3.0 microns standard error provided a 2 centimeter reseau were exposed simultaneously with the opening of the shutter. In the test case, the reseau was exposed several days prior to use in the aircraft. For reasons discussed in section 2.2.3, the uncompensated film shrinkage appeared to amount to about ±8.0 microns standard error even after linear scaling in the transverse direction.

The magnitude of uncorrected atmospheric refraction was estimated to be 0.72 microns for the extreme ray of 45° off the nadir point. The error introduced by the assumption that the earth is a sphere with radius equal to a mean radius at the latitude of the test range as compared to the more nearly correct assumption of an ellipsoidal surface was computed to be about -0.50×10^{-9} micron for the extreme ray. The error introduced by gravity anomalies in the McClure, Ohio area was determined to be 0.25×10^{-6} micron for the extreme ray.

The MPR computation using four photos simultaneously over the McClure, Ohio range produced the parameters of the model to describe the complete airborne photographic system. The corrections for the (x) and (y) photo coordinates which are expressed by this final calibration are presented in

Figures 27 and 28. By inspection, it is apparent that the camera constant used in the computation does not provide a symmetry in the sense of the photo coordinate corrections. The symmetry could be arbitrarily improved by assigning an appropriate value to the camera constant in the MPR computation. Such a procedure, however, would also require corresponding changes to all parameters of the calibration. It is the opinion of the investigator that in spite of the asymmetry of the corrections, the calibration is valid for the mathematical model adopted for this calibration. The results are satisfactory for computational photogrammetric applications since these need not depend on symmetry. The standard error of a representative photo coordinate observation computed from the residuals after adjustment of 145 points (290 observations) was $\pm$8.0 microns. The primary cause of the large error after adjustment is believed to be due to unmodeled film shrinkage caused by marked changes in relative humidity.

The CER computation for the purpose of including the camera constant as a parameter was investigated using various combinations of artificial data. It was generally concluded that the calibration range should provide a minimum of 32 well distributed targets for relief to flight height ratios of 1/3 and a minimum of 40 points for a ratio of 1/4. For investigations concerning the characteristics of the CER computation a $\pm$ 5 micron random photo coordinate deviation was used. For the conditions mentioned above, the computed camera constant agreed with the true value within 6 microns.

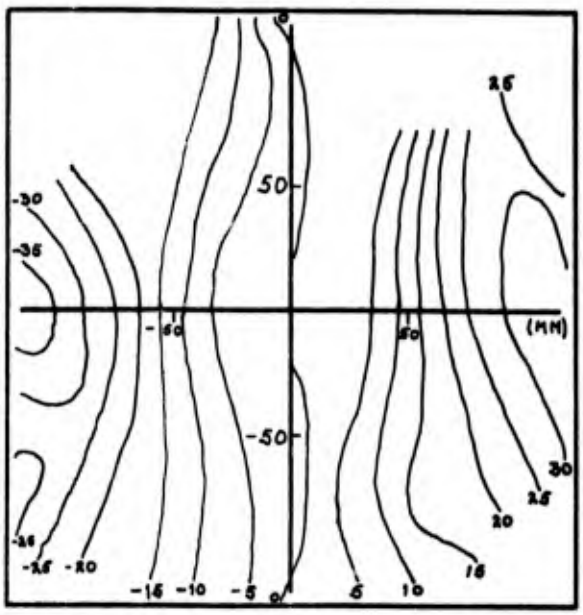

Figure 27. Plot of Corrections to the (x) Photo Coordinates After the MPR Computation Using the Fiducial Center as an Origin.

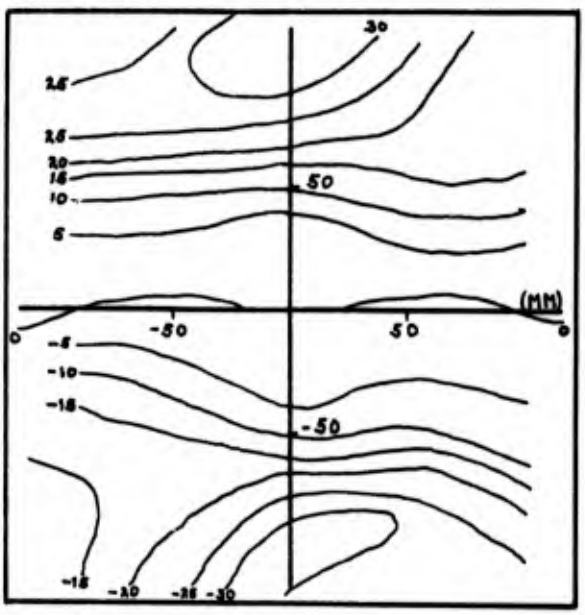

Figure 28. Plot of Corrections to the (y) Photo Coordinates After the MPR Computation Using the Fiducial Center as an Origin.

III

CONCLUSION AND RECOMMENDATIONS

This investigation was made for the purpose of studying the problems in connection with undertaking a realistic calibration of the complete airborne photographic system. Emphasis was placed on obtaining photography for purposes of the calibration under circumstances which in every respect were equivalent to those which would be expected operationally.

Application of this type of calibration is most valuable for photographic systems intended for use with purely computational data handling procedures. Its use on photo systems intended to provide photography solely for analog reduction is limited to verification of the fact that the system is performing within expected bounds. Those who are developing the AN/USQ-28 geodetic sybsystem for the U.S.A.F. should show particular interest in the problem of calibration of the photographic system. The KC6A camera intended for use with the USQ-28 subsystem is well suited to this type of calibration.

Results derived from actual photography over the McClure, Ohio camera calibration range indicated a need for improvement in the technique for correction of irregular film shrinkage. The author suggested equipment and procedures adapted to the control of this problem. The suggestion is in keeping with the requirement that no departure from anticipated operational conditions would be permitted.

A primary objection to the use of reseau type photography is the laborious reduction of observations. The author developed a procedure whereby a separate transformation of comparator coordinates to photo coordinates was made for each image point. The observer is relieved of the need to identify reseau points. This work was accomplished in a digital computer by exploitation of its characteristic truncation process.

Correlation between flying height and camera constant is near unity. There results a mutual compensation between the effects of these two parameters when they are computed in a common adjustment. This is of no particular significance unless the photo system is to be used over mountainous terrain. Under these circumstances, the use of a camera calibration performed over a level calibration range would not be appropriate. Accordingly, the author has developed and investigated a procedure in which flying height and thereby correlation with the camera constant is eliminated as a parameter

in the computation of the calibration. This was accomplished by pairing high and low points in a hypothetical camera calibration in which significant amounts of control point elevation differences existed.

3.1 Conclusions

The results of this limited investigation into the problem of airborne photographic system calibration indicate that such calibrations are feasible. The nature of the intended application of the photographic system must justify the added costs particularly in man hours for this form of field calibration.

The problem of compensation of film shrinkage requires careful attention. The proposed "reseau bonnet" will do much to correct for irregular film shrinkage without need for alteration of the conventional cartographic photographic system.

The influence of atmospheric refraction can be adequately eliminated by use of presently available standard atmospheric models. Actual daily variations from the model are of little significance. The seasonal variations are of marginal magnitude (-1.2 microns at 45° nadir distance) only for the winter months. The remainder of the year, the atmosphere conforms sufficiently close to the standard ICAN Model atmosphere.

The use of a sphere as an approximation to the geoid in the region of the McClure Ohio camera calibration range does not introduce a significant error into the calibration of the aerial camera system.

The method developed and investigated for correlation elimination between the camera constant and flying height will compute the true focal length within 6 microns, provided at least 40 well distributed points are used and that the ratio of control field depth to flying height is 1/4 or more. The convergence of the solution improves most rapidly by increasing the number of control points. This increase in control point density is also preferred from the standpoint of more thorough consideration of the total photographic field. Under these circumstances, little improvement in the accuracy of the results was noted by increasing the depth/height ratio.

3.2 Recommendations

The goal in aerial camera calibration as with any calibration according to Eisenhart [1963] is the achievement of the condition of statistical control of the measurement system. Accordingly, it is recommended that the "reseau bonnet" device be developed and employed in connection with photography over the McClure camera calibration range. The remaining procedures developed during the course of this investigation may then be applied under control of established observational specifications. The results would lead to improvement in the calibration procedures developed during this investigation and to the realistic calibration of a given photographic system.

Further work is recommended for the development of a feasible calibration scheme for photo systems intended for use in mountainous regions. The development would be most useful along the following lines:

a) use of a small number of closely spaced towers located within the control field by which tower heights can be introduced as direct observations into a conventional resection solution

b) use of an independent direct measurement of exposure station elevation by means of an electronic ranging device such as the Cubic "Autotape". Such a device may be used during daylight hours precluding the need for artificially illuminating the ground targets thereby not departing from the desired operational conditions.

Finally, it is recommended that a program of calibration and periodic recalibration be established for the photographic components of the USAF's USQ-28 geodetic subsystems. Without such knowledge of calibration, much of the value of these photographic systems will most certainly be lost.

List of References

1. Ahrend, M. (1966) Analysis of Photogrammetric Errors, 30th Photogrammetric Weeks, Karlsruhe, Germany.

2. American Society of Photogrammetry (1966) Manual of Photogrammetry, 3rd Edition, Banta Publishing Co.

3. Aschenbrenner, (1937), Bildmessung und Luftbildwesen, vol. 1.

4. Brandenberger, A. J. (1951) The Practice of Spatial Aerial Traiangulation, Federal Institute of Technology, Zurich, Switzerland.

5. Brock, R., Faulds, A. (1961) Investigation of Atmospheric Refraction and Film Shrinkage, Syracuse University Research Institute for USAF (RADC-TR-61-301).

6. Brown, Duane C. (1964) An Advanced Reduction and Calibration for Photogrammetric Cameras, Instrument Corp. of Florida.

7. Brown, D. (1966) Decentering Distortion of Lenses, Photogrammetric Engineering, Vol. XXXII, No. 3.

8. Calhoun, J. M., Leister, D. A. (1959) Effect of Gelatin Layers on the Dimensional Stability of Photographic Film, Photographic Science and Engineering, Vol. 3, pp. 8-17.

9. Clark, J. M., Cooper, G. R. (1964) Some Investigations on Film Flatness in Air Survey Cameras, 10th Congress, Int'l. Society of Photogram. Lisbon, Portugal.

10. Cole, A. E., Nee, P. F. (1965) Correlations of Pressure, Temperature and Density, to 30 Kilometers, Air Force Cambridge Research Laboratories, Air Force Surveys in Geophysics No. 160.

11. Commission 1, I.S.P.(1952) Report ot the Seventh International Congress, Sept. 1952.

12. Conrady, Prof. A. E. (1919) Decentered Lens Systems, Astronomical Society Monthly Notices, Mar. 1919.

13. Eisenhart, Churchill (1963) Realistic Evaluation of the Precision and Accuracy of Instrument Calibration Systems, Journal of Research of the National Bureau of Standards, Vol. 67C, No. 2, April, June, 1963.

14. Flight Log. (1965) ASFIR Evaluation Airborne Data, Personnal Files.

15. Fortney, C. W. (1965) Environmental Control and Installation of a Precision Aerial Camera, Technical Report No. RADC-TR-65-375, Griffiss Air Force Base, New York.

16. Gast, (1937) Bildmessung und Luftbildwessen, vol. 3.

17. Gossett, Cmdr. F. R. (1950) Manual of Geodetic Triangulation, U.S. C and GS, Sp. Pub. No. 247, U. S. Gov't Printing Office.

18. Hallert, B. (1962) Investigations of Basic Geometric Quality of Aerial Photographs and Some Related Problems, GIMRADA, Research Note No. 4.

19. Hallert, B. (1962a) Determination of the Geometrical Quality of Comparators for Image Coordinate Measurements, U.S. Army GIMRADA Research Note No. 31, August.

20. Hallert, B. (1965) Why Research on Image Coordinates?, Photogrammetria, Vol. 20, pp. 125-126.

21. Harris, W. D., Tewinkel, G. C., and Whitten, C. A. (1962) Analytic Aerotriangulation, Technical Bulletin No. 21, U.S. Coast and Geodetic Survey.

22. Heiskanen, W. A., Vening Meinesz, F. A. (1958) The Earth and Its Gravity Field. New York.

23. Heiskanen, W. A., Uotila, U. A. (1956) Gravity Survey of the State of Ohio, Institute of Geodesy, Photogrammetry and Cartography, the Ohio State University, Rpt. No. 30.

24. Keller, M., Tewinkel, G. C., (1966) Space Resection in Photogrammetry, ESSA Technical Report C and GS 32.

25. Kodak, (1965) Manual of Physical Properties, Aerial and Special Materials, Rochester, N.Y.: Eastman Kodak Co.

26. Leyonhufvud, A. (1952) On Photogrammetric Refraction, Photogrammetria, Vol. 9, pp. 93-113.

27. Military Specification, MIL-G-1366 Glass Window, Aerial Photographic.

28. Norton, C. (1963) Calibration Certificate, Camera No. 63-027, Fairchild Camera and Instrument Co., Syosset, N.Y.

29. Parratt, L. G. (1961) Probability and Experimental Errors in Science, John Wiley and Sons, Inc., New York.

30. Raytheon Co. (1965) Engineering Report on Stellar Calibration for ASFR Camera, Raytheon Co., Space and Infor. Systems Div. Autometric Operation, Alexandria, Va.

31. Rosenfield, Geo., (1959) The Problem of Exterior Orientation in Photogrammetry, Photogrammetric Engineering, Vol. XXV, No. 4, pp. 536-550.

32. Schutte, (1937), Zeitschr. f. Vermessungswesen, vol. 17.

33. Uotila, U. (1963) Lecture Notes, for a series of courses in adjustment computations, The Ohio State University.

34. Uotila, U. (1967) Communications concerning the Ohio Gravity Survey.

35. Woodcock, L. F., Lampton, F. B. (1964) Measurement of Crustal Movements by Photogrammetric Methods, Photogrammetric Engineering, Vol. 30, pp. 912-16.

36. Zakrzewski, C. W. (1966) Calibration Report for Mann Comparator 422C31, 19 April, 1966. On file in Syracuse University comparator lab.

APPENDIX A. FLOW DIAGRAMS

The material in this appendix consists of the flow diagrams of both subroutines and main programs developed and used during the course of this investigation. Detailed discussions of their development and use appear in pertinent sections of this report. References may be conveniently made to the discussion of individual programs through the "Table of Contents" of this report.

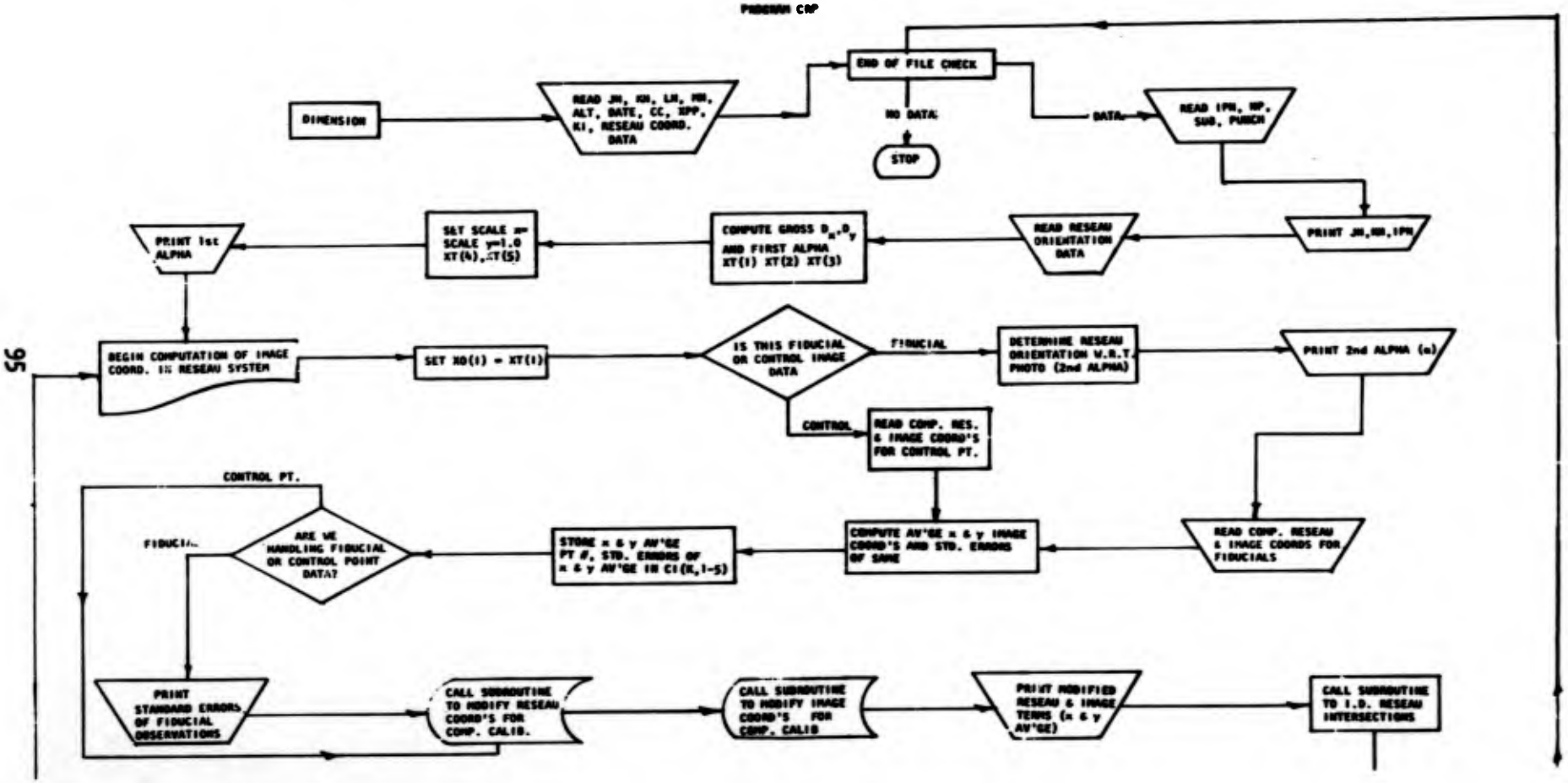
PROGRAM CRP
DIMENSION
READ JH, KH, LH, MH, ALT, DATE, CC, XPP, KI, RESEAU COORD. DATA
END OF FILE CHECK
NO DATA
STOP
DATA
READ IPH, MP, SUB, PUNCH
PRINT JH, KH, IPH
READ RESEAU ORIENTATION DATA
COMPUTE GROSS D_x, D_y AND FIRST ALPHA XT(1) XT(2) XT(3)
SET SCALE x= SCALE y=1.0 XT(4), XT(5)
PRINT 1st ALPHA
BEGIN COMPUTATION OF IMAGE COORD. IN RESEAU SYSTEM
SET XO(I) = XT(I)
IS THIS FIDUCIAL OR CONTROL IMAGE DATA
FIDUCIAL
DETERMINE RESEAU ORIENTATION W.R.T. PHOTO (2nd ALPHA)
PRINT 2nd ALPHA (a)
CONTROL
READ COMP. RES. & IMAGE COORD'S FOR CONTROL PT.
CONTROL PT.
FIDUCIAL
ARE WE HANDLING FIDUCIAL OR CONTROL POINT DATA?
STORE x & y AV'GE PT #, STD. ERRORS OF x & y AV'GE IN CI(K,I-5)
COMPUTE AV'GE x & y IMAGE COORD'S AND STD. ERRORS OF SAME
READ COMP. RESEAU & IMAGE COORDS FOR FIDUCIALS
PRINT STANDARD ERRORS OF FIDUCIAL OBSERVATIONS
CALL SUBROUTINE TO MODIFY RESEAU COORD'S FOR COMP. CALIB.
CALL SUBROUTINE TO MODIFY IMAGE COORD'S FOR COMP. CALIB
PRINT MODIFIED RESEAU & IMAGE TERMS (x & y AV'GE)
CALL SUBROUTINE TO I.D. RESEAU INTERSECTIONS

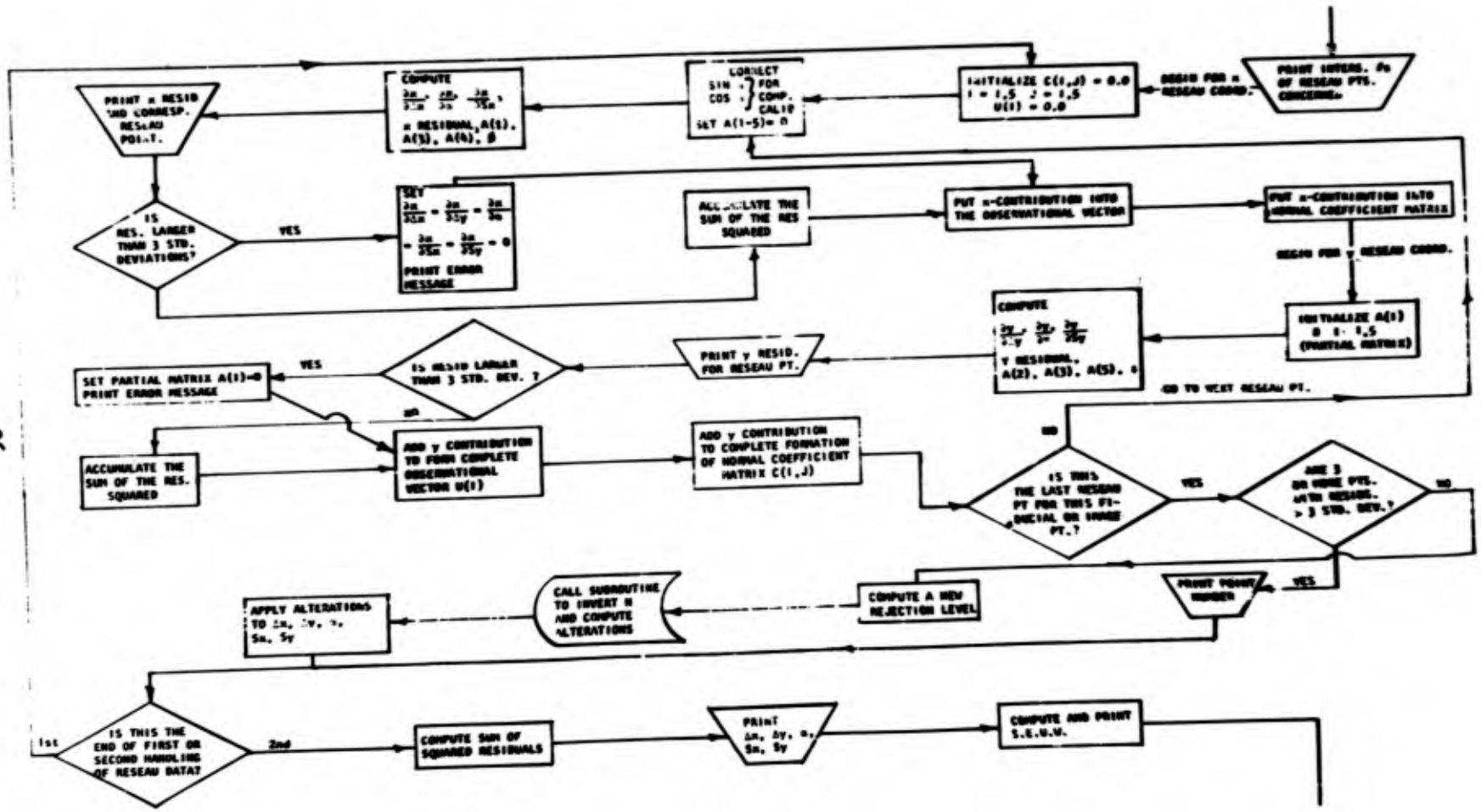
PRINT x RESID AND CORRESP. RESEAU POINT.
COMPUTE
x RESIDUAL, A(1), A(3), A(4), β
CORRECT FOR COMP. CALIP
SET A(1-5)= 0
INITIALIZE C(I,J) = 0.0
I = 1,5 J = 1,5
U(I) = 0.0
BEGIN FOR x RESEAU COORD.
POINT NUMBERS, No OF RESEAU PTS. CONCERNED
IS RES. LARGER THAN 3 STD. DEVIATIONS?
YES
SET
PRINT ERROR MESSAGE
ACCUMULATE THE SUM OF THE RES SQUARED
PUT x-CONTRIBUTION INTO THE OBSERVATIONAL VECTOR
PUT x-CONTRIBUTION INTO NORMAL COEFFICIENT MATRIX
BEGIN FOR y RESEAU COORD.
INITIALIZE A(I)
0 I 1,5
(PARTIAL MATRIX)
COMPUTE
y RESIDUAL, A(2), A(3), A(5),
PRINT y RESID. FOR RESEAU PT.
IS RESID LARGER THAN 3 STD. DEV. ?
YES
SET PARTIAL MATRIX A(I)=0
PRINT ERROR MESSAGE
NO
GO TO NEXT RESEAU PT.
ACCUMULATE THE SUM OF THE RES. SQUARED
ADD y CONTRIBUTION TO FORM COMPLETE OBSERVATIONAL VECTOR U(I)
ADD y CONTRIBUTION TO COMPLETE FORMATION OF NORMAL COEFFICIENT MATRIX C(I,J)
IS THIS THE LAST RESEAU PT FOR THIS FIDUCIAL OR IMAGE PT.?
YES
NO
ARE 3 OR MORE PTS. WITH RESIDS. > 3 STD. DEV.?
YES
PRINT POWER NUMBER
COMPUTE A NEW REJECTION LEVEL
CALL SUBROUTINE TO INVERT N AND COMPUTE ALTERATIONS
APPLY ALTERATIONS TO Δx, Δy, a, Sx, Sy
1st
IS THIS THE END OF FIRST OR SECOND HANDLING OF RESEAU DATA?
2nd
COMPUTE SUM OF SQUARED RESIDUALS
PRINT Δx, Δy, a, Sx, Sy
COMPUTE AND PRINT S.E.U.W.

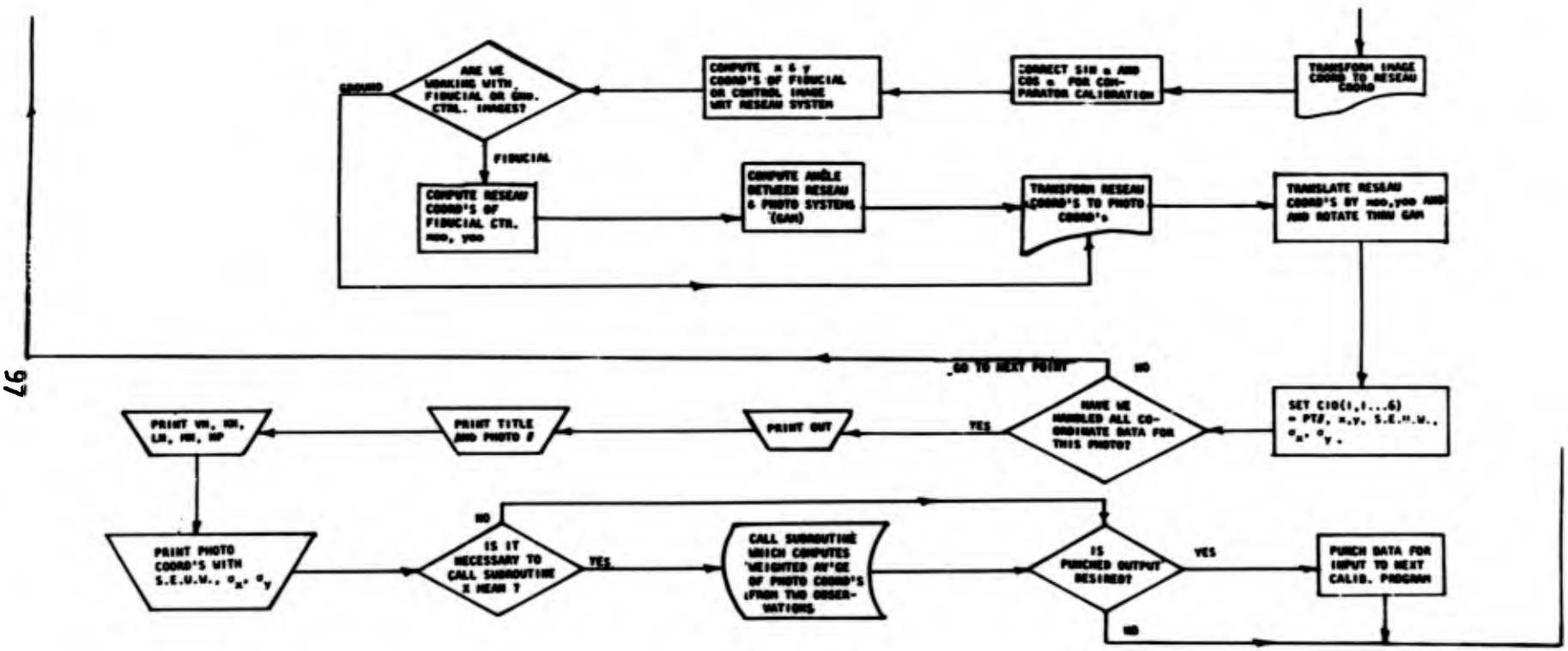
TRANSFORM IMAGE COORD TO RESEAU COORD
CORRECT SIN α AND COS α FOR COMPARATOR CALIBRATION
COMPUTE x & y COORD'S OF FIDUCIAL OR CONTROL IMAGE WRT RESEAU SYSTEM
ARE WE WORKING WITH FIDUCIAL OR CONT. CTRL. IMAGES?
GROUND
FIDUCIAL
COMPUTE RESEAU COORD'S OF FIDUCIAL CTR. x00, y00
COMPUTE ANGLE BETWEEN RESEAU & PHOTO SYSTEMS (GAM)
TRANSFORM RESEAU COORD'S TO PHOTO COORD'S
TRANSLATE RESEAU COORD'S BY x00, y00 AND AND ROTATE THRU GAM
SET C10(1,1...6) = PT#, x, y, S.E.U.W., σx, σy.
HAVE WE HANDLED ALL CO-ORDINATE DATA FOR THIS PHOTO?
NO
GO TO NEXT POINT
YES
PRINT OUT
PRINT TITLE AND PHOTO #
PRINT VH, HH, LH, HH, HP
PRINT PHOTO COORD'S WITH S.E.U.W., σx, σy
IS IT NECESSARY TO CALL SUBROUTINE X MEAN ?
NO
YES
CALL SUBROUTINE WHICH COMPUTES WEIGHTED AV'GE OF PHOTO COORD'S (FROM TWO OBSERVATIONS
IS PUNCHED OUTPUT DESIRED?
YES
NO
PUNCH DATA FOR INPUT TO NEXT CALIB. PROGRAM

PROGRAM SPR

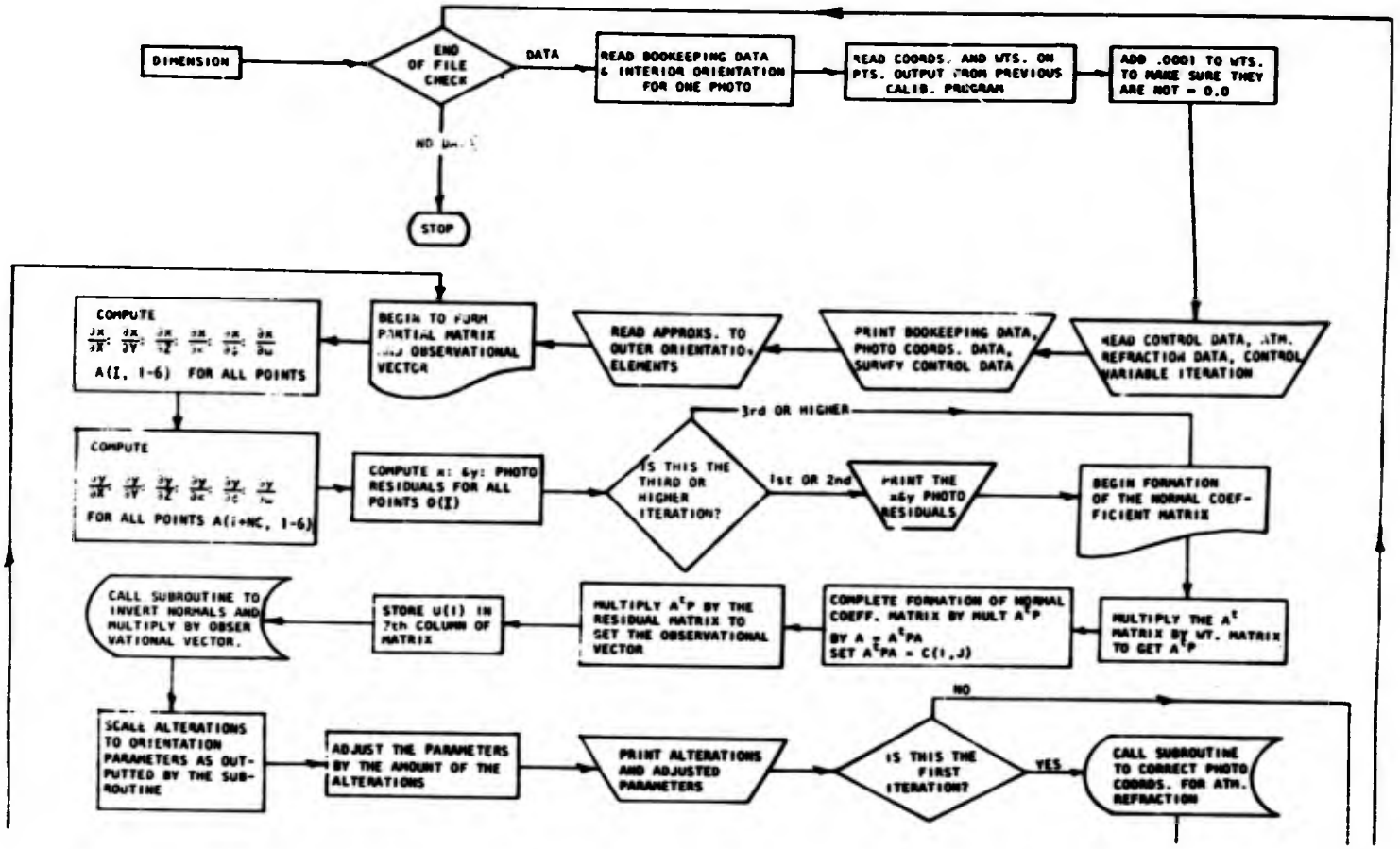
DIMENSION
END OF FILE CHECK
DATA
NO
STOP
READ BOOKEEPING DATA & INTERIOR ORIENTATION FOR ONE PHOTO
READ COORDS. AND WTS. ON PTS. OUTPUT FROM PREVIOUS CALIB. PROGRAM
ADD .0001 TO WTS. TO MAKE SURE THEY ARE NOT = 0.0
READ CONTROL DATA, ATM. REFRACTION DATA, CONTROL VARIABLE ITERATION
PRINT BOOKEEPING DATA, PHOTO COORDS. DATA, SURVEY CONTROL DATA
READ APPROXS. TO OUTER ORIENTATION ELEMENTS
BEGIN TO FORM PARTIAL MATRIX AND OBSERVATIONAL VECTOR
COMPUTE
A(I, 1-6) FOR ALL POINTS
COMPUTE
FOR ALL POINTS A(I+NC, 1-6)
COMPUTE x: &y: PHOTO RESIDUALS FOR ALL POINTS O(I)
IS THIS THE THIRD OR HIGHER ITERATION?
3rd OR HIGHER
1st OR 2nd
PRINT THE x&y PHOTO RESIDUALS
BEGIN FORMATION OF THE NORMAL COEFFICIENT MATRIX
MULTIPLY THE A^T MATRIX BY WT. MATRIX TO GET A^TP
COMPLETE FORMATION OF NORMAL COEFF. MATRIX BY MULT A^TP BY A = A^TPA SET A^TPA = C(I,J)
MULTIPLY A^TP BY THE RESIDUAL MATRIX TO GET THE OBSERVATIONAL VECTOR
STORE U(I) IN 7th COLUMN OF MATRIX
CALL SUBROUTINE TO INVERT NORMALS AND MULTIPLY BY OBSERVATIONAL VECTOR.
SCALE ALTERATIONS TO ORIENTATION PARAMETERS AS OUTPUTTED BY THE SUBROUTINE
ADJUST THE PARAMETERS BY THE AMOUNT OF THE ALTERATIONS
PRINT ALTERATIONS AND ADJUSTED PARAMETERS
IS THIS THE FIRST ITERATION?
NO
YES
CALL SUBROUTINE TO CORRECT PHOTO COORDS. FOR ATM. REFRACTION

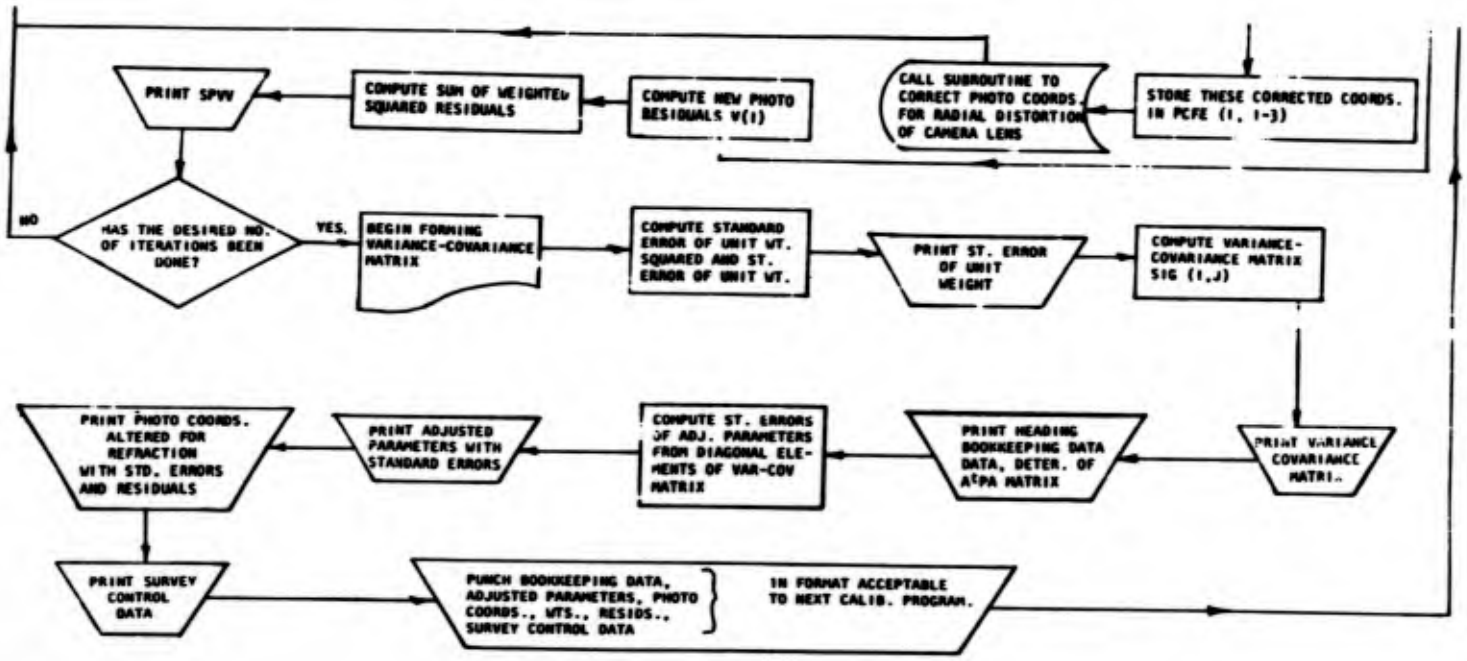
PRINT SPVV
COMPUTE SUM OF WEIGHTED SQUARED RESIDUALS
COMPUTE NEW PHOTO RESIDUALS V(I)
CALL SUBROUTINE TO CORRECT PHOTO COORDS. FOR RADIAL DISTORTION OF CAMERA LENS
STORE THESE CORRECTED COORDS. IN PCFE (I, 1-3)
NO
HAS THE DESIRED NO. OF ITERATIONS BEEN DONE?
YES.
BEGIN FORMING VARIANCE-COVARIANCE MATRIX
COMPUTE STANDARD ERROR OF UNIT WT. SQUARED AND ST. ERROR OF UNIT WT.
PRINT ST. ERROR OF UNIT WEIGHT
COMPUTE VARIANCE-COVARIANCE MATRIX SIG (I,J)
PRINT VARIANCE COVARIANCE MATRI..
PRINT HEADING BOOKKEEPING DATA DATA, DETER. OF A^tPA MATRIX
COMPUTE ST. ERRORS OF ADJ. PARAMETERS FROM DIAGONAL ELEMENTS OF VAR-COV MATRIX
PRINT ADJUSTED PARAMETERS WITH STANDARD ERRORS
PRINT PHOTO COORDS. ALTERED FOR REFRACTION WITH STD. ERRORS AND RESIDUALS
PRINT SURVEY CONTROL DATA
PUNCH BOOKKEEPING DATA, ADJUSTED PARAMETERS, PHOTO COORDS., WTS., RESIDS., SURVEY CONTROL DATA
IN FORMAT ACCEPTABLE TO NEXT CALIB. PROGRAM.

PROGRAM NPR

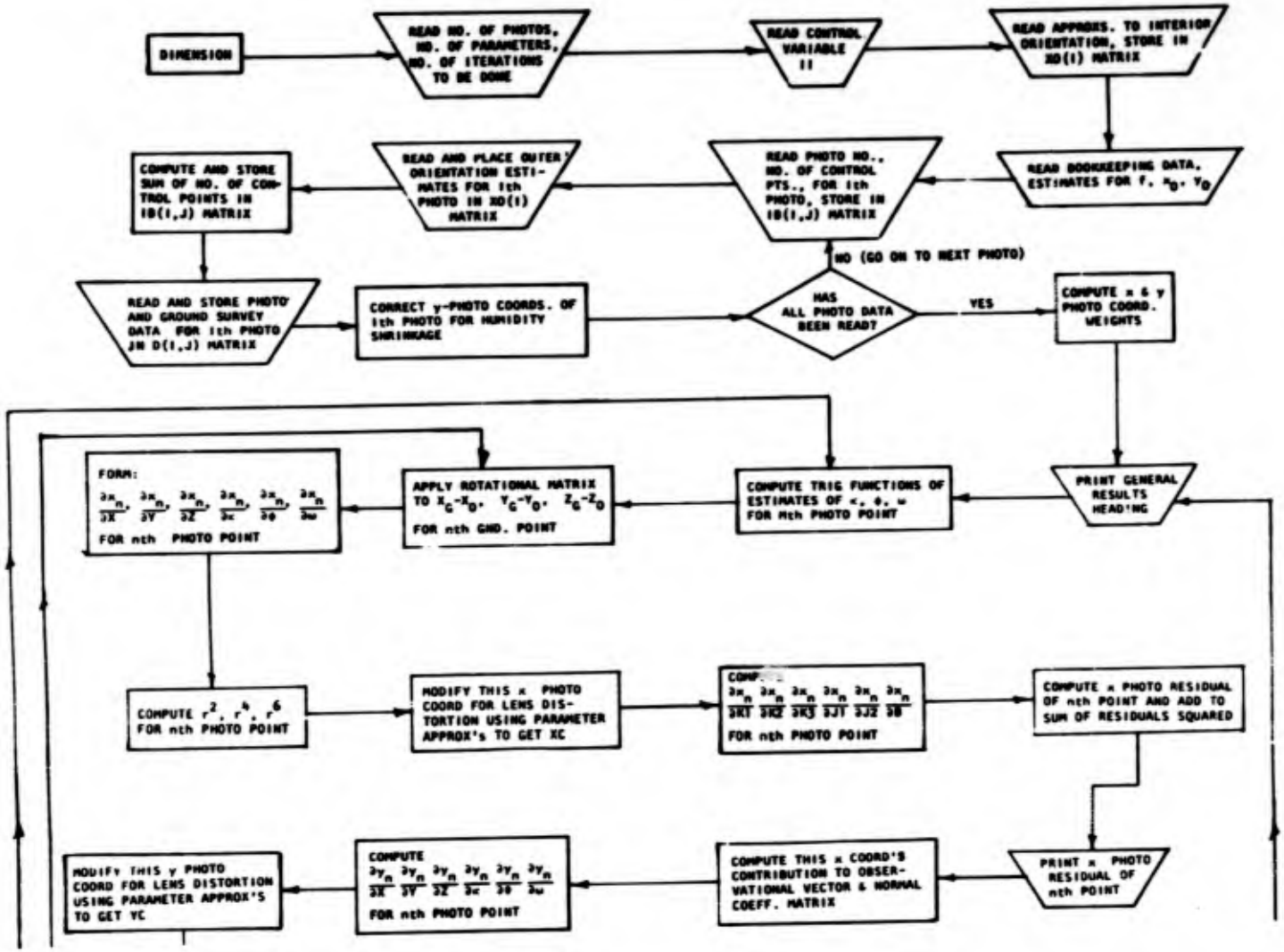
DIMENSION
READ NO. OF PHOTOS, NO. OF PARAMETERS, NO. OF ITERATIONS TO BE DONE
READ CONTROL VARIABLE II
READ APPROXS. TO INTERIOR ORIENTATION, STORE IN XO(I) MATRIX
READ BOOKKEEPING DATA, ESTIMATES FOR f, x_0, y_0
READ PHOTO NO., NO. OF CONTROL PTS., FOR Ith PHOTO, STORE IN ID(I,J) MATRIX
READ AND PLACE OUTER ORIENTATION ESTIMATES FOR Ith PHOTO IN XO(I) MATRIX
COMPUTE AND STORE SUM OF NO. OF CONTROL POINTS IN ID(I,J) MATRIX
READ AND STORE PHOTO AND GROUND SURVEY DATA FOR Ith PHOTO IN D(I,J) MATRIX
CORRECT y-PHOTO COORDS. OF Ith PHOTO FOR HUMIDITY SHRINKAGE
HAS ALL PHOTO DATA BEEN READ?
NO (GO ON TO NEXT PHOTO)
YES
COMPUTE x & y PHOTO COORD. WEIGHTS
PRINT GENERAL RESULTS HEADING
COMPUTE TRIG FUNCTIONS OF ESTIMATES OF <, ϕ, ω FOR Nth PHOTO POINT
APPLY ROTATIONAL MATRIX TO X_G-X_0, Y_G-Y_0, Z_G-Z_0 FOR nth GND. POINT
FORM: $\frac{\partial x_n}{\partial X}, \frac{\partial x_n}{\partial Y}, \frac{\partial x_n}{\partial Z}, \frac{\partial x_n}{\partial <}, \frac{\partial x_n}{\partial \phi}, \frac{\partial x_n}{\partial \omega}$ FOR nth PHOTO POINT
COMPUTE r^2, r^4, r^6 FOR nth PHOTO POINT
MODIFY THIS x PHOTO COORD FOR LENS DISTORTION USING PARAMETER APPROX's TO GET XC
COMP... $\frac{\partial x_n}{\partial K1}\frac{\partial x_n}{\partial K2}\frac{\partial x_n}{\partial K3}\frac{\partial x_n}{\partial J1}\frac{\partial x_n}{\partial J2}\frac{\partial x_n}{\partial B}$ FOR nth PHOTO POINT
COMPUTE x PHOTO RESIDUAL OF nth POINT AND ADD TO SUM OF RESIDUALS SQUARED
PRINT x PHOTO RESIDUAL OF nth POINT
COMPUTE THIS x COORD'S CONTRIBUTION TO OBSERVATIONAL VECTOR & NORMAL COEFF. MATRIX
COMPUTE $\frac{\partial y_n}{\partial X}\frac{\partial y_n}{\partial Y}\frac{\partial y_n}{\partial Z}\frac{\partial y_n}{\partial <}\frac{\partial y_n}{\partial \phi}\frac{\partial y_n}{\partial \omega}$ FOR nth PHOTO POINT
MODIFY THIS y PHOTO COORD FOR LENS DISTORTION USING PARAMETER APPROX'S TO GET YC

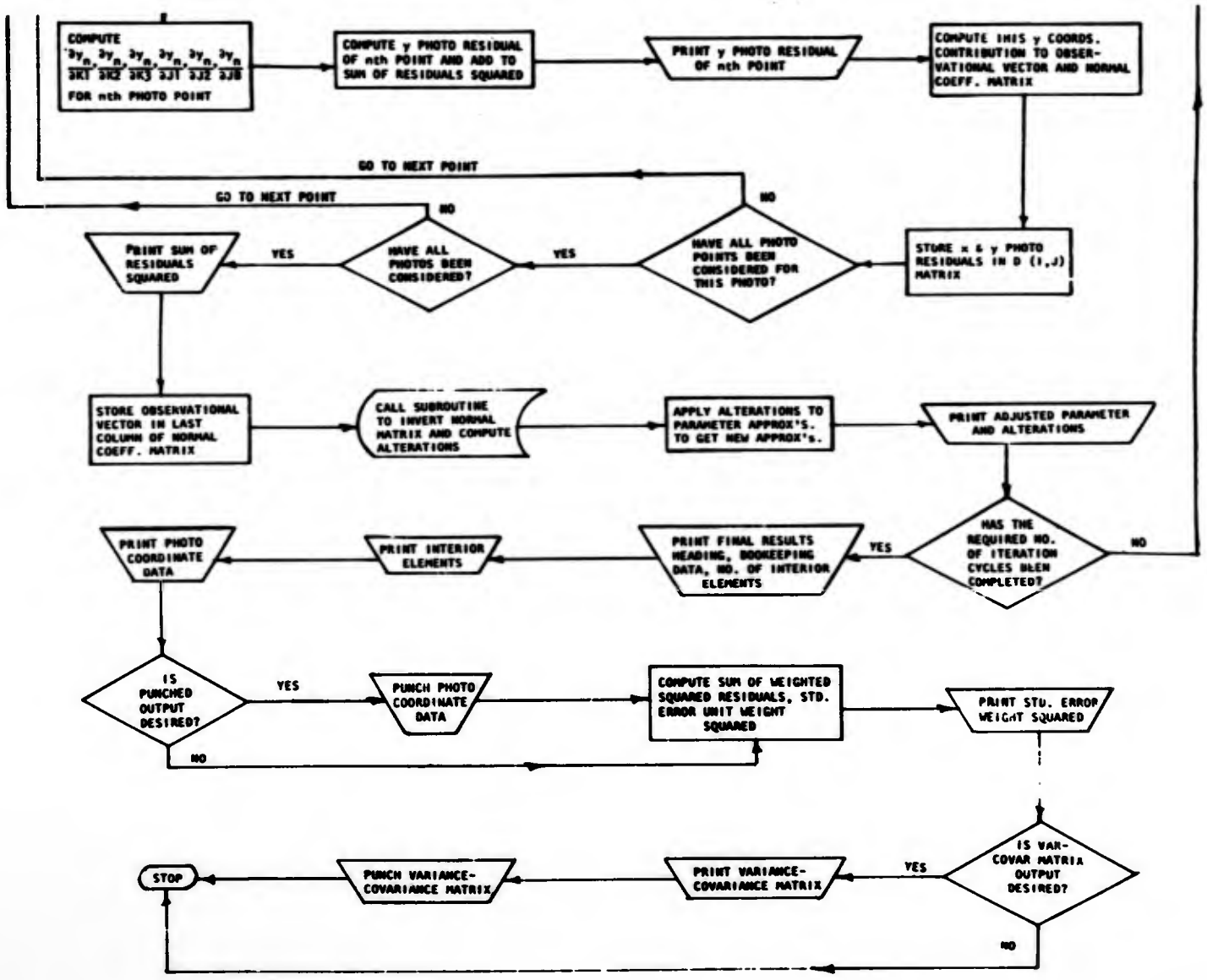
COMPUTE $\frac{\partial y_n}{\partial K1}, \frac{\partial y_n}{\partial K2}, \frac{\partial y_n}{\partial K3}, \frac{\partial y_n}{\partial J1}, \frac{\partial y_n}{\partial J2}, \frac{\partial y_n}{\partial J3}$ FOR nth PHOTO POINT
COMPUTE y PHOTO RESIDUAL OF nth POINT AND ADD TO SUM OF RESIDUALS SQUARED
PRINT y PHOTO RESIDUAL OF nth POINT
COMPUTE THIS y COORDS. CONTRIBUTION TO OBSERVATIONAL VECTOR AND NORMAL COEFF. MATRIX
GO TO NEXT POINT
GO TO NEXT POINT
NO
NO
PRINT SUM OF RESIDUALS SQUARED
YES
HAVE ALL PHOTOS BEEN CONSIDERED?
YES
HAVE ALL PHOTO POINTS BEEN CONSIDERED FOR THIS PHOTO?
STORE x & y PHOTO RESIDUALS IN D (I,J) MATRIX
STORE OBSERVATIONAL VECTOR IN LAST COLUMN OF NORMAL COEFF. MATRIX
CALL SUBROUTINE TO INVERT NORMAL MATRIX AND COMPUTE ALTERATIONS
APPLY ALTERATIONS TO PARAMETER APPROX'S. TO GET NEW APPROX's.
PRINT ADJUSTED PARAMETER AND ALTERATIONS
HAS THE REQUIRED NO. OF ITERATION CYCLES BEEN COMPLETED?
NO
YES
PRINT FINAL RESULTS HEADING, BOOKEEPING DATA, NO. OF INTERIOR ELEMENTS
PRINT INTERIOR ELEMENTS
PRINT PHOTO COORDINATE DATA
IS PUNCHED OUTPUT DESIRED?
YES
PUNCH PHOTO COORDINATE DATA
COMPUTE SUM OF WEIGHTED SQUARED RESIDUALS, STD. ERROR UNIT WEIGHT SQUARED
PRINT STD. ERROR WEIGHT SQUARED
NO
IS VAR-COVAR MATRIX OUTPUT DESIRED?
YES
PRINT VARIANCE-COVARIANCE MATRIX
PUNCH VARIANCE-COVARIANCE MATRIX
STOP
NO

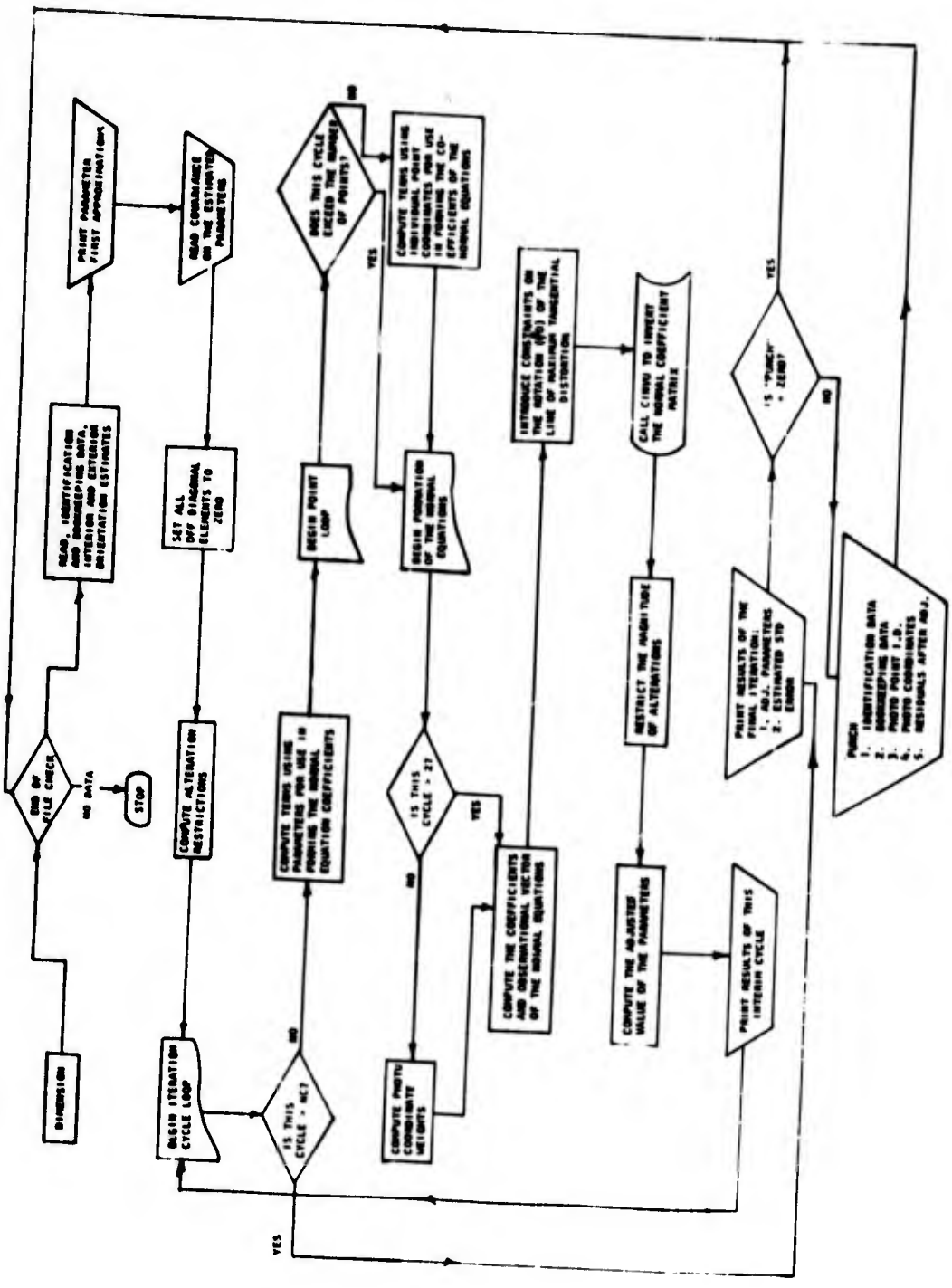
PROGRAM CER
DIMENSION
END OF FILE CHECK
NO DATA
STOP
READ, IDENTIFICATION AND BOOKKEEPING DATA, INTERIOR AND EXTERIOR ORIENTATION ESTIMATES
PRINT PARAMETER FIRST APPROXIMATIONS
READ COVARIANCE OF THE ESTIMATED PARAMETERS
SET ALL OFF DIAGONAL ELEMENTS TO ZERO
COMPUTE ALTERATION RESTRICTIONS
BEGIN ITERATION CYCLE LOOP
IS THIS CYCLE = MC?
NO
YES
DOES THIS CYCLE EXCEED THE NUMBER OF POINTS?
NO
YES
BEGIN POINT LOOP
COMPUTE TERMS USING PARAMETERS FOR USE IN FORMING THE NORMAL EQUATION COEFFICIENTS
COMPUTE TERMS USING INDIVIDUAL POINT COORDINATES FOR USE IN FORMING THE COEFFICIENTS OF THE NORMAL EQUATIONS
BEGIN FORMATION OF THE NORMAL EQUATIONS
IS THIS CYCLE = 2?
NO
YES
COMPUTE PHOTO COORDINATE WEIGHTS
COMPUTE THE COEFFICIENTS AND DISCREPANCY VECTOR OF THE NORMAL EQUATIONS
INTRODUCE CONSTRAINTS ON THE ROTATION (ΦΩ) OF THE LINE OF PASSAGE TANGENTIAL DISTORTION
CALL CINVU TO INVERT THE NORMAL COEFFICIENT MATRIX
RESTRICT THE MAGNITUDE OF ALTERATIONS
COMPUTE THE ADJUSTED VALUE OF THE PARAMETERS
PRINT RESULTS OF THIS ITERATION CYCLE
PRINT RESULTS OF THE FINAL ITERATION: 1. ADJ. PARAMETERS 2. ESTIMATED STD ERRORS
IS "FUNCT" = ZERO?
YES
NO
PUNCH
1. IDENTIFICATION DATA
2. BOOKKEEPING DATA
3. PHOTO POINT I.D.
4. PHOTO COORDINATES
5. RESIDUALS AFTER ADJ.

SUBROUTINE - CINVU - (INVERSION AND ALTERATION ROUTINE)

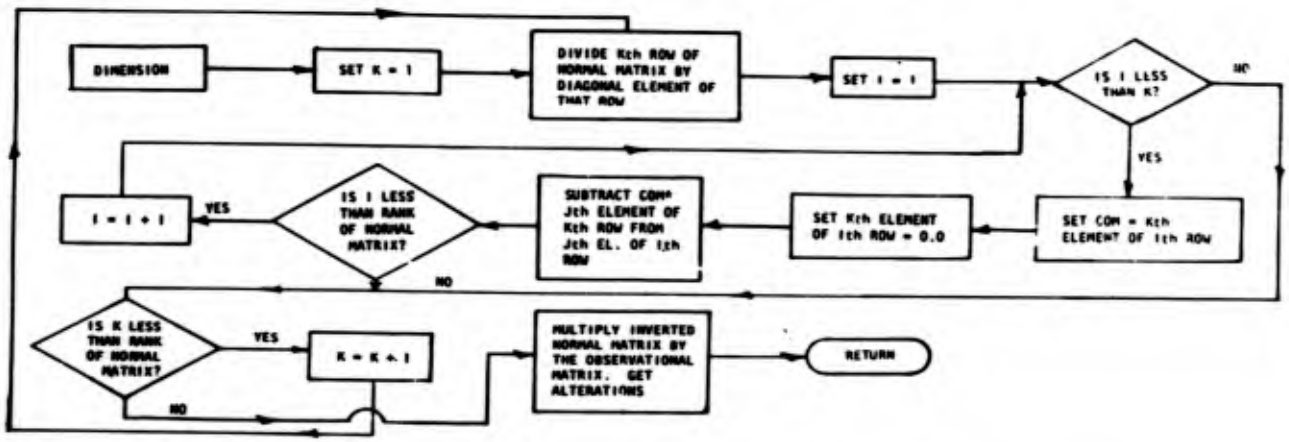

SUBROUTINE - CONCO (CORRECTS COMPARATOR COORDINATES FOR COMPARATOR ERRORS)

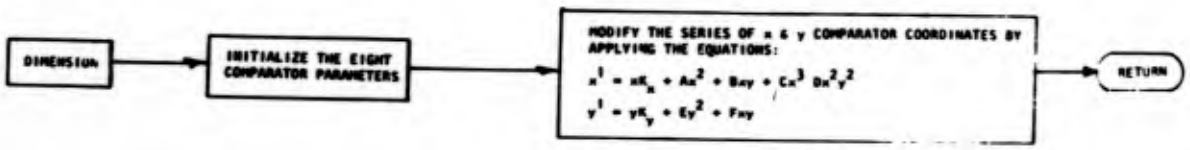

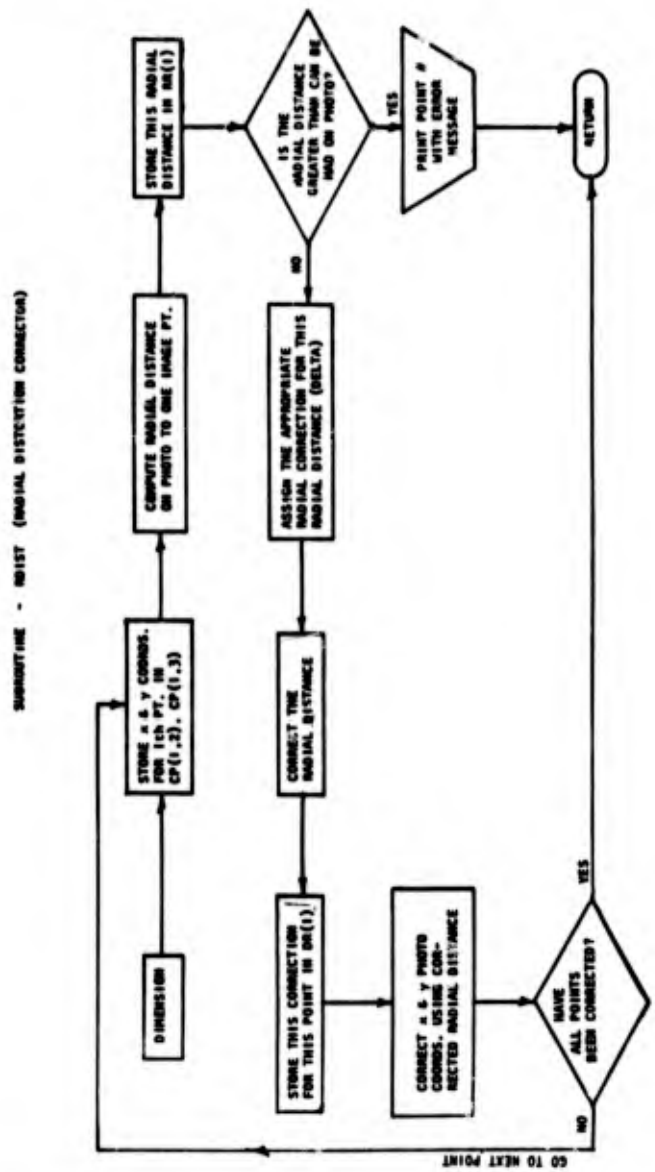
SUBROUTINE - RDIST (RADIAL DISTORTION CORRECTION)
DIMENSION
STORE x & y COORDS. FOR Ith PT. IN CP(I,1), CP(I,2)
COMPUTE RADIAL DISTANCE OF PHOTO TO ONE IMAGE PT.
STORE THIS RADIAL DISTANCE IN RR(I)
IS THE RADIAL DISTANCE GREATER THAN CAN BE HAD ON PHOTO?
YES
PRINT POINT # WITH ERROR MESSAGE
RETURN
NO
ASSIGN THE APPROPRIATE RADIAL CORRECTION FOR THIS RADIAL DISTANCE (DELTA)
CORRECT THE RADIAL DISTANCE
STORE THIS CORRECTION FOR THIS POINT IN DR(I)
CORRECT x & y PHOTO COORDS, USING CORRECTED RADIAL DISTANCE
HAVE ALL POINTS BEEN CORRECTED?
YES
NO
GO TO NEXT POINT

SUBROUTINE - REFRA (ATM. REFRACTION CORRECTOR)

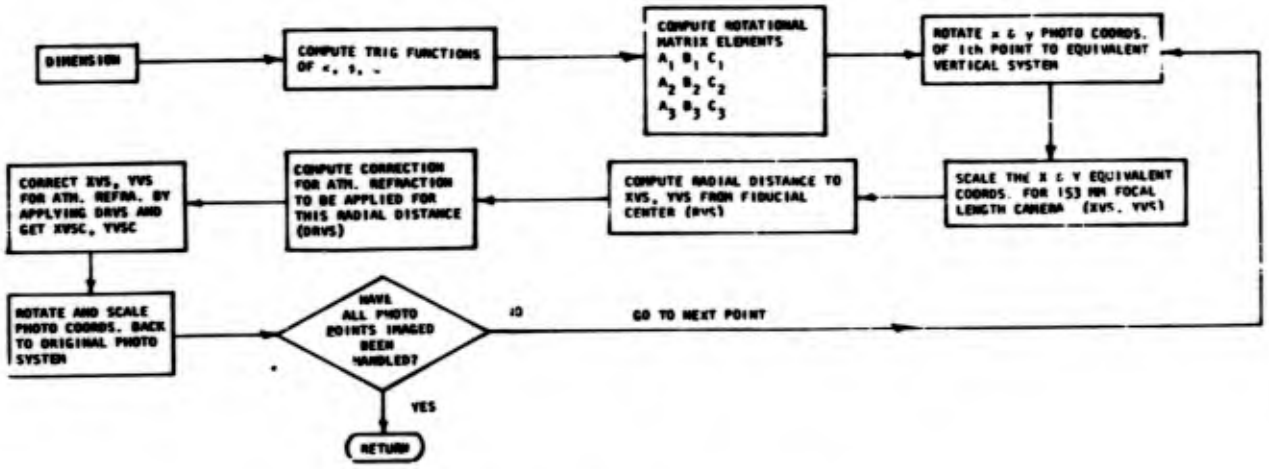

SUBROUTINE RID (RESEAU INTERSECTION IDENTIFICATION)

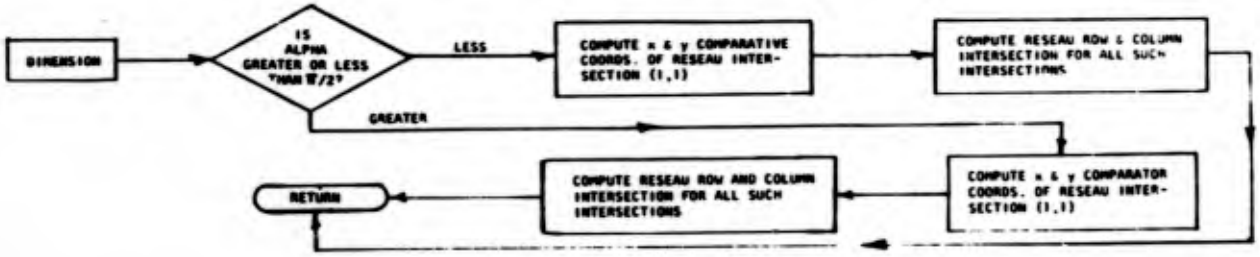

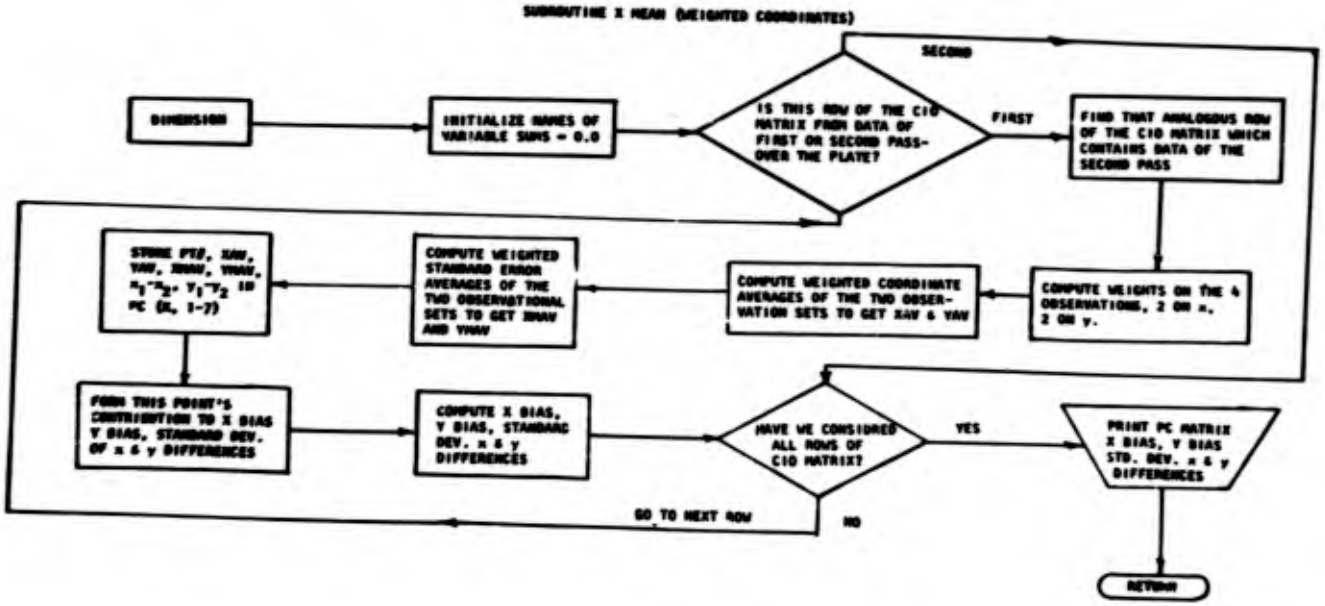
SUBROUTINE X MEAN (WEIGHTED COORDINATES)
DIMENSION
INITIALIZE NAMES OF VARIABLE SUMS = 0.0
IS THIS ROW OF THE C10 MATRIX FROM DATA OF FIRST OR SECOND PASS-OVER THE PLATE?
FIRST
SECOND
FIND THAT ANALOGOUS ROW OF THE C10 MATRIX WHICH CONTAINS DATA OF THE SECOND PASS
COMPUTE WEIGHTS ON THE 4 OBSERVATIONS, 2 ON x, 2 ON y.
COMPUTE WEIGHTED COORDINATE AVERAGES OF THE TWO OBSERVATION SETS TO GET XAV & YAV
COMPUTE WEIGHTED STANDARD ERROR AVERAGES OF THE TWO OBSERVATIONAL SETS TO GET XWAV AND YWAV
STORE PTD, XAV, YAV, XWAV, YWAV, x_1-x_2, y_1-y_2 IN PC (K, I-7)
FORM THIS POINT'S CONTRIBUTION TO X BIAS Y BIAS, STANDARD DEV. OF x & y DIFFERENCES
COMPUTE X BIAS, Y BIAS, STANDARD DEV. x & y DIFFERENCES
HAVE WE CONSIDERED ALL ROWS OF C10 MATRIX?
YES
NO
GO TO NEXT ROW
PRINT PC MATRIX X BIAS, Y BIAS STD. DEV. x & y DIFFERENCES
RETURN

APPENDIX B. FORTRAN LISTS

The FORTRAN Lists for programs flow diagrammed in Appendix A appear in this Appendix. The program language used was "PEST" which is essentially a sub-set of FORTRAN II. The programs were designed for use on the IBM 7074 computer. No external storage was required.

PROGRAM CRP

```
C     COMPARATOR TO RESEAU SUB-PROGRAM
C     CALLS COMCO,RID,CINVU
  100 DIMENSION CR(8,3),CI(8,5),IR(8,2),RX(17,17),RY(17,17),CCD(9),XO(5)
     1,U(5),C(5,5),A(5),XC(5),XB(8),YB(8),CIO(99,6),XT(5),CIT(8,9),CRT(8
     2,3),CII(4,2),PC(50,7)
      TYPE 1046
 1046 FORMAT(24HCHECK FOR PUNCHED OUTPUT)
      READ 10, JN,KN,LN,MN,IALT,IDATE,CC,XPP,YPP,K1
   10 FORMAT( 6I10/3F10.3,I10)
      READ 11, ((RX(I,J),RY(I,J),J=1,K1),I=1,K1)
   11 FORMAT (8F10.3)
    9 FORMAT (3E20.8)
C     READ PHOTO DATA
  110 CONTINUE
      READ 12,267,IPN,NP,SUB,PUNCH
   12 FORMAT(4I10)
      PRINT 20, JN,KN,IPN
C     READ  RESEAU ORIENTATION DATA
      READ 13, ALPHA,X19,Y19,XCT,YCT
      XA9=X19
      YA9=Y19
   13 FORMAT (5F10.3)
      KK=0
C     READ RESEAU AND ASSOC. IMAGE COMPAR. COORD.
C     ASSUMES 8 RESEAU AND 4 FIDUCIALS FOLLOWED BY 4 RESEAU AND 1 IMAGE
```

```
      NP1=NP+1
C     COMPUTE GROSS DX, DY, ALPHA
  121 PI=3.1415927
      COSA=COSF(ALPHA)
      SINA=SINF(ALPHA)
      XT(1)=XCT-134.739*COSA+127.060*SINA
      XT(2)=YCT-134.739*SINA-127.060*COSA
      XT(3)=ATANF(ABSF((XCT-XA9)/(YA9-YCT)))
      XT(4)=1.
      XT(5)=1.0
      PRINT 40, XT(3)
   40 FORMAT(/11HFIRST ALPHA,E16.6)
C     BEGIN COMPUTATION OF IMAGE COORD IN RESEAU SYSTEM
      DO 230 LL=1,NP1
      REJ=1.0
      DO 114 I=1,5
  114 XO(I)=XT(I)
      LLM1=LL-1
  115 IF(KK) 122,120,122
  120 IRN=8
      IIN=4
C     QUAD IDENTIFICATION
  136 IF(XCT-XA9)138,149,137
  137 IF(YA9-YCT)142,149,141
  138 IF(YA9-YCT)143,149,144
  141 GO TO 148
  142 XO(3)=PI-XO(3)
      GO TO 148
  143 XO(3)=PI+XO(3)
      GO TO 148
  144 XO(3)= 2.0*PI-XO(3)
  148 CONTINUE
      PRINT 41,XO(3)
   41 FORMAT(/12HSECOND ALPHA, E16.6)
```

```
      DO 1140 I=5,9,2
 1140 YM=YM+CIT(K,I)
      YM=YM/3.0
      YVV=0.0
      DO 1145 I=5,9,2
 1145 YVV=YVV+(YM-CIT(K,I))**2
      SEY= SQRTF(YVV/6.0)
      CI(K,1)=XM
      CI(K,2)=YM
      CI(K,3)=CIT(K,1)
      CI(K,4)=SEX
      CI(K,5)=SEY
       IF(KK)135,1146,135
 1146 CII(K,1)=SEX
      CII(K,2)=SEY
      PRINT 51
      PRINT 50,(CII(K,J),J=1,2)
   51 FORMAT(//// 84H RESULTS OF RESEAU TO FIDUCIAL CENTER TRANSFORMATIO
     1N/(TAKEN AS IMAGE OF POINT 1.000)//28H  S.E. X-FID    S.E. Y-FID
     1 )
   50 FORMAT(2E14.5)
  135 CONTINUE
      RI =12.5
  150 CALL COMCO(CCD,CR,IRN)
      PRINT 45, CI(1,3)
   45 FORMAT (///22HRESULTS-IMAGE OF POINT,F10.4,/)
  151 CALL COMCO(CCD,CI,IIN)
  152 CALL RID (CR,IR,IRN,RI,ALPHA,XCT,YCT)
  155 DO 177 LLL=1,2
      IREJ=0
      OS=0.0
      DO 160 K=1,5
      U(K)=0.0
      DO 160 L=1,5
      C(K,L)=0.0
  160 CONTINUE
      DO 173 LOOP=1,IRN
      I=IR(LOOP,1)
      J=IR(LOOP,2)
C     BEGIN ADJUST FOR PARAMETERS OF TRANS.
```

```
      GO TO 130
  149 XO(3)=ALPHA
      GO TO 130
   16 FORMAT (/6HREGION,I5,12HRESEAU POINT,I5,13HREJECTED IN Y)
   17 FORMAT(/6HREGION,I5,12HRESEAU POINT,I5,13HREJECTED IN X)
  122 IRN=4
      IIN=1
      GO TO 130
  130 READ 14, ((CRT(I,J),J=2,3),I=1,IRN)
      READ 15, ((CIT(I,J),J=1,9),I=1,IIN)
   14 FORMAT(8X,2F8.3)
   15 FORMAT (9F8.3)
      XT(3)=XO(3)
      DO 133 I=1,IRN
      DO 133 J=1,2
      JJP=J+1
  133  CR(I,J)=CRT(I,JJP)
      DO 135 K=1,IIN
      XM=0.0
      DO 134 I=4,8,2
  134 XM=XM+CIT(K,I)
      XM=XM/3.0
      XVV=0.0
      DO 1135 I=4,8,2
 1135 XVV=XVV+(XM-CIT(K,I))**2
      SEX= SQRTF(XVV/6.0)
      YM=0.0
```

```
      SINA=SINF(XO(3))
      COSA=COSF(XO(3))
      SINAB=SINF(XO(3)-CCD(3))
      COSAB= COSF(XO(3)-CCD(3))
C      FOR X
      DO 161 K=1,5
  161 A(K)=0.0
      A(1)=1.0
      A(3)=-(RX(I,J)*SINA+RY(I,J)*COSA)/XO(4)
      A(4)= -(RX(I,J)*COSA-RY(I,J)*SINA)/XO(4)**2
      O=CR(LOOP,1)-XO(1)+A(4)*XO(4)
      PRINT 33,O,LOOP
   33 FORMAT(E16.6,18H X RISID FOR POINT,I10)
      IF(REJ-ABSF (O))900,900,905
  900 DO 901 III=1,5
  901 A(III)=0.0
      LLM1=LL-1
      PRINT 17, LLM1,LOOP
      IREJ=IREJ+1
      GO TO 906
  905 OS=OS+O**2
  906 DO 163 K=1,5
      U(K)=U(K)+A(K)*O
      DO 162 L=1,5
  162 C(K,L)=C(K,L)+A(K)*A(L)
  163 CONTINUE
C     FOR Y
  170 CONTINUE
      DO 171 K=1,5
  171 A(K)=0.0
      A(2)=1.0
      A(3)=(RX(I,J)*COSAB-RY(I,J)*SINAB)/XO(5)
      A(5)=-(RX(I,J)*SINAB+RY(I,J)*COSAB)/XO(5)**2
      O=CR(LOOP,2)-XO(2)+A(5)*XO(5)
```

```
      PRINT 34,O
   34 FORMAT(E16.6,8H Y RESID)
      IF(REJ-ABSF(O))998,998,1000
  998 DO 999 III=1,5
  999 A(III)=0.0
      LLM1=LL-1
      PRINT 16, LLM1,LOOP
      IREJ=IREJ+1
      GO TO 1001
 1000 OS=OS+O**2
 1001 DO 173 K=1,5
      U(K)=U(K)+A(K)*O
      DO 172 L=1,5
  172 C(K,L)=C(K,L)+A(K)*A(L)
  173 CONTINUE
      PREJ=IREJ
      TIRN=IRN
      TEST=2.0*TIRN-5.0-PREJ
      IF(TEST) 1173,1173,174
 1173 PRINT 48, CI(1,3)
   48 FORMAT(/6HREGION,F10.4,9HREJECTED )
      GO TO 177
  174 REJ=3.0*SQRTF(OS/TEST)
  175 CALL CINVU(C,U,5,XC)
      DO 176 N=1,5
  176 XO(N)=XO(N)+XC(N)
  177 CONTINUE
      OS=0.0
      DO 178 I=1,IRN
      O=CR(LOOP,1)-XO(1)+A(4)*XO(4)
      OS=O**2
      O=CR(LOOP,2)-XO(2)+A(5)*XO(5)
  178 OS=O**2
```

```
      PRINT 46,(XO(I),I=1,5)
   46 FORMAT(/7HDELTA X,6X,7HDELTA Y,10X,5HALPHA,8X,7HSCALE X,8X,7HSCALE
     1 Y/2F10.4,3E16.6)
      TIRN=IRN
      OSS=SQRTF(OS/(2.0*TIRN-5.0))
      PRINT 47,OSS
   47 FORMAT  (/27HSTD. ERROR OF UNIT WT. (MM),E12.4//)
C     TRANSFORM IMAGE COORD TO RESEAU COORD
      SINA=SINF(XO(3))
      COSA=COSF(XO(3))
      SINAB=SINF(XO(3)-CCD(3))
      COSAB=COSF (XO(3)-CCD(3))
      DEN= COSA*COSAB+SINA*SINAB
      DO 180 I=1,IIN
      X=CI(I,1)
      Y=CI(I,2)
      DX = XO(4)*(X-XO(1))
      DY=XO(5)*(Y-XO(2))
      CI(I,1)=(DY*SINA+DX*COSAB)/DEN
  180 CI(I,2)=(DY*COSA-DX*SINAB)/DEN
C     BRANCH TO COMPUTE PHOTO COORD
      IF(KK)225,200,225
  200 KK=1
      DO 210 I=1,4
      XB(I)=CI(I,1)
  210 YB(I)=CI(I,2)
      DENO=(XB(4)-XB(2))*(YB(3)-YB(1))-(XB(1)-XB(3))*(YB(2)-YB(4))
  215 XOO= ((XB(1)-XB(3))*(XB(2)*YB(4)-YB(2)*XB(4))-(XB(4)-XB(2))*(XB(3)
     1*YB(1)-XB(1)*YB(3)))/DENO
  216 YOO= ((YB(2)-YB(4))*(XB(3)*YB(1)-XB(1)*YB(3))+(YB(3)- YB(1))*(XB(4
     1)*YB(2)-XB(2)*YB(4)))/DENO
      PI2=2.0*PI
      GAM=ATANF(ABSF((XB(4)-XB(2))/(YB(2)-YB(4))))
      IF(ALPHA-PI/2.0)2001,2001,1002
```

```
 2001 IF(XB(4)-XB(2))1011,2000,2000
 1011 GAM=PI2-GAM
      GO TO 2000
 1002 IF(XB(4)-XB(2)) 1014,1012,1012
 1012 GAM=PI-GAM
      GO TO 2000
 1014 GAM=PI+GAM
 2000 CONTINUE
      SING =SINF(GAM)
      COSG =COSF(GAM)
  222 GO TO 230
C     TRANSFORM RESEAU TO PHOTO
  225 CIO(LLM1,1)=CI(1,3)
      DX=CI(1,1)-XOO
      DY=CI(1,2)-YOO
      CIO  (LLM1,2)=DX*COSG+DY*SING
      CIO(LLM1,3)=-DX*SING+DY*COSG
      CIO(LLM1,4)=OSS
      CIO(LLM1,5)=SEX
      CIO(LLM1,6)=SEY
  230 CONTINUE
C     PRINT OUT
   20 FORMAT(/49HCOMPARATOR TO PHOTO COORDINATES THROUGH A RESEAU,/10HJO
     1B NUMBER,I10,/13HCAMERA NUMBER,I10,/13H PHOTO NUMBER,I10)
      PRINT 52, IPN
   52 FORMAT (C 2,62HCOMPARATOR TO PHOTO TRANSFORMATION-COMPOSITE RESULT
     1S FOR PHOTO,I10)
      PRINT 53, JN,KN,LN,MN,NP
   53 FORMAT(//6HJOB NO,I10,/9HCAMERA NO,I10,/7HLENS NO,I9,/6HMAG NO,I9,
     1/16HNUMBER OF POINTS,I10)
  240 PRINT 21
   21 FORMAT (/17HPHOTO COORDINATES)
   22 FORMAT(/9HPOINT NO.,6X,4HXMM,6X,4HYMM,4X,18HSTD ERROR UNIT WT.
```

```
   1,4X,16HSTD ERROR X MEAN,4X,16HSTD ERROR Y MEAN)
242 PRINT 22
244 PRINT 23, ((CIO(I,J),J=1,6),I=1,NP)
 23 FORMAT (3F10.4,3E20.4)
     IF(SUB)265,265,255
255 NP=NP/2
    CALL XMEAN(NP,CIO,PC)
    DO 280 I=1,NP
    CIO(I,1)=PC(I,1)
    CIO(I,2)=PC(I,2)
    CIO(I,3)=PC(I,3)
    CIO(I,5)=PC(I,4)
280 CIO(I,6)=PC(I,5)
265 IF(PUNCH)250,250,245
245 PUNCH 24, JN,KN,LN,MN,IALT,IDATE,CC,XPP,YPP
 24 FORMAT (6I10/3F10.3)
    PUNCH 26, IPN,NP
 26 FORMAT (2I10)
    PUNCH 25, (CIO(I,1),CIO(I,2),CIO(I,3),CIO(I,5),CIO(I,6),IPN,I=1,NP
   1)
 25 FORMAT (5F10.4,I10)
250 CONTINUE
    GO TO 110
267 CONTINUE
    STOP
    END
```

PROGRAM SPR

```
C    PROGRAM CALLS MATIN,REFRA,RDIST
  101 DIMENSION C(30,30),PC(50 ,5),XO(6),SIGX(6,6),SC(50 ,4),X(6),D(100
  1011),V(100),SEXA(6),PRT(6),A(100,6),ATP(6,100),U(6),XA(6),PCE(50 ,5),
  1012PCFE(50,8),RR(50),DR(50),CCP(50,5)
  110 READ 10,710, JN,KN,LN,MN,IALT,IDATE,CC,XPP,YPP
   10 FORMAT (6I10/3F10.3)
      CC=-CC
      READ1,IPN,NC
    1 FORMAT (2I10)
      READ 2, ((PC(I,J),J=1,5),I=1,NC)
    2 FORMAT (5F10.3)
      DO 112 I=1,NC
      PC(I,4)=PC(I,4)+.0001
  112 PC(I,5)=PC(I,5)+.0001
      READ 3,((SC(I,J),J=1,4),I=1,NC)
    3 FORMAT (F10.3,3F10.2)
      READ 4,(PRT(I),I=1,6)
    4 FORMAT (6F10.3)
      READ 42, RK1,RK2,IQUIT
   42 FORMAT (E10.1,E10.2,I10)
      PRINT 70
   70 FORMAT(C 2)
      PRINT 5,JN,KN,LN,MN,IALT,IDATE,IPN
    5 FORMAT(/11HJOB NUMBER ,I10,/14HCAMERA NUMBER ,I10,/12HLENS NUMBER
    51,I10,/12HMAG. NUMBER ,I10,/20HALT ABOVE DATUM (M) ,I10,/14HDATE OF
```

```
   52 PHOTOG,I10,/13HPHOTO NUMBER ,I10)
      PRINT 6
    6 FORMAT(/19HSURVEY CONTROL DATA,/15X,5HPOINT,15X,1HX,20X,1HY,19X,1HZ)
     1Z)
      PRINT 63,((SC(I,J),J=1,4),I=1,NC)
   63 FORMAT(4F20.3)
      PRINT 7
    7 FORMAT(//21HPHOTO COORD. AND WTS.,/  50H   POINT      X (MM)     Y. (
     71MM)     MX (MM)    MY (MM))
      PRINT83,((PC(I,J),J=1,5),I=1,NC)
   83 FORMAT(3F10.3,2F10.4)
      READ 8,(XO(I),I=1,6)
    8 FORMAT(3F10.3,3F10.8)
      KCYCL=0
   37 FORMAT(F15.6,10H XO-MATRIX)
C     A'MATRIX AND L'MATRIX
  120 SK=SINF(XO(4))
      SP=SINF(XO(5))
      SW=SINF(XO(6))
      CK=COSF(XO(4))
      CP=COSF(XO(5))
      CW=COSF(XO(6))
  125 CONTINUE
  130 DO 135 I=1,NC
      NY=NC+I
      DX=SC(I,2)-XO(1)
      DY=SC(I,3)-XO(2)
      DZ=SC(I,4)-XO(3)
  172 XT=DX*CP*CK+DY*(CW*SK+SW*SP*CK)+DZ*(SW*SK-CW*SP*CK)
      YT=-DX*CP*SK+DY*(CW*CK-SW*SP*SK)+DZ*(SW*CK+CW*SP*SK)
      ZT=DX*SP-DY*SW*CP+DZ*CW*CP
      COZ=CC*(1.0/ZT**2)
      A(I,1  )=-COZ*(ZT*CP*CK-XT*SP)*100.
      A(I,2  )=-COZ*(ZT*(CW*SK+SW*SP*CK)+XT*SW*CP)*100.
```

```
      A(I,3   )=-COZ*(ZT*(SW*SK-CW*SP*CK)-XI*CW*CP)*100.
 2100 A(I,4   )=COZ*(-DX*CP*SK+DY*(CW*CK-SW*SP*SK)+DZ*(SW*CK+CW*SP*SK)
 21001)*ZT*.01
  212 A(I,5   )=COZ*(ZT*(-DX*SP*CK+DY*SW*CP*CK-DZ*CW*CP*CK)-XT*(DX*
  2121CP+DY*SW*SP-DZ*CW*SP))*.01
  214 A(I,6   )=COZ*(ZT*(DY*(CW*SP*CK-SW*SK)+DZ*(CW*SK+SW*SP*CK))+
     1XT*(DY*CW*CP+DZ*SW*CP))*.01
  220 CONTINUE
  230 A(NY,1   )=COZ*(ZT*CP*SK+YT*SP)*100.
      A(NY,2   )=-COZ*(ZT*(CW*CK-SW*SP*SK)+YT*SW*CP)*100.
      A(NY,3   )=-COZ*(ZT*(SW*CK+CW*SP*SK)-YT*CW*CP)*100.
  232 A(NY,4   )=COZ*(ZT*(-DX*CP*CK-DY*(CW*SK+SW*SP*CK)+DZ*(CW*SP*CK
     1-SW*SK)))*.01
  234 A(NY,5)  =COZ*(ZT*(DX*SP*SK-DY*SW*CP*SK+DZ*CW*CP*
     1SK)-YT*(DX*CP+DY*SW*SP-DZ*CW*SP))*.01
  236 A(NY,6   )=COZ*(ZT*(-DY*(SW*CK+CW*SP*SK)+DZ*(CW*CK-SW*SP*SK))+
     1YT*(DY*CW*CP+DZ*SW*CP))*.01
      O(I)=PC(I,2)-CC*XT*(1.0/ZT)
      O(NY)=PC(I,3)-CC*YT*(1.0/ZT)
  135 CONTINUE
      IF(KCYCL-1)239,239,248
  239 PRINT 69
  240 DO 249 I=1,NC
      NY=NC+I
       PRINT 68,PC(I,1),O(I),O(NY)
   68 FORMAT(F10.3,2E15.3)
   69 FORMAT(//9HRESIDUALS,/5X,5HPOINT,10X,1HX,15X,1HY)
  249 CONTINUE
  248 CONTINUE
      NC2=2*NC
   31 FORMAT(6E15.5,9H A-MZTRIX)
   32 FORMAT(E14.6,9H O-MATRIX)
C     N°MATRIX
      DO 200 I=1,NC
      DO 200 J=1,6
  200 ATP(J,I)=A(I,J)*(1.0/PC(I,4)**2)
```

```
      NCP1=NC+1
      DO 210 K=NCP1,NC2
      DO 210 J=1,6
      I=K-NC
  210 ATP(J,K)=A(K,J)*(1.0/PC(I,5)**2)
  250 DO 260 J=1,6
      DO 260 K=1,6
      C(J,K)=0.0
      DO 260 I=1,NC2
```

```
      PRINT 64,KP1
   64 FORMAT(///45HALTERATIONS AND ADJUSTED PARAMETERS FOR CYCLE,I10,/)
      PRINT 35,(X(I),I=1,6)
      PRINT 36,(XA(I),I=1,6)
   35 FORMAT( /E20.8,9H X-MATRIX  )
   36 FORMAT (/E20.8,10H XA MATRIX)
  283 CONTINUE
  300 DO 305 I=1,6
  305 XO(I)=XA(I)
      IF(KCYCL) 310,310,320
  310 CALL REFRA(PC,RK1,RK2,NC,XO,CC)
      DO 312 I1=1,NC
      DO 312 J1=1,3
  312 PCFE(I1,J1)=PC(I1,J1)
      CALL RDIST(PC,CCP,NC,RR,DR)
      DO 313 I1=1,NC
      DO 313 I2=2,3
  313 PC(I1,I2)=CCP(I1,I2)
      KCYCL=KCYCL+1
   50 FORMAT(5F10.4,7H ALT PC)
      GO TO 120
C     V MATRIX
  320 DO 392 I=1,NC2
      V(I)=0.
      DO 390 J=1,3
  390 V(I)=V(I)+A(I,J)*X(J)*0.01
      DO 391 J=4,6
  391 V(I)=V(I)+A(I,J)*X(J)*100.
      V(I)=V(I)-O(I)
  392 CONTINUE
   38 FORMAT(E15.8,9H V MATRIX)
  395 CONTINUE
      KCYCL=KCYCL+1
  406 SPVV=0.
      DO 408 I=1,NC
      NY=NC+I
```

```
      SPVV=SPVV+(V(I)**2)*(1./PC(I,4)**2)
  408 SPVV=SPVV+(V(I)**2)*(1./PC(I,5)**2)
  410 CONTINUE
      PRINT 39,SPVV,KP1
   39 FORMAT(/E15.4,15H SPVV FOR CYCLE,I10,///)
      IF(KCYCL-IQUIT)  465,465,470
  465 GO TO 120
C     VAR'COVAR MATRIX
  470 DENO=2*NC-6
      SEUWS=SPVV/DENO
      SEUW=SQRTF(SEUWS)
      PRINT 40, SEUW
   40 FORMAT(/30HSTANDARD ERROR OF UNIT WT (MM),E15.4,//)
      DO 472 K=1,6
      DO 472 L=1,6
  472 SIGX(K,L)=C(K,L)*SEUWS
      DO 473 I=1,3
      DO 473 J=1,6
      SIGX(I,J)=SIGX(I,J)*100.
  473 SIGX(J,I)=SIGX(J,I)*100.
      DO 475 I=4,6
      DO 475 J=1,6
      SIGX(I,J)=SIGX(I,J)*.01
  475 SIGX(J,I)=SIGX(J,I)*0.01
  480 CONTINUE
      PRINT 65
   65 FORMAT(//26HVARIANCE-COVARIANCE MATRIX)
      PRINT 41,((SIGX(I,J),J=1,6),I=1,6)
   41 FORMAT(6E12.4)
C     OUTPUT
      PRINT 66
   66 FORMAT( C 2,44HCOMPOSITE RESULTS FOR SINGLE PHOTO RESECTION)
  500 PRINT 20,IPN,NC,DET
   20 FORMAT(//14HPHOTO NUMBER   ,I10,/26HNUMBER OF CONTROL POINTS  ,I10,
```

```
 201/40HDETERMINANT OF NORMAL COEFFICIENT MATRIX ,E12.2)
510 DO 512 I=1,6
512 SEXA(I)=SQRTF(SIGX(I,I))
    CONTINUE
520 PRINT 21
 21 FORMAT(/44HORIENTATION WITH RESPECT TO RANGE (RADIANS).)
    PRINT 22
 22 FORMAT(8H   KAPPA,9X,47H+OR-      PHI          +OR-      OMEGA       +O
   1R-          )
    PRINT 23,(XA(I),SEXA(I) ,I=4,6)
 23 FORMAT(6F11.7)
530 PRINT 24
 24 FORMAT(/33HAIR STATION COORDINATES          ,/7X,1HX,15X,4H+OR-,13
 241X,1HY,12X,4H+OR-,13X,1HZ,12X,4H+OR-)
    PRINT 25,(XA(I),SEXA(I) ,I=1,3)
 25 FORMAT(6F15.4)
540 PRINT 26
 26 FORMAT(/40HPHOTO COORDINATES ALTERED FOR REFRACTION,/70H      POINT
 261      X MM       Y MM      MX MM      MY MM      VX MM      VY MM )
    CONTINUE
560 DO 570 I=1,NC
    DO 561 J=4,5
561 PCFE(I,J)=PC(I,J)
562 PCFE(I,6)=V(I)
    NY=I+NC
    PCFE(I,7)=V(NY)
    PCFE(I,8)=IPN
570 PRINT 27,(PCFE(I,J),J=1,7)
    CONTINUE
 27 FORMAT(F10.3,6F10.4)
    PRINT 67
 67 FORMAT(//14HSURVEY CONTROL,/2X,8HPOINT NO,7X,1HX,14X,1HY,14X,1HZ)
 28 FORMAT(F10.3,3F15.3)
582 PRINT 28,((SC(I,J),J=1,4),I=1,NC)
```

```
594   PUNCH 10, JN,KN,LN,MN,IALT,IDATE,CC,XPP,YPP
      PUNCH1,IPN,NC
      PUNCH 53,(XA(I),I=1,6)
 53   FORMAT (3F10.2,3F10.6)
      DO 60 I=1,NC
      PUNCH 56,(PCFE(I,J),J=1,8)
 60   PUNCH 57,(SC(I,J),J=2,4)
 56   FORMAT(3F10.3,4F10.4,F10.3)
 57   FORMAT (3F10.2)
700   CONTINUE
      GO TO 110
 52   FORMAT(I10)
710   STOP
      END
```

PROGRAM MPR

```
  101 DIMENSION XOI(8),XO(32),IB(5,3),D(200,10),C(36,36),U(32),II(7)
     1,A(32),S(32),AS(32)
  110 READ 1, NP,IEO,IIO,KOUNT
    1 FORMAT (4I10)
      NRANK=IEO+IIO
      READ 18,(II(I),I=1,7)
      READ 3,(XOI(I),I=1,IIO)
    3 FORMAT(3E15.8)
      READ2, JN,KN,LN,MN,IALT,IDATE,CC,XPP,YPP
    2 FORMAT(6I10/3F10.3)
C     FORM XO,D,IB
      DO 115 I=1,IIO
      J=NP*6+I
  115 XO(J)=XOI(I)
      IB(1,3)=0
  120 DO 138 M=1,NP
      READ 4, (IB(M,J),J=1,2)
    4 FORMAT(2I10)
      IB(M+1,3)=IB(M,2)+IB(M,3)
      READ 5,(XOI(I),I=1,6)
      DO 132I=1,6
      J=(M-1)*6+I
  132 XO(J)=XOI(I)
      L3=IB(M,3)+1
      L4=IB(M,2)+IB(M,3)
  136 DO 138 J=L3,L4
      READ 6,(D(J,K),K=1,5)
```

```
    6 FORMAT(5F10.3)
      READ 7,(D(J,K),K=6,8)
    7 FORMAT(3F10.3)
C     INTRODUCE HUMIDITY SCALE CORR IN Y ONLY
      D(J,3)=D(J,3)*1.000258
  138 CONTINUE
C     WEIGHTS
      DO 146 M=1,NP
      L3=IB(M,3)+1
      L4=IB(M,2)+IB(M,3)
      DO 145 J=L3,L4
      D(J,4)=1./D(J,4)**2
  145 D(J,5)=1./D(J,5)**2
  146 CONTINUE
C     BEGIN LOOPS
      KOUNT=4
  150 DO 330 KCYCL=1,KOUNT
C     BEGIN ITTERATION LOOP
      DO 155 I=1,NRANK
      U(I)=0.
      DO 155 J=1,NRANK
  155 C(I,J)=0.
      SB=SINF(XO(IEO+6))
      CB=COSF(XO(IEO+6))
      OS=0.
      PRINT 42
   42 FORMAT(33HGENERAL RESULTS FOR PHOTO NUMBERS)
      DO 164 M=1,NP
      PRINT 43, IB(M,1)
   43 FORMAT(I10)
  164 CONTINUE
C     BEGIN PHOTO LOOP
  163 DO 911 M=1,NP
      PRINT 41, IB(M,1),KCYCL
```

```
      MM=(M-1)*6
      SK=SINF(XO(MM+4))
      SP=SINF(XO(MM+5))
      SW=SINF(XO(MM+6))
      CK=COSF(XO(MM+4))
      CP=COSF(XO(MM+5))
      CW=COSF(XO(MM+6))
C     BEGIN POINT LOOP
      L3=IB(M,3)+1
      L4=IB(M,2)+IB(M,3)
      DO 910 N=L3,L4
      DX=D(N,6)-XO(MM+1)
      DY=D(N,7)-XO(MM+2)
      DZ=D(N,8)-XO(MM+3)
  172 XT=DX*CP*CK+DY*(CW*SK+SW*SP*CK)+DZ*(SW*SK-CW*SP*CK)
      YT=-DX*CP*SK+DY*(CW*CK-SW*SP*SK)+DZ*(SW*CK+CW*SP*SK)
      ZT=DX*SP-DY*SW*CP+DZ*CW*CP
      COZ=CC*(1.0/ZT**2)
      A(MM+1 )=-COZ*(ZT*CP*CK-XT*SP)
      A(MM+2 )=-COZ*(ZT*(CW*SK+SW*SP*CK)+XT*SW*CP)
      A(MM+3 )=-COZ*(ZT*(SW*SK-CW*SP*CK)-XT*CW*CP)
 2100 A(MM+4 )=COZ*(-DX*CP*SK+DY*(CW*CK-SW*SP*SK)+DZ*(SW*CK+CW*SP*SK)
 21001)*ZT
  212 A(MM+5 )=COZ*(ZT*(-DX*SP*CK+DY*SW*CP*CK-DZ*CW*CP*CK)-XT*(DX*
  2121CP+DY*SW*SP-DZ*CW*SP))
  214 A(MM+6 )=COZ*(ZT*(DY*(CW*SP*CK-SW*SK)+DZ*(CW*SK+SW*SP*CK))+
     1XT*(DY*CW*CP+DZ*SW*CP))
      RL2= (D(N,2)-XPP)**2+(D(N,3)-YPP)**2
      RL4=RL2**2
      RL6=RL2**3
      RC=1.0+XO(IEO+1)*RL2+XO(IEO+2)*RL4+XO(IEO+3)*RL6
      RCI=1.0/RC
      EJ=XO(IEO+4)*RL2+XO(IEO+5)*RL4
      XC=CC*XT*(1.0/ZT)
      XC=XC*RCI+EJ*SB
      DXOR=(D(N,2)-XPP)/RC**2
```

```
      A(IEO+1)=-DXOR*RL2
      A(IEO+2)=-DXOR*RL4
      A(IEO+3)=-DXOR*RL6
      A(IEO+4)=SB*RL2/RC
      A(IEO+5)=SB*RL4/RC
      A(IEO+6)=CB*(XO(IEO+4)*RL2+XO(IEO+5)*RL4)/RC
      O=D(N,2)-XPP-XC
      OS=OS+O**2
      PRINT 31,O,D(N,1)
   31 FORMAT(E12.5,7H O OF X,2X,5HPOINT,2X,F10.4)
 2500 GO TO(2501,2502,2503,2504),M
 2501 L7=1
      L8=6
      GO TO 2550
 2502 L7=7
      L8=12
      GO TO 2550
 2503 L7=13
      L8=18
      GO TO 2550
 2504 L7=19
      L8=24
      GO TO 2550
 2550 CONTINUE
 2552 CONTINUE
 2600 CONTINUE
      DO 810 I=1,NRANK
      U(I)=U(I)+A(I)*D(N,4)*O
      DO 808 J=1,NRANK
  808 C(I,J)=C(I,J)+A(I)*D(N,4)*A(J)
  810 CONTINUE
      DO 811 I=1,NRANK
  811 A(I)=0.
  230 A(MM+1  )=COZ*(ZT*CP*SK+YT*SP)
```

```
      A(MM+2   )=-COZ*(ZT*(CW*CK-SW*SP*SK)+YT*SW*CP)
      A(MM+3   )=-COZ*(ZT*(SW*CK+CW*SP*SK)-YT*CW*CP)
  232 A(MM+4   )=COZ*(ZT*(-DX*CP*CK-DY*(CW*SK+SW*SP*CK)+DZ*(CW*SP*CK
     1-SW*SK)))
  234 A(MM+5   )=COZ*(ZT*(DX*SP*SK-DY*SW*CP*SK           +DZ*CW*CP*
     1SK)-YT*(DX*CP+DY*SW*SP-DZ*CW*SP))
  236 A(MM+6   )=COZ*(ZT*(-DY*(SW*CK+CW*SP*SK)+DZ*(CW*CK-SW*SP*SK))+
     1YT*(DY*CW*CP+DZ*SW*CP))
      YC=CC*YT*(1.0/ZT)
      YC=YC*RCI-EJ*CB
      DYOR=(D(N,3)-YPP)/RC**2
      A(IEO+1)=-DYOR*RL2
      A(IEO+2)=-DYOR*RL4
      A(IEO+3)=-DYOR*RL6
      A(IEO+4)=-CB*RL2/RC
      A(IEO+5)=-CB*RL4/RC
      A(IEO+6)=SB*(XO(IEO+4)*RL2+XO(IEO+5)*RL4)/RC
      O=D(N,3)-YPP-YC
      OS=OS+O**2
      PRINT 32,O,D(N,1)
   32 FORMAT(E12.5,7H O OF Y,2X,5HPOINT,2X,F10.4)
 3500 GO TO(3501,3502,3503,3504),M
 3501 L7=1
      L8=6
      GO TO 3550
 3502 L7=7
      L8=12
      GO TO 3550
 3503 L7=13
      L8=18
```

```
      GO TO 3550
 3504 L7=19
      L8=24
      GO TO 3550
 3550 CONTINUE
 3600 CONTINUE
      DO 910 I=1,NRANK
      U(I)=U(I)+A(I)*D(N,5)*O
      DO 908 J=1,NRANK
  908 C(I,J)=C(I,J)+A(I)*D(N,5)*A(J)
  912 D(N,9)=D(N,2)-XPP-XC
      D(N,10)=D(N,3)-YPP-YC
  910 CONTINUE
      DO 911 I=1,NRANK
      A(I)=0.
  911 CONTINUE
  309 CONTINUE
      PRINT 49,OS
  310 CONTINUE
C     INVERSION BY GAUSS JORDAN WITH PIVOTING
      NRP1=NRANK +1
      DO 311 I=1,NRANK
  311 C(I,NRP1)=U(I)
      M=NRANK
      N=1
  320 CALL MATIN(C,M,N,ISING,DET)
      DO 330 I=1,NRANK
  325 XO(I)=XO(I)+C(I,NRANK+1)
      PRINT 17,I,XO(I),C(I,NRANK+1)
  330 CONTINUE
```

```
C       BIGIN OUTPUT
        PRINT 45
   45 FORMAT(C 2,24HFINAL RESULTS FOR PHOTOS)
        DO 335 I5=1,NP
        PRINT 43,IB(I5,1)
  335 CONTINUE
        PRINT 8, JN,KN,LN,MN,NP,IIO
    8 FORMAT (// 6HJOB NO,I10,/·9HCAMERA NO,I10,/7HLENS NO,I10,/ 6HMAG N
     1O,I10,/16HNUMBER OF PHOTOS,I10,/27HNUMBER OF INTERIOR ELEMENTS,I10
     2)
        L5=IE0+IIO
        L6=IB(NP,2)+IB(NP,3)
        L7=IE0+1
        PRINT 9
    9 FORMAT (//5X,2HK1,13X,2HK2,13X,2HK3,13X,2HJ1,13X,2HJ2,13X,4HRETA )
        PRINT 10,(XO(I),I=L7,L5)
   10 FORMAT (6E15.8)
        PRINT 11
   11 FORMAT (//11HDATA MATRIX,/4X,5HPT NO,6X,4HX MM,6X4HY MM,6X,2HPX,8X
     12HPY,8X,2HVX,8X,2HVY)
        PRINT 12,((D(I,J),J=1,5),(D(I,K),K=9,10),I=1,L6)
   12 FORMAT (3F10.3,2E10.3,2E10.3)
  350 CONTINUE
        IF(II(1))354,354,352
  352 PUNCH 13,((D(I,J),J=2,3),(D(I,J),J=9,10),D(I,1),I=1,L6)
   13 FORMAT(4F10.4,13HCONTROL PT NO,F8.3)
  354 CONTINUE
C       BEGIN ANALSIS OF RESIDUALS
        SPVV=0.
        L2=IB(NP,3)+IB(NP,2)
        DO 362 I=1,L2
```

```
      SPVV=SPVV+D(I,4)*D(I,9)**2+D(I,5)*D(I,10)**2
      DENO=2*L2-IEO-IIO
  362 SEUWS=SPVV/DENO
      PRINT 14, SEUWS
   14 FORMAT (/23HSTD ERROR OF UNIT WT SO,E16.6)
      IF(II(2)) 390,390,370
  370 CONTINUE
      IF(NP-2)273,274,275
  273 L8=1
      GO TO 280
  274 L8=2
      GO TO 280
  275 IF(NP-4)276,277,277
  276 L8=2
      GO TO 280
  277 L8=3
      GO TO 280
  280 DO 285 M=1,L8
      PRINT 16
      K=(M-1)*12+1
      DO 285 I=1,NRANK
      KP11=K+11
  285 PRINT 15,(C(I,J),J=K,KP11)
  286 PUNCH 48, ((C(I,J),J=K,KP11),I=1,NRANK)
   48 FORMAT (8E10.3)
    5 FORMAT(3F10.3,3F10.6)
   15 FORMAT(12E10.3)
   16 FORMAT(C 2,26HVARIANCE-COVARIANCE MATRIX)
   17 FORMAT(/I10,2E16.8,17H ADJ PAR AND ALT )
   18 FORMAT(7I10)
   40 FORMAT(6E10.3)
   41 FORMAT(/5HPHOTO,2X,I10,2X,5HCYCLE,2X,I10)
   49 FORMAT(/37HNON WIEGHTED SUM OF SQUARED RESIDUALS,E15.4,/)
  390 CONTINUE
  395 STOP
      END
```

PROGRAM CER

```
C      RESECTION ON ONE PHOTO WITH CORRELATION ELIMINATION
C      PROGRAM CALLS CINVU
       DIMENSION ALT(30),OUT(50,2),XO(12),D(50,13),C(30,30),U(30),A(12)
      1,DEL(30),CV(30,30),XOO(12),P(12,12),PL(12)
  100 READ 1,550,JN,KN,LN,MN,IEO,NP,PN
    1 FORMAT(6I10,F10.4)
      READ2,NC,NU,NR
    2 FORMAT(3I10)
      READ3,XPP,YPP
    3 FORMAT(2F10.3)
  105 READ 4,(XO(I),I=1,5)
    4 FORMAT(2F10.3,3F10.6)
      READ5,(XO(I),I=6,11)
    5 FORMAT(3E15.8)
      READ6,XO(12)
    6 FORMAT(F10.3)
      XO(12)=-XO(12)
   30 FORMAT(6F10.0)
      LOOP=0
      PRINT 10,LOOP,(XO(I),I=1,NU)
      PHIO=XO(11)
      COJ1=XO(9)
C     COVARIANCE INPUT AND MOD
      READ 36, ((CV(I,J),J=1,NU),I=1,NU)
```

```
   36 FORMAT (8E10.3)
      DO 1110 I=1,12
      DO 1109 J=4,12
      JM1=J-1
 1109 CV(I,JM1)=CV(I,J)
 1110 CONTINUE
      DO 1120 J=1,11
      DO 1119 I=4,12
      IM1=I-1
 1119 CV(IM1,J)=CV(I,J)
 1120 CONTINUE
      PRINT 37
   37 FORMAT(//9HMOD COVAR)
      PRINT 38,((CV(I,J),J=1,11),I=1,11)
   38 FORMAT(11E10.2)
      DO 107 I=1,12
  107 XOO(I)=XO(I)
      DO 108 I=1,12
  108 CV(I,12)=0.
      DO 109 J=1,12
  109 CV(12,J)=0.
      CV(12,12)=.00001
      DO 1121 I=1,12
      J=I
      P(I,J)=1./CV(I,J)
 1121 CONTINUE
   31 FORMAT(//16HINTIAL ESTIMATES,/2F15.2,4E15.5)
   32 FORMAT(5E15.5,F10.3)
      DO110I=1,NP
  110 READ7,(D(I,J),J=1,8)
    7 FORMAT(5F10.3/3F10.3)
```

```
      PUNCH=0.
      PRT1=0.
      DEL(6)=0.5*EXPF(-8.0)
      DEL(7)=0.5*EXPF(-11.)
      DEL(8)=0.2*EXPF(-15.)
      DEL(9)=0.1*EXPF(-6.)
      DEL(10)=0.1*EXPF(-11.)
      DEL(11)=0.1
      DEL(12)=0.01
C     BEGIN LOOP
  120 CONTINUE
      DO 510 LOOP=1,NC
      PRT1=PRT1+1.
      DO291J=1,NU
      U(J)=0.
      DO290K=1,NU
  290 C(J,K)=0.
  291 CONTINUE
      OS=0.
  130 XCS=XO(1)
      YCS=XO(2)
      CK=COSF(XO(3))
      SK=SINF(XO(3))
      SP=SINF(XO(4))
      CP=COSF(XO(4))
      CW=COSF(XO(5))
      SW=SINF(XO(5))
  140 AK1=XO(6)
      AK2=XO(7)
      AK3=XO(8)
```

```
      AJ1=X0(9)
      AJ2=X0(10)
  150 B=X0(11)
      CC=X0(12)
      CB=COSF(B)
      SB=SINF(B)
      SINB=SB
      COSB=CB
  160 T11=CP*CK
      T12=CP*SK
      T13=-SP
      T21=-CW*SK+SW*SP*CK
      T22=CW*CK+SW*SP*SK
      T23=SW*CP
  170 T31=SW*SK+CW*SP*CK
      T32=-SW*CK +CW*SP*SK
      T33=CW*CP
  180 T11K=-CP*SK
      T11P=-SP*CK
      T11W=0.
      T12K=CP*CK
      T12P=-SP*SK
  181 T12W=0.
      T13P=-CP
      T13W=0.
  182 T21K=-CW*CK-SW*SP*SK
      T21P=SW*CP*CK
      T21W=SW*SK+CW*SP*CK
```

```
      T22K=-CW*SK+SW*SP*CK
  183 T22P=SW*CP*SK
      T22W=-SW*CK+CW*SP*SK
      T23K=0.
      T23P=-SW*SP
  184 T23W=CW*CP
      T31K=SW*CK+CW*SP*SK
      T31P=CW*CP*CK
      T31W=-SW*SP*CK+CW*SK
  185 T32K=SW*SK+CW*SP*CK
      T32P=CW*CP*SK
      T32W=-CW*CK-SW*SP*SK
      T33K=0.
      T33P=-CW*SP
  186 T33W=-SW*CP
C     COMPUTE X-PRIME,Y-PRIME,Z-PRIME
  200 DO210I=1,NP
      D(I,9)=D(I,2)*T11+D(I,3)*T12+CC*T13
      D(I,10)=D(I,2)*T21+D(I,3)*T22+CC*T23
  210 D(I,11)=D(I,2)*T31+D(I,3)*T32+CC*T33
  220 CONTINUE
      KI=-1
C     BEGIN POINT LOOP
      DO 433I=1,NP
      KI=KI*(-1)
      IA=I+KI
  226 CONTINUE
  230 R2=(D(I,2)-XPP)**2+(D(I,3)-YPP)**2
      R4=R2*R2
      R6=R4*R2
      AK=1.+R2*XO(6)+R4*XO(7)+R6*XO(8)
      CJ=R2*XO(9)+R4*XO(10)
      R2J=(D(IA,2)-XPP)**2+(D(IA,3)-YPP)**2
```

```
      R4J=R2J*R2J
      R6J=R4J*R2J
      AKJ=1.+R2J*XO(6)+R4J*XO(7)+R6J*XO(8)
      CJJ=R2J*XO(9)+R4J*XO(10)
  240 XI=AK*(D(I,2)-XPP)-CJ*SINB
      YI=AK*(D(I,3)-YPP)+CJ*COSB
      XJ=AKJ*(D(IA,2)-XPP)-CJJ*SINB
      YJ=AKJ*(D(IA,3)-YPP)+CJJ*COSB
  250 DXJ=D(IA,6)-XO(1)
      DYJ=D(IA,7)-XO(2)
      DELZ=D(I,8)-D(IA,8)
      DXI=D(I,6)-XO(1)
  260 DYI=D(I,7)-XO(2)
      XPI=XI*T11+YI*T12+CC*T13
      YPI=XI*T21+YI*T22+CC*T23
      ZPI=XI*T31+YI*T32+CC*T33
      XPJ=XJ*T11+YJ*T12+CC*T13
      YPJ=XJ*T21+YJ*T22+CC*T23
      ZPJ=XJ*T31+YJ*T32+CC*T33
      D(I,9)=XPI
      D(I,10)=YPI
      D(I,11)=ZPI
      D(IA,9)=XPJ
      D(IA,10)=YPJ
      D(IA,11)=ZPJ
      XD=DELZ+ZPJ*DXJ/XPJ
  280 YD=DELZ+ZPJ*DYJ/YPJ
      SBX=DXI*ZPI/XD-YI*T12-CC*T13
      SBY=DYI*ZPI/YD-XI*T21-CC*T23
C     BEGIN FORMATION OF NORMALS
      PXSB=1./(AK*T11)
```

```
C    COMPUTATION OF WEIGHTS
       IF(PRT1-1.)294,982,294
  982 CONTINUE
       IF(XD)2281,2282,2281
 2281 IF(XPJ)282,2282,282
  282 D(I,12)=1./(D(I,4)**2+(((DXI*ZPI/XD**2)*(ZPJ*DXJ/XPJ**2)*(1./
     1AK))**2)*D(IA,4)**2)
       GO TO 2283
 2282 D(I,12)=0.
 2283 IF(YD)3281,3282,3281
 3281 IF(YPJ)283,3282,283
  283 D(I,13)=1./(D(I,5)**2+(((DYI*ZPI/YD**2)*(ZPJ*DYJ/YPJ**2)*(1./AK
     1))**2)*D(IA,5)**2)
       GO TO 294
 3282 D(I,13)=0.
  294 CONTINUE
C      FORX
       DO295J=1,NU
  295 A(J)=0.
  301 A(1)=((-XD*ZPI+DXI*ZPI*ZPJ/XPJ)*PXSB)/XD**2
       A(3)=(1./XD**2)*(XD*DXI*(XI*T31K+YI*T32K)-(DXI*ZPI*DXJ/XPJ**2)*(XP
     1J*( XJ*T31K+YJ*T32K)-ZPJ*(XJ*T11K+YJ*T12K)))-YI*T12K
  303 A(3)=(A(3)*T11-SBX*T11K)/(CK*T11**2)
       A(4)=(1./XD**2)*(XD*DXI*(XI*T31P+YI*T32P+CC*T33P)-(DXI*ZPI*DXJ/XPJ
     1**2)*(XPJ*(XJ*T31P+YJ*T32P+CC*T33P)-ZPJ*(XJ*T11P+YJ*T12P+CC*T13P))
     2)-YI*T12P-CC*T13P
  304 A(4)=(A(4)*T11-SBX*T11P)/(AK*T11**2)
       A(5)=(1./XD**2)*(XD*DXI*(XI*T31W+YI*T32W+CC*T33W)-(DXI*ZPI*DXJ/XPJ
     1**2)*(XPJ*(XJ*T31W+YJ*T32W+CC*T33W)))
  305 A(5)=A(5)/AK*T11
```

```
      306 A(6)=R2*(XPP-XI)/AK
      307 A(7)=-R4*(XI-XPP)/AK
      308 A(8)=-R6*(XI-XPP)/AK
      309 A(9)=R2*SINB/AK
      310 A(10)=R4*SINB/AK
      311 A(11)=CJ*COSB/AK
      312 A(12)=(PXSB/XD**2)*(XD*DXI*CW*CP-(DXI*ZPI*DXJ/XPJ**2)*(XPJ*CW*CP+Z
         1PJ*SP))+SP*PXSB
      320 CONTINUE
      325 O=D(I,2)-(XPP+(1./AK)*((1./T11)*(DXI*ZPI/XD-YI*T12-CC*T13)+CJ*SINB
         1))
          PRINT 8,D(I,1),O,D(I,12)
       22 FORMAT(7E16.6,6H X OBS)
       24 FORMAT(4E16.6,2I10)
          OS=OS+D(I,12)*O**2
        8 FORMAT(14HX RESID FOR PT,F10.4,3H IS,E16.4,10X ,3H WT,E16.4)
          OUT(I,1)=O
          DO333K=1,NU
          U(K)=U(K)+A(K)*O*D(I,12)
          DO332L=1,NU
      332 C(K,L)=C(K,L)+A(K)*A(L)*D(I,12)
      333 CONTINUE
C         FORY
      350 PYSB=1./(AK*T22)
          DO355J=1,NU
      355 A(J)=0.
          A(2)=(-YD*ZPI+DYI*ZPI*ZPJ/YPJ)/YD**2
      402 A(2)=PYSB*A(2)
          A(3)=(1./YD**2)*(YD*DYI*(XI*T31K+YI*T32K)-(DYI*ZPI*DYJ/YPJ**2)*(YP
         1J*(XJ*T31K+YJ*T32K)-ZPJ*(XJ*T21K+YJ*T22K)))-XI*T21K
      403 A(3)=(A(3)*T22-SBY*T22K)/(CK*T22**2)
```

```
      A(4)=(1./YD**2)*(YD*DYI*(XI*T31P+YI*T32P+CC*T33P)-(DYI*ZPI*DYJ/YPJ
     1**2)*(YPJ*(XJ*T31P+YJ*T32P+CC*T33P)-ZPJ*(XJ*T21P+YJ*T22P+CC*T23P))
     2)-XI*T21P-CC*T23P
  404 A(4)=(A(4)*T22-SBY*T22P)/(AK*T22**2)
      A(5)=(1./YD**2)*(YD*DYI*(XI*T31W+YI*T32W+CC*T33W)-(DYI*ZPI*DYJ/YPJ
     1**2)*(YPJ*(XJ*T31W+YJ*T32W+CC*T33W)-ZPJ*(XJ*T21W+YJ*T22W)))-XI*T21
     2W-CC*T23W
  405 A(5)=(A(5)*T22-SBY*T22W)/(AK*T22**2)
      DYOK=-(YI-YPP)/AK
  406 A(6)=R2*DYOK
  407 A(7)=R4*DYOK
  408 A(8)=R6*DYOK
  409 A(9)=-R2*CB/AK
  410 A(10)=-R4*CB/AK
  411 A(11)=(CJ/CK)*SB
  412 A(12)=(1./(AK*T22*YD**2))*(YD*DYI*T33-(DYI*ZPI*DYJ/YPJ**2)*(YPJ*T3
     13-ZPJ*T23))-T23/(AK*T22)
  420 CONTINUE
  425 O=D(I,3)-(YPP+(1./AK)*((1./T22)*(DYI*ZPI/YD-XI*T21-CC*T23)-CJ*CB)
     1)
      PRINT 9,D(I,1),O,D(I,13)
   23 FORMAT(7E16.6,6H Y OBS)
   25 FORMAT(4E16.6)
      OS=OS+D(I,13)*O**2
      OUT(I,2)=O
    9 FORMAT(14HY RESID FOR PT,F10.4,3H IS,E16.4,10X ,3H WT,E16.4)
      DO433K=1,NU
      U(K)=U(K)+A(K)*O*D(I,13)
      DO432L=1,NU
  432 C(K,L)=C(K,L)+A(K)*A(L)*D(I,13)
```

```
  433 CONTINUE
      PRINT 21,OS
   21 FORMAT(/23HSUM OF WEIGHTED SQUARES,E16.4)
      IF(PRT1-1.) 440,434,440
  434 PRINT 19
   19 FORMAT(//22HNORMALS ON FIRST CYCLE)
      PRINT 20,((C(K,L),L=1,12),K=1,12)
   20 FORMAT(12E10.2)
  440 CONTINUE
C     INTRODUCE CONSTRAINTS ON X-AIR STATION THROUGH BETA
      IF(PRT1-2. ) 4442,4442,4445
 4442 CONTINUE
      DO 4444K=1,12
      PL(K)=0.
 4444 CONTINUE
      DO 442 K=1,12
      DO 441 L=1,12
  441 PL(K)=PL(K)+P(K,L)*(XOO(L)-XO(L))
  442 CONTINUE
      DO 444K=1,12
      U(K)=U(K)+PL(K)
      DO 443 L=1,12
  443 C(K,L)=C(K,L)+P(K,L)
  444 CONTINUE
 4445 CONTINUE
C     INTRODUCE CONSTRAINT ON PHIO = TO STD ERROR OF .1 RADIAN
      C(11,11)=C(11,11)+100.
      U(11)=U(11)+100.  *(PHIO-XO(11))
C    INTRODUCE CONSTRAINT ON J1=TO STD ERROR OF 0.1E-6
      PCOJ1=EXPF(14.)
      C(9,9)=C(9,9)+PCOJ1
```

```
      U(9)=U(9)+PCOJ1*(COJ1-XO(9))
C     COMPUTE ALTERATIONS
      CALL CINVU(C,U,NU,ALT)
      DO 451 I=1,5
  451 XOO(I)=XO(I)
      XOO(12)=XO(12)
C     RESTRICT ALTERATIONS
      DO 450 I=6,NU
  445 ABSX=ABSF(ALT(I))
      IF(ABSX-DEL(I)) 450,450,446
  446 ALT(I)=(ALT(I)/ABSX)*DEL(I)
  450 CONTINUE
      DO 500 I=1,NU
  500 XO(I)=XO(I)+ALT(I)
      PRINT 41
   41 FORMAT(C 2)
      PRINT10,LOOP,(XO(I),I=1,NU)
   10 FORMAT(//17HRESULTS FOR CYCLE,I5,/13HX AIR STATION,F15.4,/13HY AIR
     1 STATION,F15.4,/5HKAPPA,E12.5,/3HPHI,E12.5,/5HOMEGA,E12.5,/2HK1,
     2E16.8,/2HK2,E16.8,/2HK3,E16.8,/2HJ1,E16.8,/2HJ2,E16.8,/1HB,E16.8,/
     316HCAL FOCAL LENGTH,E16.8)
  510 CONTINUE
C     PRINT RESULTS
      FNP=NP
      SEUWS=OS/(2.*FNP-12.)
      SEUW=SQRTF(SEUWS)
      PRINT 33
   33 FORMAT(C 2)
      PRINT 11,LOOP,NU
   11 FORMAT(///20HFINAL RESULTS ON THE, I5,10H CYCLE FOR,I5,9H UNKNOWNS
```

```
     1)
      PRINT12,JN,KN,LN,MN,NR,IPN,NP
   12 FORMAT(/6HJOB NO,I10,/9HCAMERA NO,I10,/7HLENS NO,I10,/11HMAGAZINE
     1NO,I10,/6HRUN NO,I10,/8HPHOTO NO,I10  ,/16HNUMBER OF POINTS,I10)
   13 FORMAT(//17HCAMERA PARAMETERS)
      PRINT 10,LOOP,(XO(I),I=1,NU)
      PRINT14,SEUWS,SEUW
   14 FORMAT(/13HUNIT VARIANCE,E16.4,/21HSTD ERROR OF UNIT WT.,E16.4)
      DO520I=1,NU
      DO519J=1,NU
  519 C(I,J)=C(I,J)*SEUWS
  520 CONTINUE
      PRINT 33
      PRINT 15,IPN
   15 FORMAT(//30HCOVARIANCE MATRIX FOR PHOTO NO,I10,/)
      PRINT16,((C(I,J),J=1,12),I=1,12)
   16 FORMAT(12E10.2)
      PRINT 34,IPN
   34 FORMAT(C 2,42HRESULTS FOR INDIVIDUAL POINTS FOR PHOTO NO,I10,
     1//8HPOINT NO,5X,4HX MM
     1,6X,4HY MM,7X,4HX WT,8X,4HY WT,6X,7HX RESID,5X,7HY RESID)
      DO 525 I=1,NP
      PRINT 35,D(I,1),D(I,2),D(I,3),D(I,12),D(I,13),OUT(I,1),OUT(I,2)
   35 FORMAT(3F10.4,4E12.3)
  525 CONTINUE
      IF(PUNCH)530,532,530
  530 PUNCH18,JN,KN,LN,MN,NR,NP,PN
   18 FORMAT(6I10,F10.4)
      DO531I=1,NP
      PUNCH17,(D(I,J),J=1,3),(OUT(I,K),K=1,2)
  531 CONTINUE
  532 CONTINUE
   17 FORMAT(5F10.4)
      GO TO 100
  550 STOP
      END
```

SUBROUTINE CINVU

```
      SUBROUTINE CINVU(C,U,NU,X)
C     MATRIX INVERSE BY JORDAN ELIMINATION WITH SOLUTION FOR ALTERATIONS
C     -C-NORMAL COEF MATRIX
C     -U-OBSERVATIONAL VECTOR
C     -NU-RANK OF NORMALS
C     -X-ALTERATIONS  X=NINV*U
      DIMENSION C(16,16),U(16).X(16)
      DO 4 K=1,NU
      COM=C(K,K)
      C(K,K)=1.0
      DO 1 J=1,NU
    1 C(K,J)=C(K,J)/COM
      DO 4 I=1,NU
      IF(I-K)2,4,2
    2 COM=C(I,K)
      C(I,K)=0.0
      DO 3 J=1,NU
    3 C(I,J)=C(I,J)-COM*C(K,J)
    4 CONTINUE
      DO 5 I=1,NU
      X(I)=0.0
      DO 5 J=1,NU
    5 X(I)=X(I)+C(I,J)*U(J)
    6 CONTINUE
      RETURN
      END
```

SUBROUTINE COMCO

```
      SUBROUTINE COMCO(CCD,CO,NP)
C     MODEL AND COEFFICIENTS SELECTED FOR SYRACUSE UNIVERSITY MANN.
C     INST. 422C31
C     ESTIMATED VALIDITY 1.0 MICRON STD ERROR IN Y, 1.6 MICRON IN X
C     OBSERVATIONS MADE IN NOVEMBER 1966
      DIMENSION CCD(9),CO(300,3)
      XK=1.0000346
      YK=0.99999245
      A=-0.55570178*EXPF(-6.)
      B=-0.21397495*EXPF(-6.)
      C=0.20500064*EXPF(-8.)
      D=0.64311187*EXPF(-11.)
      E=-0.15111637*EXPF(-6.)
      F=0.34367281*EXPF(-7.)
   50 DO 100 I=1,NP
      X=CO(I,1)
      Y=CO(I,2)
      XS=X*X
      YS=Y*Y
      XC=XS*X
      YC=YS*Y
      XY=X*Y
      CO(I,1)=X*XK+A*XS+B*XY+C*XC+D*XS*YS
      CO(I,2)=Y*YK+E*YS+F*XY
  100 CONTINUE
  120 RETURN
  125 END
```

SUBROUTINE RDIST

```
      SUBROUTINE RDIST(PC,CP,NP,RR,DR)
   10 DIMENSION CP(50,5),PC(50,5),RR(50),DR(50)
   14 DO 15 I=1,NP
   15 DR(I)=0.0
   20 DO 840 I=1,NP
   30 CP(I,2)=PC(I,2)
   40 CP(I,3)=PC(I,3)
   50 R=SQRTF(CP(I,2)**2+CP(I,3)**2)
   55 RR(I)=R
   70 IF(R-10.)840,490,80
   80 IF(R-30.)490,510,90
   90 IF(R-42.)510,490,100
  100 IF(R-46.)490,470,110
  110 IF(R-51.)470,840,120
  120 IF(R-55.)840,650,130
  130 IF(R-60.)650,670,140
  140 IF(R-64.)670,690,150
  150 IF(R-66.)690,710,160
  160 IF(R-69.)710,730,170
  170 IF(R-72.)730,750,180
  180 IF(R-74.)750,770,190
  190 IF(R-91.)770,790,200
  200 IF(R-91.)790,770,210
  210 IF(R-94.)770,750,220
  220 IF(R-98.)750,730,230
  230 IF(R-102.)730,710,240
```

```
240 IF(R-106.)710,690,250
250 IF(R-109.)690,670,260
260 IF(R-110.)670,650,270
270 IF(R-112.)650,840,280
280 IF(R-113.)840,470,290
290 IF(R-114.)470,490,300
300 IF(R-115.)490,510,310
310 IF(R-117.)510,530,320
320 IF(R-120.)530,550,330
330 IF(R-122.)550,570,340
340 IF(R-125.)570,590,350
350 IF(R-128.)590,610,360
360 IF(R-131.)610,590,370
370 IF(R-134.)590,570,380
380 IF(R-137.)570,550,390
390 IF(R-140.)550,570,400
400 IF(R-143.)570,590,410
410 IF(R-146.)590,610,420
420 IF(R-149.)610,630,430
430 IF(R-152.)630,630,435
435 PRINT 436, PC(I,1)
436 FORMAT(20HERROR STOP POINT NO.F10.4)
440 GO TO 850
470 DELTR=.001
480 GO TO 800
490 DELTR=.002
500 GO TO 800
510 DELTR=.003
520 GO TO 800
530 DELTR=.004
```

```
540 GO TO 800
550 DELTR=.005
560 GO TO 800
570 DELTR=.006
580 GO TO 800
590 DELTR=.007
600 GO TO 800
610 DELTR=.008
620 GO TO 800
630 DELTR=.009
640 GO TO 800
650 DELTR=-.001
660 GO TO 800
670 DELTR=-.002
680 GO TO 800
690 DELTR=-.003
700 GO TO 800
710 DELTR=-.004
720 GO TO 800
730 DELTR=-.005
740 GO TO 800
750 DELTR=-.006
760 GO TO 800
770 DELTR=-.007
780 GO TO 800
790 DELTR=-.008
800 R=R+DELTR
805 DR(I)=DELTR
810 CP(I,2)=(DELTR*CP(I,2))/(R-DELTR)+CP(I,2)
820 CP(I,3)=(DELTR*CP(I,3))/(R-DELTR)+CP(I,3)
840 CONTINUE
850 RETURN
860 END
```

SUBROUTINE REFRA

```
      SUBROUTINE REFRA(PC,RK1,RK2,NC,XO,CC)
      DIMENSION PC(50 ,5),XO(6)
      SK=SINF(XO(4))
      SP=SINF(XO(5))
      SW=SINF(XO(6))
      CK=COSF(XO(4))
      CP=COSF(XO(5))
      CW=COSF(XO(6))
      A1=CP*CK
      A2=CW*SK+SW*SP*CK
      A3=SW*SK-CW*SP*CK
      B1=CP*SK
      B2=CW*CK-SW*SP*SK
      B3=SW*CK+CW*SP*SK
      C1=SP
      C2=SW*CP
      C3=CW*CP
      DO 3140 I=1,NC
      XV=A1*PC(I,2)-B1*PC(I,3)-C1*CC
      YV=A2*PC(I,2)+B2*PC(I,3)+C2*CC
      ZV=A3*PC(I,2)+B3*PC(I,3)-C3*CC
      XVS=-(XV/ZV)*153.000
      YVS=-(YV/ZV)*153.000
      RVS=SQRTF(XVS**2+YVS**2)
      RVS3=RVS**3
      DRVS=RVS*RK1+RVS3*RK2
      XVSC=XVS-(XVS*DRVS)/RVS
```

```
      YVSC=YVS-(YVS*DRVS)/RVS
      CSC=-XVSC*C1+YVSC*C2+153.0*C3
      PC(I,2)=(CC/CSC)*(XVSC*A1+YVSC*A2-153.0*A3)
      PC(I,3)=(CC/CSC)*(-XVSC*B1+YVSC*B2-153.0*B3)
 3140 CONTINUE
      RETURN
      END
```

SUBROUTINE RID

```
      SUBROUTINE RID(CR,IR,IRN,RI,ALPHA,XCT,YCT)
C     LIMITED TO ALPHA = 0 OR 180 DEGREES +,- .3 DEG.
C     CR-COMPARATOR COORDINATE OF RESEAU,IRNX2
C     IR-MATRIX OF IDENTIFICATION, IRNX2
C     IRN-NUMBER OF POINTS IN SET
C     RI-RESEAU INTERVAL IN UNITS OF OBS.
C     XCT,YXT-COMPARATOR COORDINATE OF CENTER RESEAU
  100 DIMENSION CR(8,3),IR(8,2)
      IF( ALPHA)108,110,108
  108 IF(ALPHA-1.57)110,110,115
  110 X11=XCT+8.*RI
      Y11=YCT+8.*RI
      DO 112 I=1,IRN
      IR(I,1)=(Y11-CR(I,2))/RI+1.5
      IR(I,2)=(X11-CR(I,1))/RI+1.5
  112 CONTINUE
      GO TO 120
  115 X11=XCT-8.*RI
      Y11= YCT-8.*RI
      DO 117 I=1,IRN
      IR(I,1)=(CR(I,2)-Y11)/RI+1.5
      IR(I,2)=(CR(I,1) -X11)/RI+1.5
  117 CONTINUE
  120 RETURN
  125 END
```

SUBROUTINE X-MEAN

```
      SUBROUTINE XMEAN(N,CIO,PC)
C     N=NO OF PHOTO POINTS MEASURED
C      PC=(NX5)MATRIX, PT. NO., XP, YP, XM, YM
C     PC IS PUNCHED ACCORDING TO 5F10.3,ACCEPTABLE TO CALIB-B
   10 DIMENSION CIO(99,6),PC(50,7)
   12 II=2*N
   16 FORMAT (12HINPUT MATRIX)
   18 FORMAT (6F10.4)
   20 K=1
      QSUMX=0.
      QSUMY=0.
      QSQX=0.
      QSQY=0.
   40 DO 330 I=1,II
   50 PPT = (CIO(I,1)/2.0)*10000.0
   60 NPT=PPT
   70 SPT=NPT
   80 IF(PPT-SPT)110,330,110
  100 FORMAT (5HCIO =F10.4)
  110 INDX1=I
  120 TEST=CIO(I,1)+.0001
  130 DO 150 J=1,II
  140 IF(TEST-CIO(J,1))150,160,150
  150 CONTINUE
  160 INDX2=J
  180 FORMAT(10HCIO(4,1) =,F10.4)
```

```
190 PX1=1.0/(CIO(I,4)**2+CIO(I,5)**2)
200 PX2= 1.C/(CIO(J,4)**2+CIO(J,5)**2)
210 PY1= 1.0/(CIO(I,4)**2+CIO(I,6)**2)
220 PY2= 1.0/(CIO(J,4)**2+CIO(J,6)**2)
230 XAV=(PX1*CIO(I,2)+PX2*CIO(J,2))/(PX1+PX2)
240 YAV= (PY1*CIO(I,3)+PY2*CIO(J,3))/(PY1+PY2)
250 XMAV=SQRTF((1.0/((PX1+PX2)**2))*((PX1**2)*CIO(I,5)**2+(PX2**2)*
   1(CIO(J,5)**2)))
260 YMAV=SQRTF((1.0/((PY1+PY2)**2))*((PY1**2)*(CIO(I,6)**2)+(PY2**2)
   1*(CIO(J,6)**2)))
270 PC(K,1)=CIO(I,1)
280 PC(K,2)=XAV
290 PC(K,3)=YAV
300 PC(K,4)=XMAV
310 PC(K,5)=YMAV
313 PC(K,6)=   CIO(J,2)-CIO(I,2)
314 PC(K,7)= CIO(J,3)-CIO(I,3)
    OSUMX =OSUMX+PC(K,6)
    OSUMY=OSUMY+PC(K,7)
    OSQX=OSQX+PC(K,6)**2
    OSQY=OSQY+PC(K,7)**2
    FPN=N
    XMB=OSUMX/FPN
    YMB=OSUMY/FPN
    SDDX=SQRTF(OSQX/(FPN-1.))
    SDDY=SQRTF(OSQY/(FPN-1.))
320 K=K+1
```

```
330 CONTINUE
    PRINT 335
335 FORMAT(///18HCOMBINED OBS. SETS,/)
355 PRINT 356
356 FORMAT (2X,5HPOINT,5X,5HXMEAN,5X,5HYMEAN,4X,9HS.E.XMEAN,1X,9HS.E.Y
   1MEAN,3X,7HDELTA X,3X,7HDELTA Y/)
357 PRINT 361,((PC(I,J),J=1,7),I=1,N)
    PRINT 358, XMB,SDDX,YMB,SDDY
358 FORMAT(//30HANALYSIS OF PAIRED DIFFERENCES ,//14HMEAN X BIAS,MM,F1
   14.5,/24HSTD DEV OF X-DIFFERENCES,E16.4,//14HMEAN Y BIAS,MM,F14.5,/
   224HSTD DEV OF Y DIFFERENCES,E16.4)
360 FORMAT(5F10.3)
361 FORMAT(3F10.3,4F10.4)
370 RETURN
380 END
```

UNCLASSIFIED

Security Classification

DOCUMENT CONTROL DATA - R & D

(Security classification of title, body of abstract and indexing annotation must be entered when the overall report is classified)

1. ORIGINATING ACTIVITY (Corporate author) Syracuse University Research Institute Department of Civil Engineering Syracuse, New York 13210	2a. REPORT SECURITY CLASSIFICATION Unclassified 2b. GROUP N/A

3. REPORT TITLE

CALIBRATION OF THE AERIAL PHOTOGRAPHIC SYSTEM

4. DESCRIPTIVE NOTES (Type of report and inclusive dates)

Final Report

5. AUTHOR(S) (First name, middle initial, last name)

Dean C. Merchant

6. REPORT DATE	7a. TOTAL NO. OF PAGES	7b. NO. OF REFS
December 1967	156	36

8a. CONTRACT OR GRANT NO AF 30(602)-4329 b. PROJECT NO 5569 c. Task 556902 d.	9a. ORIGINATOR'S REPORT NUMBER(S) 9b. OTHER REPORT NO(S) (Any other numbers that may be assigned this report) RADC-TR-67-552

10. DISTRIBUTION STATEMENT

This document is subject to special export controls and each transmittal to foreign governments or foreign nationals may be made only with prior approval of RADC (EMIRA), Griffiss Air Force Base, New York 13440.

11. SUPPLEMENTARY NOTES	12. SPONSORING MILITARY ACTIVITY
RADC Project Engineer. Joseph J. Del Vecchio, EMIRA AC 315-330-2624	Rome Air Development Center (EMIRA) Griffiss Air Force Base, New York 13440

13. ABSTRACT

Emphasis on greater accuracy from photogrammetric methods has stimulated interest in the problem of calibration of the aerial photographic system. To be realistic, the calibration procedures must be accomplished under circumstances of environment and technique which are equivalent to those to be expected operationally. It was the purpose of this study to develop and investigate the feasibility of providing a realistic aerial photographic system calibration.

Computational procedures were developed, programmed, and verified with artificial data. These computations included comparator calibration, single photo resection and multiple photo resection. The multiple photo resection employed up to four photographs using a common six parameter model to express interior orientation.

All procedures were verified further by use of real photography made at 14,000 feet over the U.S. Coast and Geodetic Survey, McClure, Ohio, camera calibration range. Results of the computations using real data indicated a need for improvement in the reseau techniques employed for compensation of film shrinkage. Recommendations were made for this purpose.

Procedures were developed and studied for determination of the camera constant independently from the flying height of the aircraft. This is of particular importance for photographic systems intended for use over mountainous regions. The characteristics of this method of aerial calibration were discussed.

DD FORM 1 NOV 65 1473

UNCLASSIFIED

Security Classification

14 KEY WORDS	LINK A		LINK B		LINK C	
	ROLE	WT	ROLE	WT	ROLE	WT
Photogrammetry						
Computers (Programming)						